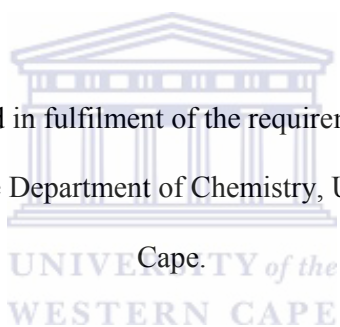


AMPEROMETRIC BIOSENSOR SYSTEMS PREPARED ON POLY(ANILINE-
FERROCENIUM HEXAFLUOROPHOSPHATE) COMPOSITES DOPED WITH
POLY(VINYL SULFONIC ACID SODIUM SALT).

PETER MUNYAO NDANGILI

A full thesis submitted in fulfilment of the requirements for the degree of
Magister Scientiae in the Department of Chemistry, University of the Western



Supervisors: Prof. Emmanuel I. Iwuoha and Prof. Priscilla Baker.

November 2008.

Key words.

Amperometric biosensor

Poly(aniline-ferrocenium hexafluorophosphate) [Pani-FcPF₆]

Poly(vinyl sulfonic acid sodium salt) –PVS-Na

Nano-composites

Horseradish peroxide (HRP)

Hydrogen peroxide

Scanning Electron Microscopy (SEM)

Cyclic voltammetry (CV)

Steady-state amperometry.

Tooth whitening products.



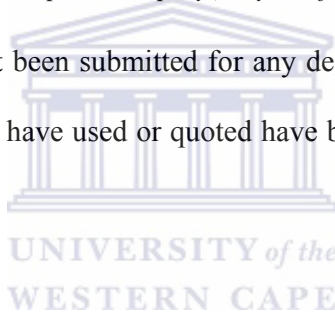
Abstract.

An amperometric biosensor was prepared by physically depositing horseradish peroxidase (HRP) enzyme on a poly(aniline-ferrocenium hexafluorophosphate) nano-composite modified glassy carbon electrode (GCE). The poly(aniline-ferrocenium hexafluorophosphate) nano-composites were electrochemically deposited on the electrode surface by scanning ten cycles from -100 mV to +1000 mV at a scan rate of 100 mV s⁻¹. Surface morphology of the electrodeposited composites was studied by Scanning electron microscopy (SEM) and showed nano-fibrous composites formed; with a cross-sectional diameter of 100 nm. Electrochemical characterization of the nano-composites, studied in 1 M hydrochloric acid (HCl) showed that the surface concentration of the adsorbed composite material was 1.2478×10^{-8} mol cm⁻². Biosensor analysis of standard hydrogen peroxide; studied using cyclic voltammetry (CV), square wave voltammetry (SWV) and steady state amperometric techniques gave a linear range of 6.60×10^{-5} M to 2.23×10^{-3} M, Michaelis-Menten constant (K_m^{app}) of 1.6890 mmol L⁻¹ and a maximum current under saturated substrate concentration (i_{max}) of 7.1560×10^{-6} A. Further studies of this biosensor with tooth whitening products showed that the biosensor developed was able to successfully detect, isolate and reduce hydrogen peroxide in both DAYWHITE® teeth whitening gel and Colgate Plax Whitening Blacheua (CPWB); leading to quantitative evaluation of the level of hydrogen peroxide concentration in the two products.

Declaration

I declare that *Amperometric biosensor systems prepared on poly(aniline-ferrocenium hexafluorophosphate) composites doped with poly(vinyl sulfonic acid sodium salt).*

is my own work, that it has not been submitted for any degree or examination in any other university, and that all sources I have used or quoted have been indicated and acknowledged by complete references.



Peter Munyao Ndangili

November 2008

Signed

Acknowledgements

First and foremost, I dearly thank the Almighty God for His grace in the period over which I carried out this study.

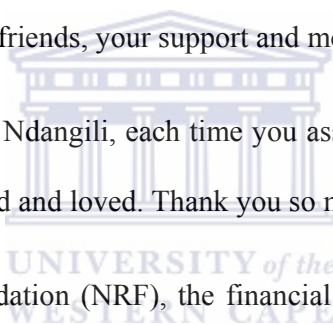
To my supervisors, thank you so much for the progressive evaluation of this work and facilitation that ensured successful completion. Kindly, feel highly appreciated.

To the staff of the departments of Chemistry and Physics, UWC, thank you so much for the kind support that you accorded me during this period.

To sensor lab colleagues and all friends, your support and motivation is highly appreciated.

To my mother, Mrs. Rosalia M. Ndangili, each time you assured me of your blessings while studying, I felt highly encouraged and loved. Thank you so much.

To the National Research Foundation (NRF), the financial assistance of the Department of Labour (DST) towards this research is hereby acknowledged.



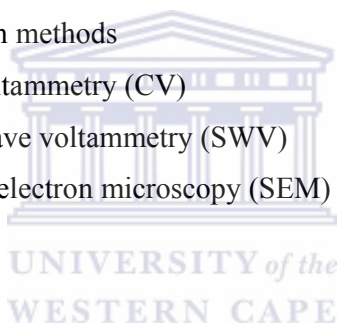
List of publications

1. Peter M. Ndangili, Munkombwe Muchindu, Priscilla G Baker, Catherine J Ngila, Emmanuel I Iwuoha, Tesfaye T Waryo. Polyanilino-polyvinyl sulphonate nanofibrillarity and application in wired-enzyme amperometric biosensor, 2009 (in press).
2. Tesfaye T. Waryo, Everlyne A. Songa, Mangaka C. Matoetoe, Rachel F. Ngece, Peter M. Ndangili, Amir Al-Ahmed, Nazeem M. Jahed, Priscilla G.L. baker, Emmanuel I. Iwuoha. Functionalization of polyaniline nanomaterials for amperometric biosensors: In *“Nanostructured Materials for Electrochemical Biosensors”* NOVA publishers, NY, USA, 2009 (in press).

Table of contents

Title page	i
Key words	ii
Abstract	iii
Declaration	iv
Acknowledgements	v
List of publications	vi
List of figures	xi
List of tables	vii
List of schemes	xiii
Chapter 1	1
1.0 Introduction	1
1.1 Tooth whitening	2
1.2 Risks associated with tooth whitening	3
1.3 Motivation of the study	5
1.4 Objectives of study	7
1.5 Research framework	8
1.6 Delimitations of the thesis	9
1.7 Outline of the thesis	9
Chapter 2	11
2.0 Literature review	11
2.1 Introduction to biosensors	11
2.1.1 The bio-element (Bio-recognition element)	13
2.1.2 The transducer	18
2.1.3 Types of biosensors	18
2.1.3.1 Electrochemical biosensors	18
2.1.3.1.1 Potentiometric biosensors	19
2.1.3.1.2 Conductrometric/impedimetric biosensors	19

2.1.3.1.3 Amperometric biosensors	19
2.2 Enzymes	20
2.2.1 Horseradish peroxidase (HRP) enzyme	25
2.3 Immobilization methods	27
2.3.1 Cross linking	28
2.3.2 Carrier bonding	29
2.3.2.1 Physical adsorption mode	30
2.3.2.2 Ionic bonding mode	31
2.3.2.3 Covalent bonding mode	31
2.3.3 Entrapping of enzymes	34
2.4 Conducting polymers containing metals (composites or metallopolymers)	35
2.4.1 Polyaniline	39
2.4.2 Ferrocenium hexafluorophosphate (FcPF ₆)	42
2.4.3 Characterization methods	45
2.4.3.1 Cyclic voltammetry (CV)	45
2.4.3.2 Square wave voltammetry (SWV)	48
2.4.3.3 Scanning electron microscopy (SEM)	50
Chapter 3	52
3.0 Experimental	52
3.1 Instrumentation	52
3.2 Reagents	52
3.3 Preparation of Pani-FcPF ₆ nano-composites	53
3.4 Characterization of the Pani-FcPF ₆ nano-composites	54
3.4.1 Electrochemical characterization	54
3.4.2 Scanning Electron Microscopy (SEM)	54
3.5 Fabrication of the biosensor	55
3.5.1 Illustrating the necessity of the HRP in the biosensor	55
3.5.2 Choice of potential window	56
3.5.3 Choice of scan rate	56
3.6 Biosensor measurements	56
3.6.1 Preparation and analysis of standard hydrogen peroxide	56
3.6.2 Preparation and analysis of commercial tooth whiteners	57
3.7 Interference studies	58



Chapter 4	60
4.0 Results and discussion 1	60
4.1 The Pani-FcPF ₆ composites	60
4.2 Characterization of the Pani-FcPF ₆ composites	65
4.2.1 Electrochemical characterization	65
4.2.2 Scanning Electron Microscopy (SEM)	71
Chapter 5	74
5.0 Results and discussion 2	74
5.1 The necessity of horseradish peroxidase (HRP) enzyme in the biosensor	74
5.2 Choice of potential window	76
5.3 Choice of scan rate	78
5.4 Response characteristics of the hydrogen peroxide biosensor	80
5.5 Interference to hydrogen peroxide detection by the biosensor	88
5.6 Biosensor response to hydrogen peroxide in selected tooth whiteners	91
5.6.1 DAYWHITE®	91
5.6.2 Colgate Plax Whitening Blacheua (CPWB).	93
5.6.3 Quantitative evaluation of H ₂ O ₂ in DAYWHITE® and CPWB.	96
Chapter 6	98
6.0 Conclusions and recommendations	98
6.1 Conclusions	98
6.2 Recommendations	99
References	100
Appendices	112

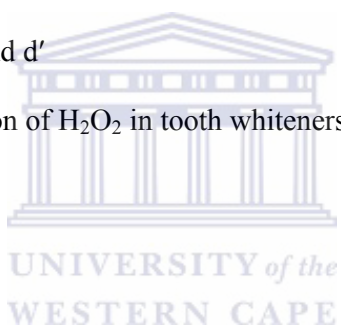
List of figures.

- Figure 1: Structure of ferrocenium hexafluorophosphate. 41
- Figure 2: A typical cyclic voltammogram showing the basic peak parameters, $E_{p,a}$, $E_{p,c}$, $i_{p,a}$ and $i_{p,c}$. 46
- Figure 3: A typical square wave voltammogram. 49
- Figure 4: Voltammograms for the electropolymerization of poly(aniline-ferrocenium hexafluorophosphate) nano-composites in 1 M HCl, initial potential: -100 mV; scan rate 100 mV s⁻¹. 62
- Figure 5: Voltammograms for electropolymerization of polyaniline in 1 M HCl, initial potential: -100 mV; scan rate 100 mV s⁻¹. 63
- Figure 6: Voltammograms of 0.02 M FcPF₆ in 1 M HCl, initial potential: 100 mV, scan rates: 20, 50, 80 and 100 mV s⁻¹. 64
- Figure 7: Multiscan voltammograms of Pani-FcPF₆ characterization in 1 M HCl at different scan rates (20 to 90 mV s⁻¹ in steps of 10 mV s⁻¹). Initial potential: -100 mV. 66
- Figure 8: A plot of scan rate versus peak current for peak a'. 70
- Figure 9: Scanning electron micrograph of (a) Pani-FcPF₆ and (b) PANI. 72
- Figure 10: Multiscan voltammograms of Pani-FcPF₆/Glu/BSA/HRP, Pani-FcPF₆, Pani-FcPF₆/Glu and Pani-FcPF₆/Glu/BSA; all with 20 μL of 5 mmol L⁻¹ of H₂O₂ as well as Pani-FcPF₆/Glu/BSA/HRP without H₂O₂; each performed in PBS, pH 7.0 at a scan rate of 10 mV s⁻¹. 75
- Figure 11: Multiscan voltammograms of the enzyme electrode in presence of 5 μL of 5 mmol L⁻¹ H₂O₂ in PBS, pH 7.0 at a scan rate of 10 mV s⁻¹ within different potential windows. 77

Figure 12: Multiscan voltammograms of enzyme electrode in presence of 20 μL of 5 mmol L^{-1} H_2O_2 in PBS, pH 7.0 at different scan rates.	79
Figure 13: Cyclic Voltammetric biosensor response to successive additions of standard H_2O_2 in PBS, pH 7.0 at a scan rate of 10 mV s^{-1}	81
Figure 14: Square wave voltammetric response to successive additions of standard H_2O_2 in PBS, pH 7.0	82
Figure 15: Current-time plot for biosensor response to standard H_2O_2 at a constant potential of -400 mV in PBS, pH 7.0 (inset are similar plots for days 1, 3, 7 and 13)	84
Figure 16: Calibration curve for the biosensor response to standard H_2O_2 in PBS, pH 7.0 with a freshly prepared enzyme electrode.	86
Figure 17: A current- H_2O_2 concentration plot for the biosensor response to standard H_2O_2 in PBS, pH 7.0	88
Figure 18: Square wave voltammetric biosensor response to 3 mmol L^{-1} H_2O_2 alone and $\text{H}_2\text{O}_2 + \text{C}_2\text{H}_5\text{OH}$ in PBS, pH 7.0.	90
Figure 19: Current-time plot for the biosensor response to successive additions of DAYWHITE® at a constant potential of -400 mV in PBS, pH 7.0.	92
Figure 20: Square wave voltammetric response to successive additions of DAYWHITE® in PBS, pH 7.0.	93
Figure 21: Square wave voltammetric response to successive additions of CPWB in PBS, pH 7.0.	94
Figure 22: Current-time plot for the biosensor response to successive additions of CPWB at a constant potential of -400 mV in PBS, pH 7.0.	95

List of tables.

Table 1: Different groups of enzymes.	21
Table2: Different forms of covalent binding.	33
Table 3: The slopes and correlation coefficients for various plots of peaks a, a', d, and d'	68
Table 4: Quantitative composition of H ₂ O ₂ in tooth whiteners.	96



List of Schemes

Scheme 1: Research framework.	8
Scheme 2: Schematic representation of a biosensor.	12
Scheme 3: Catalytic pathway of HRP.	26
Scheme 4: Cross linking reactions of glutaraldehyde	29
Scheme 5: Structural formulae for the conducting polymers (a) polypyrrole, (b) polythiophene and (c) polyaniline.	36
Scheme 6: Aniline to polyaniline electrochemical polymerization mechanism	39
Scheme 7: Different forms of polyaniline	41



Chapter 1

1.0 Introduction

Life quality in the modern society is an important and a key parameter determining the life expectancy of human beings. It is closely linked to the quality of environment, the quality of consumer products such as food or aesthetic products and general health status. However industrial developments have led to emissions and effluents that pollute the environment (air, water and soil). Moreover, poor health conditions emanating from uncontrolled levels of metabolites such as glucose, urea, cholesterol and lactate among others in whole blood have led to terminal diseases thus reducing the life expectancy of the population. Products consumed by human beings for food such as food additives or for beauty purposes such as cosmetics contain established and well defined proportions of ingredients. Too much or too little of one or more of these ingredients in the products may pose health dangers. Therefore, the control of diseases, food quality and safety, and quality of our environment are important aspects that require attention for improved life quality and increased life expectancy. For instance, identification of the type of pollutants and establishment of the level of pollution is an essential practice in environmental monitoring. The estimation of the above mentioned metabolites is of central importance in clinical diagnostics [1]. A system of monitoring the proportional composition of ingredients in consumer products with a view of standardizing them thus making them fit for human consumption is also essential for a healthy population. This calls for a continuous, fast and sensitive monitoring to control key parameters of the all the above. For this reason improvement of life quality has been one of the most important objectives of global research efforts [2].

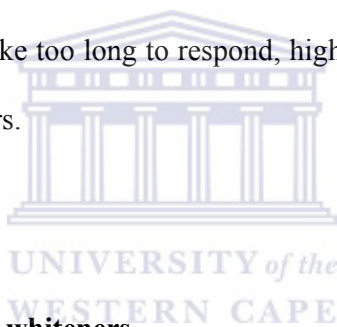
One chemical found in most household products and whose level of concentration in these products require monitoring is hydrogen peroxide. Hydrogen peroxide (H_2O_2) is an essential

chemical in many fields, including food production, pulp and paper bleaching, sterilization, chemical and biological sectors [3]. It is also a powerful oxidizing agent which can be used for synthesis of many other compounds [3]. Of particular interest in this study is the inclusion of hydrogen peroxide in tooth whitening products.

1.1 Tooth Whitening

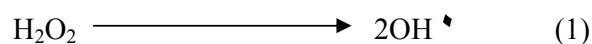
Tooth whitening, also known as tooth bleaching is a common procedure in cosmetic dentistry. It involves changing the colour of the teeth without changing their physical structure. In the recent years, tooth whitening has become one of the most rapidly growing oral care sectors [4]. This is due to patients demand for both healthy and cosmetically attractive smiles. Tooth whitening is also meant address the ever increasing problems of tooth darkening emanating from changes of the mineral structure of the tooth, staining by bacterial pigments, food stuffs and tobacco. In tooth bleaching, either carbamide peroxide ($\text{CH}_4\text{N}_2\text{O}\cdot\text{H}_2\text{O}_2$) or hydrogen peroxide (H_2O_2) is usually used as the bleaching agent [5-7]. Carbamide peroxide breaks down in the mouth into hydrogen peroxide and urea [8]. Tooth whitening action by hydrogen peroxide involves its diffusion through the enamel, causing bleaching of the pigments found in the enamel-dentine junction [4]. Eventually, the teeth appear whiter and less yellow. Peroxide containing tooth whiteners have recently been classified into three categories [9]. In the first category are tooth whiteners containing high concentrations of peroxides; usually 30 to 35% H_2O_2 concentration or 35% $\text{CH}_4\text{N}_2\text{O}\cdot\text{H}_2\text{O}_2$ concentration [9]. These are made for professional use only. The second category includes those tooth whiteners dispensed by dentists, a procedure commonly known as office bleaching or used by patients at home (home bleaching). They contain up to 10% H_2O_2 or 16% $\text{CH}_4\text{N}_2\text{O}\cdot\text{H}_2\text{O}_2$. The third category includes the over-the counter products, normally sold

to consumers directly for home use. The H₂O₂ content in these products is usually up to 6%. However, the concentration of the active ingredient (hydrogen peroxide or carbamide peroxide) in most over-the counter tooth whitening products is not indicated. For instance, Colgate Plax Whitening Blacheua (CPWB); which is an over-the counter tooth bleaching product contains hydrogen peroxide among other ingredients as indicated by the manufacturers. However, its concentration is not indicated. Moreover, manufacturers may not give the exact concentrations of hydrogen peroxide in tooth whitening products for purposes of marketing. This makes it necessary for the consumers of these products to have an idea of how they can precisely quantify the amount of hydrogen peroxide in the tooth whiteners. This is because, whereas low levels of hydrogen peroxide in tooth whiteners either do not effectively bleach the teeth or take too long to respond, high levels of hydrogen peroxide are associated with health risk factors.

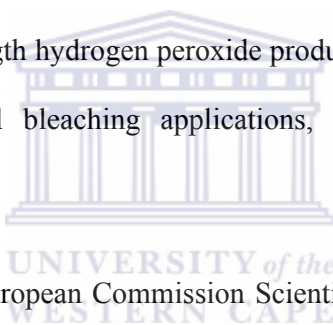


1.2 Risks associated with tooth whiteners.

Tooth whitening is associated with risks such as chemical burns especially if a high concentration of the bleaching agent is used, sensitive teeth and over bleaching. Talking about possible burns from highly concentrated bleaching agent poses the question of “how high is high?!” Deleterious effects of hydrogen peroxide arising from tooth whitening procedures have also been reported. These include ulceration of the oral cavity, inflammation of the gingival and inactivation of the pulpal enzymes [8]. Moreover, peroxides are commonly characterized by their ability to form free radicals [9], according to the equation;



The free radicals undergo oxidative reactions and have been reported to damage proteins, lipids and nucleic acids [10-13]. In particular, hydroxyl radicals derived from H₂O₂ have been reported to take part in various stages of carcinogenesis [14, 15]. The oxidative reactions and subsequent damage of cells by free radicals emanating from hydrogen peroxide are believed to be the major mechanisms responsible for observed toxicity of peroxide compounds [9]. The process may be associated with carcinogenesis, aging, stroke and other degenerative diseases [10-13]. Hydrogen peroxide has been established to be cytotoxic at concentration levels ranging from 0.05 mmol L⁻¹ to 0.58 mmol L⁻¹ in cell culture studies [16-20]. It is for this reason that health Canada has not authorized any hydrogen peroxide product advertised to treat AIDS, cancer, emphysema or any other serious and life-threatening diseases. There are, however, several high strength hydrogen peroxide products authorized for sale in Canada as disinfectants and as dental bleaching applications, which are health products for professional use only.



According to a report by the European Commission Scientific Committee on Consumer Products (SCCP) in 2005 about opinion on hydrogen peroxide in tooth whitening products, the use of tooth whiteners containing up to 0.1% hydrogen peroxide are safe for home bleaching purposes and up to 6% up on approval by a dentist. For this reason, restrictions on availability of bleaching products and concentration of the peroxides have been imposed by some countries in Europe and US. For instance, the US Food and Drug Administration (FDA) has accepted both hydrogen peroxide (1.5 - 3%) and carbamide peroxide (10 - 15%) as oral antiseptic agents [9]. FDA allows same concentrations of the two products for use as home tooth whitening products.

1.3 Motivation

In view of the above risks associated with tooth whitening procedures and fair restrictions imposed on tooth whitening products, it leaves no doubt that monitoring of the level of hydrogen peroxide in tooth whiteners is an essential practice. Besides the manufacturer, it is also necessary for the consumer of tooth whitening products to have an idea of how much hydrogen peroxide is present in the products. Several methods for determining hydrogen peroxide in samples have been reported. These methods include volumetric, calorimetric, chemiluminisence, spectrophotometric and titrimetry [21, 22]. In aqueous solutions, volumetric methods can suitably detect hydrogen peroxide at levels ranging from 0.1% to 5% [23]. Although this method detects such low levels of hydrogen peroxide, it involves several other chemicals. These chemicals include potassium iodide (KI), ammonium molybdate $[(\text{NH}_4)_8\text{Mo}_7\text{O}_{24}]$, potassium iodate (KIO_3), starch solution and potassium thiosulphate ($\text{K}_2\text{S}_2\text{O}_3$). It is thus an expensive, complicated and laborious method. Calorimetric methods with a linear range of 3.125×10^{-2} M to 1 M have been developed [24]. Titrimetry method is most accurate in the range of peroxide concentration of 0.5 mg L^{-1} to 5 mg L^{-1} (1.46×10^{-5} M to 1.46×10^{-4} M) in buffer solution [25] whereas that obtained by chemilluminisce method in a similar media is 2.44 ng mL^{-1} to 2500 ng mL^{-1} [26]. However, these methods are time consuming, complex, suffer from interferences [21], require long pre-treatment and involve utilization of expensive and toxic reagents [22]. Recent studies have shown that electrochemical methods are inexpensive and effective [3]. Moreover, more sensitive methods have been developed using peroxidase modified electrodes [22]. In this study, an electrochemical method, in form of a biosensor will be developed for quantitative evaluation of hydrogen peroxide in tooth whiteners.

An existing body of knowledge that, hydrogen peroxide is a substrate for horseradish peroxidase enzyme offers an insight into the principle behind this electrochemical method.

Upon application of a suitable potential, catalytic reduction of hydrogen peroxide is usually accompanied by generation of current. This current is proportional to the amount of hydrogen peroxide available in the sample under investigation. By monitoring this current, the amount of hydrogen peroxide in a sample can be inferred. On its part, horseradish peroxidase is a low molecular weight enzyme, with a relatively thin insulating protein shell surrounding its active centre [27]. For this reason, horseradish peroxidase is able to exhibit direct electron communication between its active centre and common electrodes [27]. This process is however slow. This can be enhanced by incorporation of an electroactive compound (mediator) into the biosensor. It is therefore envisaged that, incorporation of horseradish peroxidase enzyme and a suitable electron transfer mediator will present promising tools (biosensors) for monitoring the levels of hydrogen peroxide in tooth whiteners. Conducting polymers containing metals (metallopolymers or composites) are emerging compounds that find applications as sensor mediators [28]. These new materials combine the processing advantages of polymers with the functionality provided by the presence of metal centres [28]. The metal centres usually contained in the metallopolymers range from main group metals such as Sn and Pb to transition metals such as Fe, Ir and Pt (and their complexes) as well as lanthanides such as Eu [28]. On their part, the conducting polymers include polyaniline (PANI), polypyrrole (PPY) and polythiophene. For instance, complexes of iron (ferrocenes) have been successfully been incorporated into polythiophenes and the resulting metallopolymers used in biosensors [29]. Therefore, both polypyrrole and polyaniline are potential candidates for co-polymerization with ferrocenes and the resulting compounds used as electron transfer mediators in biosensor fabrication. In this study, polyaniline will be polymerized in presence of ferrocenium hexafluorophosphate (FcPF_6); giving rise to poly(aniline-ferrocenium hexafluorophosphate) - $[\text{Pani-FcPF}_6]$ composites.

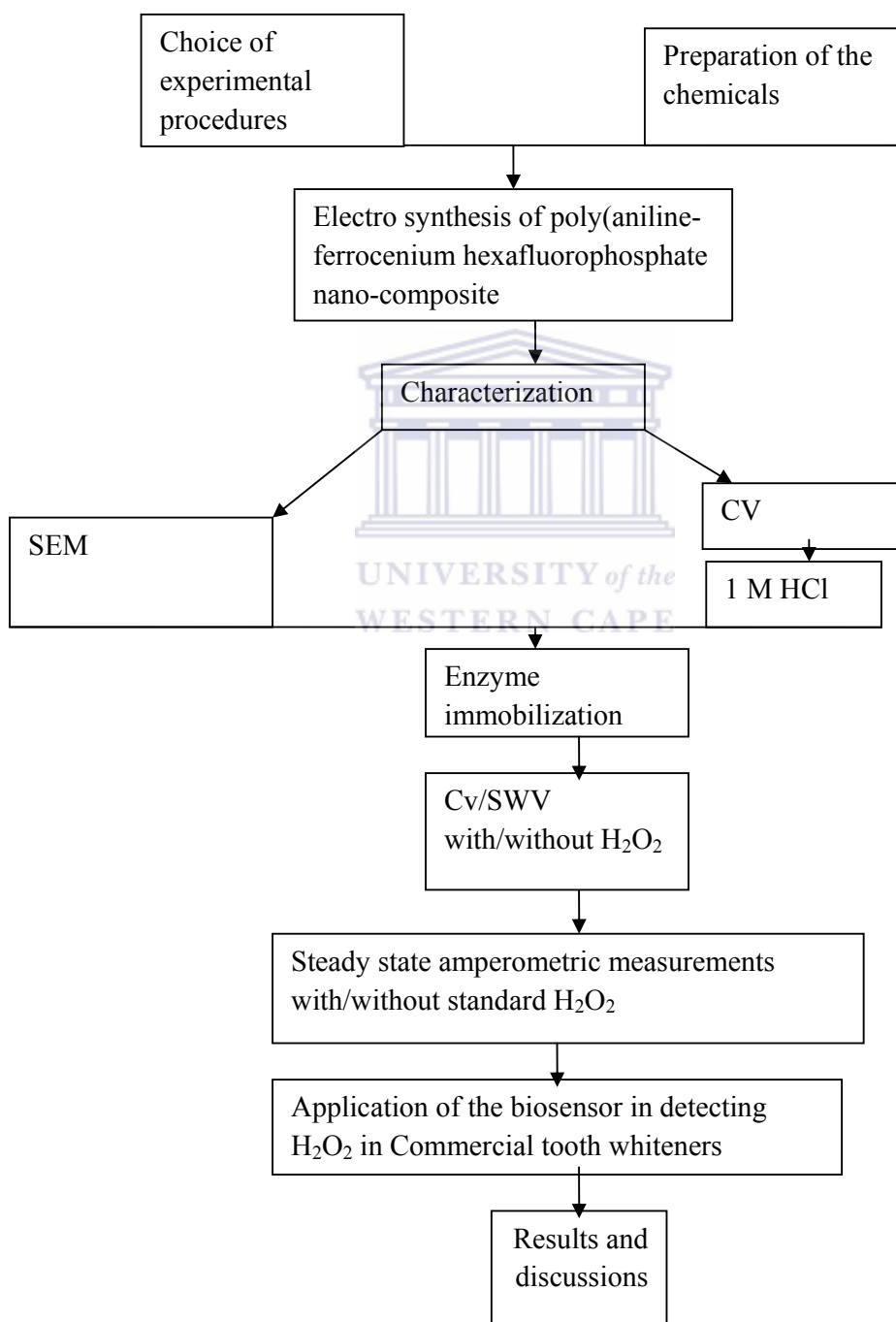
1.4 OBJECTIVES

The main hypothesis in this study is the development of a nanocomposite mediated amperometric biosensor for detection of hydrogen peroxide. The aim is to combine the electrochemical properties of both polyaniline and ferrocenium hexafluorophosphate into highly conductive nano composites capable of exhibiting electrochemistry in non acidic media; shuttling electrons between HRP and GCE for biosensor applications. The main sub-objectives of this study include:

- i. Development of poly(aniline-ferrocenium hexafluorophosphate) nano-composites on glassy carbon electrode (GCE) surface
- ii. Investigate the electrochemical properties of the developed nano-composite material.
- iii. Study the surface morphology of the nano-composite using Scanning Electron Microscopy (SEM).
- iv. Suitably immobilize HRP enzyme on the nano-composite modified electrode
- v. Use the enzyme electrode to determine the potential at which hydrogen peroxide is reduced by employing cyclic voltammetry and oyster square wave voltammetry with different concentration of hydrogen peroxide
- vi. Carry out steady state amperometric measurements using the above determined potential at different concentrations of hydrogen peroxide
- vii. Investigate the analytical characteristics of the biosensor such as linear range, detection limit, sensitivity, response time and reproducibility among others.
- viii. Apply the biosensor for detection of hydrogen peroxide concentrations in commercial tooth whitening products.

1.5 Research framework.

In line with the study objectives and the experimental programme, the research framework process is shown on the scheme in

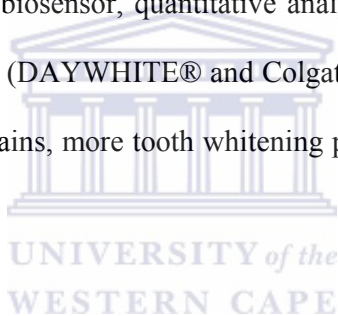


Scheme 1: Research framework.

1.6 Delimitations of the thesis

The main efforts of the thesis involve the following aspects.

- i. Poly(aniline-ferrocenium hexafluorophosphate) nano composites were developed in acidic media. Both electrochemical and physical characteristics of the developed nano-composites were investigated.
- ii. The electron shuttling ability of the developed nano-composites between a biomolecule and an electrode were demonstrated using HPR (biomolecule) and GCE in the fabrication of an amperometric biosensor for H₂O₂.
- iii. By using the developed biosensor, quantitative analysis of H₂O₂ in two commercial tooth whitening products (DAYWHITE® and Colgate Plax Whitening Blacheua) was done. Due to time constrains, more tooth whitening products were not covered in this study.



1.7 Outline of the thesis

The thesis will be presented as outlined briefly below:

An introduction giving various issues that influence human life and which require continuous monitoring are raised in this chapter. Tooth whitening practice, risks associated with the practice and need for developing biosensors for monitoring of the active ingredients in these products is also highlighted in this chapter. Various aspects of horseradish peroxidase and metallopolymers that can possibly lead to an achievable fabrication of the biosensor in study are discussed. The objectives of this study, work frame and delimitations of this study are also stated in this chapter.

A literature review relating to the various aspects of biosensors, biomolecules as well as immobilization methods will be presented in chapter two. This chapter will also cover a brief introduction to conducting polymers containing metals as well as introduction to polyaniline and ferrocenium hexafluorophosphate. Characterization methods, mainly cyclic voltammetry, square wave voltammetry and scanning electron microscopy are also briefly discussed in this chapter. In chapter 3, the chemicals, instrumentation and preparation procedures will be described. The chapters 4 and 5 will present results and discussion in which, chapter 4 will mainly present and discuss the characterization results of the developed nano-composite. Chapter 5 will present and discuss the results of biosensor response to standard H_2O_2 . It is also in this chapter that a detailed description of the biosensor and its analytical characteristics such as stability, detection limit, response time, linear range and reproducibility will be presented. In this chapter will also feature results and discussion of biosensor response to H_2O_2 in selected commercial tooth whiteners. The quantitative values of H_2O_2 concentration in the studied commercial tooth whiteners will be spelt out in this chapter. The final chapter, 6 will present the conclusions.

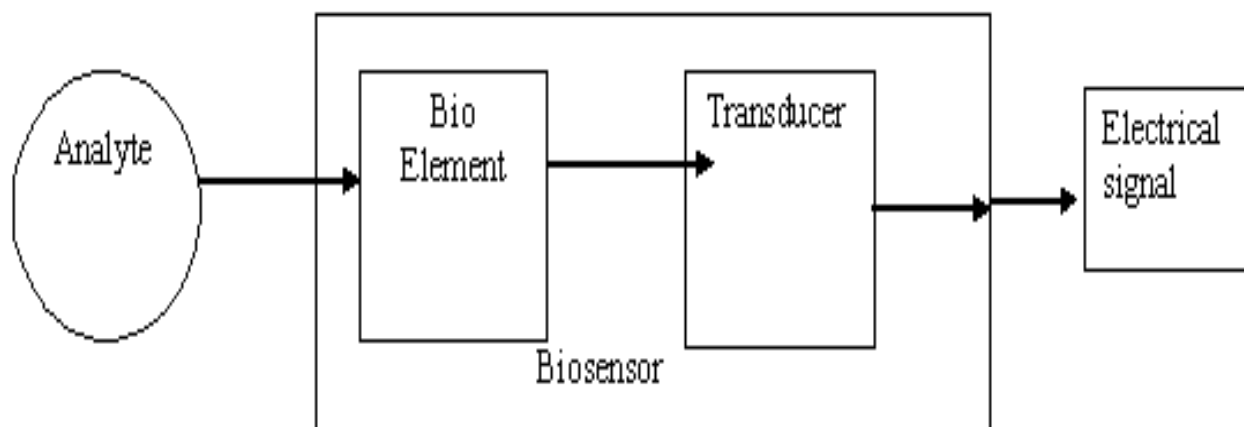
Chapter 2

2.0 Literature Review

2.1 Introduction to biosensors.

A biosensor is an analytical device made up of a combination of a specific biological component and a transducer. The specific biological element recognizes a specific analyte and the changes in the bio molecule are usually converted into a quantifiable signal (which is in turn calibrated to a certain scale) by a transducer. The use of biosensors can offer significant advantages for the continuous, fast, sensitive and inexpensive monitoring of environment, health and consumer products. Benefits arising from biosensors include efficiency, reliability and ability to find applications in many fields. Integrated with new technologies in molecular biology, macro fluids, and nano materials, biosensors have proved to provide selective identification of target analytes at ultra trace levels. This has found applications in Agricultural production, food processing, medical diagnosis and environmental monitoring for rapid, specific, inexpensive, in-field, on-line, and/or real-time detection of pesticides, antibiotics, pathogens, toxins, proteins, nutrilites, odours, microbes, and more in plants, animals, foods, soil, air, and water.

The concept of a biosensor dates back to 1962 when Clark and Lyons described the development of the first “enzyme sensor [30]. Since then, there has been a tremendous activity witnessed in this area of biosensors. A schematic representation of a biosensor is shown below.



Scheme 2: Schematic representation of a biosensor.

To maximize the detection of the generated signal, the microenvironment within which the biological molecule and the target analyte interacts, and the relay of this signal to the detector (transducer) have been extensively studied. Although there exists an extremely large number of possible combinations between different types of bio-recognition molecules and transducers, a direct communication between the biorecognition molecule and the transducer is limited to a few examples such as peroxidases or pyroloquinoline quinone dehydrogenases combined with amperometric transducers [31]. The reason behind this is that, since most biorecognition elements used are whole living cells [32] and enzymes [33], those with high molecular weight have a thick insulating protein shell surrounding the active site which prevents electrical communication between the redox centers of the biorecognition molecules and the electrode surfaces. The kinetic barrier results from the distance of the redox active site from the electrode surface. Previous studies have shown that, low molecular weight redox proteins such as peroxidases, examples being Cytochrome c peroxidase [34, 35], horseradish peroxidase [34, 36-37], microperoxidase [38], Lactoperoxidase [39] and fungal peroxidase [40] exhibit direct communication between common electrodes and their active

sites. However, this process is known to be generally slow. For this reason, and for most enzyme-based biosensors, the electro-reduction or electro-oxidation of the enzyme is facilitated by the presence of redox compounds known as mediators; either dissolved in the fluid to be analyzed or coated on the electrode (chemically modified electrode). Biosensors may be classified according to the biological specificity-conferring mechanism, the mode of physiochemical signal transduction or according to the analytes or reactions that they monitor.

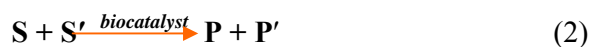
2.1.1 The bio-element (biorecognition element)

This is a biological recognition molecule that selectively detects and binds a particular molecule (target analyte) from amongst many other molecules. It translates information from the biochemical domain, usually an analyte concentration into a chemical or physical output signal with a defined sensitivity. The main purpose of the recognition system is to provide the sensor with a high degree of sensitivity for the analyte to be measured. While all biosensors are more or less selective (non-specific) for a particular analyte, some are, by design and construction only class specific, since they use class enzymes. Examples are phenolic compound biosensors, or whole cells, for instance used to measure biological oxygen demand.

The recognition molecules include enzymes, antibodies, antigens, DNA, living cells, tissues, e.t.c [1]. Biosensors that use antibodies or antigens as biorecognition elements are commonly known as immunosensors. They act on the principle that the immune response of a certain biological species to contaminants will produce antibodies which in turn can be measured. Immunosensors have been developed and applied widely in detection of food and soil contaminants. Examples include the fibre optic biosensor and the continuous flow

immunosensor which detect water and soil contaminants such as trinitrotoluene (TNT) and royal demolition explosive (RDX). Although the bio recognition element is the selective part of the biosensor, the overall function of the biosensor is determined by proper combination of the biological recognition element with the transducer with respect to the signal transduction process. Based on the biological specificity-conferring mechanism, biorecognition elements may be classified into biocatalytic recognition elements and biocomplexing or bio affinity recognition elements.

Biocatalytic recognition elements are based on reactions which are catalyzed by macromolecules, present in their original environment, having been previously isolated or manufactured. This continuous consumption of an analyte(s) is achieved by the immobilized biocatalyst incorporated into the sensor and transient or steady state responses monitored by the integrated detector. The biocatalysts commonly used in this class of biosensors are enzymes (mono or multi-enzyme), whole cells (micro organisms such as bacteria, fungi, eukaryotic cells or yeast) or cell organelles, and tissue (plant or animal tissue slice). One or more analytes, usually known as substrates **S** and **S'**, react in the presence of the corresponding enzyme, cell or tissue to yield one or several products, **P** and **P'**, according to the general reaction scheme below.

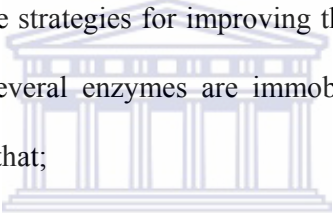


The use of adjacent transducer to monitor the substrate consumption involves a number of strategies. One such a strategy involves detection of the co-substrate (**S'**) consumption e.g O₂ depleted by oxidase, bacteria or yeast reacting layers and the corresponding signal decrease

from its initial value. The second strategy involves recycling of one of its reaction products, for example H_2O_2 , H^+ , CO_2 or NH_3 produced by oxidoreductase, hydrolase or lyase corresponding to signal increase. Thirdly, there may occur direct electron transfer between the active site of a redox enzyme and the electrochemical transducer. The fourth strategy involves detection of the state of the biocatalyst redox active centre or cofactor in the presence of the substrate using an immobilized mediator which reacts sufficiently and rapidly with the biocatalyst and easily detected by the transducer.

This last strategy eliminates the dependence of sensor response on the co-substrate, S' concentration and also decreases the effects of possible interfering species.

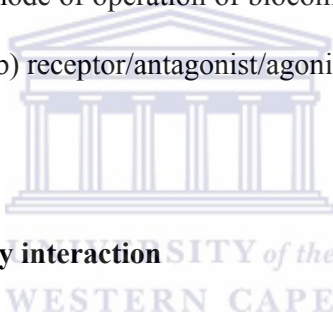
It is worth mentioning that, more strategies for improving the biosensor performance can be developed when for example several enzymes are immobilized within the same reaction layer. The three possibilities are that;

- 
- i. Several enzymes facilitate the biological recognition by sequentially converting the product of a series of enzymatic reactions into a final electro active form. This allows a much wider range of possible biosensor analytes.
 - ii. Multiple enzymes, applied in series, may generate the first enzyme co-substrate and real amplification of the biosensor output signal may be achieved by efficient regeneration of another co-substrate of the first enzyme and
 - iii. Multiple enzymes, applied in parallel may improve the biosensor selectivity by decreasing the local concentration of electrochemical interfering substrate.

Enzymes were the first bio recognition elements to be used in biosensors and still remain the most mostly used elements. The product formed from the catalytic reaction is released, thus regenerating the active binding site. The main advantage of the enzyme based biosensors

therefore is the implemented regeneration of the enzyme's active site, implying an amplification of the signal concomitantly with an intrinsic reversibility of the sensor.

In **biocomplexing or bio affinity recognition element**, the biosensor operation is based on the interaction of the analyte with macromolecules or organized molecular assemblies that have either been isolated from their original biological environment or engineered. Thus equilibrium is usually reached and there is no further consumption of the analyte by the immobilized biocomplexing agent. These equilibrium responses are monitored by the integrated detector. The biocomplexing reaction itself may in some cases be monitored using a complementary bio catalytic reaction. Steady state or transient signals are then monitored by the integrated detector. The mode of operation of biocomplexing elements is either via (a) antigen-antibody interaction or (b) receptor/antagonist/agonist.



(a) The antigen-antibody interaction

The most developed examples of biosensors using biocomplexing receptors are based on immunochemical reactions such as binding an antigen (Ag) to a specific antibody (Ab). The formation of such Ag-Ab complexes has to be detected under conditions where non-specific interactions are minimized. Each Ag determination requires the production of a particular Ab, its isolation and usually its purification. Several studies have been described involving direct monitoring of the sensitivity of Ab-Ag complex formation on ion-sensitive field effect transistors (ISFETs). In order to increase the sensitivity of immunosensors, enzyme labels are frequently coupled to Ab or Ag, thus requiring additional synthesis steps. Even in the case of the enzyme labelled Ab, these biosensors operate essentially at equilibrium, the enzyme being there only to quantify the amount complex produced. As the binding or affinity constant is very large, such systems are either irreversible (single use biosensors) or placed within flow

injection analysis (FIA) environment where Ab may be regenerated by dissociation of complexes by chaotropic agents such as glycine – HCl at pH 2.5.

(b) Receptor/antagonist/agonist.

Attempts have been made in the recent past to use ion channels, membrane receptors or binding proteins as molecular recognition systems in conductometric, ISEFT or optical sensors [41]. For example, the transporter, protein lactose permease (LP) may be incorporated into liposome bilayers thus allowing coupling of sugar proton transport with a stoichiometric ratio of 1:1, as demonstrated with the fluorescent pH probe pyranine entrapped in these liposomes [42]. The LP containing liposomes have been incorporated within planner lipid bilayer coatings of an ISEFT gate sensitive to pH. The preliminary results have shown that these modified ISEFTs enable rapid and reversible detection of lactone in an FIA system. Protein receptor based biosensors have so far been developed. The result of the binding of the analyte, here named agonist, to immobilized channel receptor protein is monitored by changes in ion fluxes through these channels. For example the glutamate, as a target agonist, may be determined in the presence of interfering agonists, by detecting Na^+ or Ca^{2+} fluxes using conductivity or ion selective electrodes. Due to the dependence of ion channel switching on agonist binding, there is usually no need of enzyme labelling of the receptor to achieve the desired sensitivity.

The most recent development in the electrochemical biosensors involves the use of chips and electrochemical methods to detect binding of oligonucleotides (gene probes). This involves the intercalation into the oligonucleotide duplex, during the formation of a double stranded DNA on the probe surface, a molecule that is electroactive or directly detecting guanine

which is electroactive. Oligonucleotides have also been immobilized on electroactive metal dendrimers attached on disk electrodes and charge transfer changes monitored [43].

2.1.2 The transducer.

This is the part of the sensor that serves to transfer the signal from the output domain of the recognition system to, mostly the electrical domain. Depending on the transduction mechanism used, biosensors can be classified into resonant biosensors, optical detection biosensors, thermal detection biosensors, ion selective field effect transistor biosensors and electrochemical biosensors; each of which is briefly discussed below with special emphasis on electrochemical biosensors which are the major focus in this study.

2.1.3 Types of biosensors

2.1.3.1 Electrochemical biosensors

The underlying principle in this class of biosensors is that many chemical reactions produce or consume ions or electrons which in turn cause some changes in electrical properties of the reaction solution and which can be sensed out and used as a measuring parameter. Based on the electrochemical parameter measured, electrochemical biosensors can further be classified into amperometric, potentiometric, and conductometric or impedimetric biosensors.

2.1.3.1.1 Potentiometric biosensors

The measured parameter in this type of biosensors is the reduction/oxidation (redox) potential of an electrochemical reaction. The principal behind this is that when a ramp voltage is applied to an electrode in solution, the electrochemical reactions cause flow of current. The voltage at which the reaction occurs indicates a particular reaction of a particular species. The

most common potentiometric devices are the pH electrodes. Other devices include ion selective electrodes (F^- , Na^+ , K^+ , NH_4^+ , Ca^{2+} , CN^- , I^-) or gas selective electrodes (CO_2 and NH_3).

2.1.3.1.2 Conductrometric/impedimetric biosensors

The measured parameter in this type of biosensors is the conductance/resistance of a solution. During electrochemical reactions, ions or electrons are either produced or consumed and this causes an overall change in the conductivity of the solution. This change is measured and calibrated to a proper scale.

2.1.3.1.3 Amperometric biosensors

This type of biosensors is based on the measurement of current resulting from electrochemical oxidation or reduction of an electro active species. It is usually performed by maintaining a constant potential at platinum, gold or carbon based working electrode or an array of electrodes with respect to a reference electrode and an auxiliary electrode. The resulting current is directly proportional to the bulk concentration of the electro active species or its production or consumption rate within the adjacent bio catalytic layer. Since bio catalytic reaction rates are often chosen to be first order dependent on the bulk analyte concentration, such steady state currents are usually proportional to the bulk analyte concentration.

Other types of biosensors include resonant biosensors, optical detection biosensors, thermal detection biosensors and ion-selective biosensors. In resonant biosensors, an acoustic wave transducer is coupled with an antibody (bio-element). When the analyte molecules (antigens)

get attached to the membrane, the mass of the membrane changes. This results in a subsequent change in the resonant frequency of the transducer. This frequency change is measured out. The output transduced signal measured in optical detection biosensors is light. The biosensors may be made based on optical diffraction or electrochemilluminence. In optical diffraction based devices, a silicon wafer is coated with a protein via covalent bonds. The wafer is exposed to UV light through a photomask and the antibodies made inactivated in the exposed regions. The diced wafer chips when incubated in analyte, antigen-antibody binding is formed in active regions, thus creating diffraction grating. This grating produces signal when illuminated with a light source such as laser. This signal can be measured or can be further amplified before measurement for improving sensitivity. Thermal detection biosensors are constructed by combining enzymes with temperature sensors. When the analyte comes into contact with the enzyme, the heat reaction of the enzyme is measured and calibrated against the analyte concentration. The ion-selective biosensors are basically composed of semiconductor field effect transistors. When the ions and the semiconductor interact, the surface electrical potential changes which can be measured.

2.2 Enzymes

Enzymes are biocatalysts involved in the performance of metabolic reactions [44]. They are high molecular weight protein compounds, principally made up of amino acid chains linked together by peptide bonds. The catalytic activity of most enzymes is aided by other compounds known as cofactors. The cofactors are mainly co-enzymes, prosthetic groups or metal-ion activators. A coenzyme is a non-protein organic substance which is dialyzable, thermostable and loosely attached to the protein part. A prosthetic group is an organic substance which is dialyzable, thermostable and firmly attached to the protein portion

whereas metal-ion activators include cations such as K^+ , Fe^{2+} , Fe^{3+} , Cu^{2+} , Co^{2+} , Zn^{2+} , Mn^{2+} , Ca^{2+} and Mo^{3+} . Enzymes exhibit specificity relative to the reactions they catalyze and this property makes them important diagnostic and research tools. The specificity of enzymes is however exhibited in four major ways. These are:-

- i. Absolute specificity where the enzyme will catalyze only one type of reaction,
- ii. Group specificity where the enzyme acts only on molecules that have specific functional groups such as amino, phosphate and methyl groups,
- iii. Linkage specificity where the enzyme acts on a particular type of a chemical bond regardless of the rest of the molecular structure and
- iv. Stereochemical specificity where an enzyme will only act on a particular steric or optical isomer. Currently, there exist a large number of enzymes that have been isolated and characterized. These enzymes have been classified according to the type of reaction they catalyze. These groups are shown in table 1.

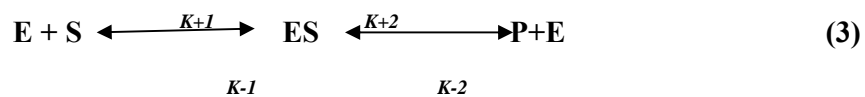
Table 1. Different groups of enzymes.

Group	Type of reaction catalyzed
Lingases	Split C-C, C-O, C-N, C-S and C-halogen bonds without hydrolysis or oxidation. The reaction is usually accompanied by the consumption of a high energy compound such as Adenosine triphosphate (ATP) and

	other nucleoside triphosphates
Lyases	Non-hydrolytically remove groups from their substrates with the concomitant formation of double bonds or alternatively add new groups across double bonds.
Hydrolases	Catalyze cleavage reactions or the reverse fragment condensations. According to the type of bond cleaved, a distinction is made between peptidases, esterases, lipases, glycosidases and phosphatases among others. Examples of this class of enzyme include; cholesterol esterase, alkaline phosphatase and glucoamylase.
Transferases	Transfer C, N, P or S containing groups (alkyl, acyl, aldehyde, amino, phosphate or glucosyl) from one substrate to another. They include transaminases,transketolases, transaldolases and transmethylases
Oxidoreductases	Catalyze oxidation and reduction reactions involving the transfer of hydrogen atoms or electrons. They include <i>Dehydrogenases</i> which catalyse hydrogen transfer from the substrate to a nicotinamide adenine dinucleotide cofactor (NAD ⁺). <i>Oxidases</i> -

	<p>catalyse hydrogen transfer from the substrate to molecular oxygen producing hydrogen peroxide as a by-product</p> <p>Peroxidases - catalyse oxidation of a substrate by hydrogen peroxide. An example of this type of enzyme is horseradish peroxidase which catalyses the oxidation of a number of different reducing substances (dyes, amines, hydroquinones etc.) and the concomitant reduction of hydrogen peroxide</p> <p>Oxygenases - catalyse substrate oxidation by molecular oxygen. The reduced product of the reaction in this case is water and not hydrogen peroxide.</p>
--	---

The catalytic activities of enzymes involve sequential reactions in which an enzyme-substrate (ES) complex is initially formed. This is followed by conversion of the substrate (S) to its corresponding product (P) and the regeneration of a free enzyme (E). This sequential reaction can be illustrated by the equation below,



Where k_{+1} and k_{-1} are the forward and reverse rate constants for the enzyme substrate complex formation whereas k_{+2} and k_{-2} are the forward and reverse rate constants for the reaction involving conversion of substrate to the product.

As mentioned earlier, enzymes were the first biological components to be used in biosensors and still remain by far the most widely used and the best understood in biosensor technology. For instance, biosensors based on the enzyme glucose oxidase have been extensively and successfully been fabricated for the detection of glucose [45-48]. Other enzymes that have been widely studied and used in biosensors include acetylcholine esterase [49], cytochrome p450 [50-54] and horseradish peroxidase [55-59] among others.

In the enzyme based biosensors, the enzyme is retained (immobilized) on the surface of an electrode, mostly a modified electrode while the substrate (analyte) is gradually increased. The signal generated from the catalytic interaction between the enzyme and the substrate is recorded. This implies that the enzyme concentration remains constant while the substrate concentration changes. Under this phenomenon, the reaction velocity increases gradually, and then reaches a maximum when the entire available enzyme is converted to enzyme-substrate complex. The substrate concentration $[S]$ at half of the maximum velocity $\left(\frac{V_{\max}}{2}\right)$ allows for an estimation of Michaelis constant (K_m) which gives information about the activity of the enzyme. The equation for this constant is given as

$$K_m = \frac{K_{+1} + K_{+2}}{K_{-1}} \quad (4)$$

This is also equal to the substrate concentration at half of the maximum velocity. The rate constants K_{+1} , K_{+2} and K_{-1} are as explained in equation (3). A small K_m value indicates that the enzyme requires only a small amount of enzyme to become saturated and therefore the

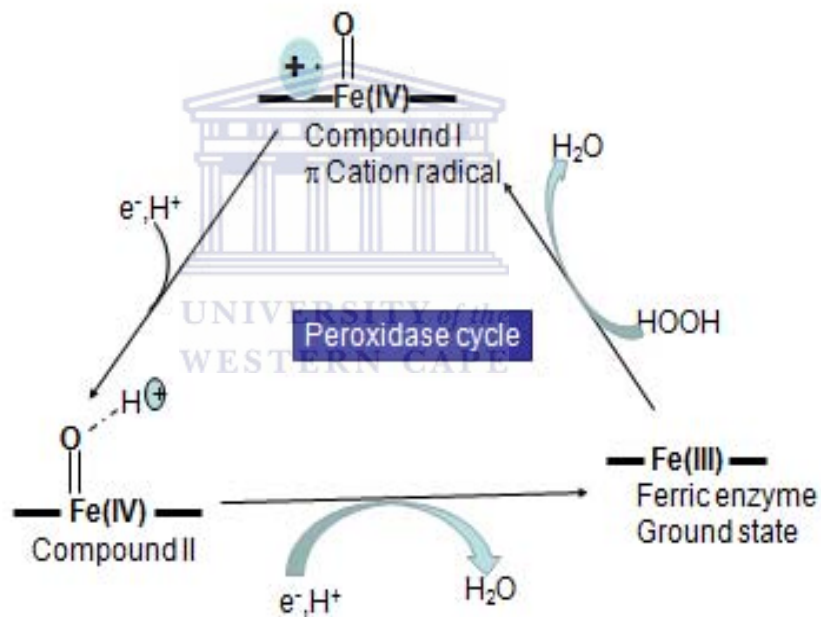
maximum velocity is reached at relatively low substrate concentration. A large K_m indicates that high substrate concentration is needed to achieve maximum reaction velocity. The substrate with the lowest K_m value upon which the enzyme acts as a catalyst is usually assumed to be the enzymes natural substrate. However this is not true for all enzymes.

2.2.1 Horseradish peroxidase (HRP) enzyme

HRP, also known as hydrogen peroxide oxidoreductase, EC-1.11.1.7 is a heme containing glycoprotein [60-61]. It is isolated from the roots of *Amoracia rusticana* and belongs to the ferroporphyrin group of peroxidases. It catalyzes the oxidation of a large number of organic and inorganic substrates by hydrogen peroxide. Like most other enzymes, the catalytic activity of HRP is aided by a cofactor which is iron(III) protoporphyrin IX prosthetic group. The iron(III) centre of HRP has six coordination positions. Four of these positions are occupied by porphyrin nitrogen atoms. The fifth coordination position is occupied by histidine (His-42) which deprotonates the hydrogen peroxide, hence facilitating the formation of HRP-H₂O₂ complex. The sixth position can be occupied by a variety of groups and it is this position that the substrate occupies during the catalytic reaction.

In its catalytic activity, HRP combines with H₂O₂ forming compound I, also designated as HRP-I. This compound is two oxidation equivalents above the resting state of HRP; iron(III). One of these oxidation equivalents is associated with oxoferryl iron(IV) centre ($\text{Fe}^{\text{IV}}=\text{O}$) while the second one is associated with a porphyrin π cation radical. Therefore compound I comprises of the oxoferryl iron(IV) centre and a porphyrin π radical cation. This compound is highly oxidizing and can abstract an electron from a suitable reducing agent to form a second intermediate designated as compound II or HRP-II. The reaction in this step involves an electron gain by the porphyrin π radical cation. Compound II is therefore one oxidation

equivalent above the resting state of HRP and comprises of the oxoferryl iron(IV) centre. This oxoferryl iron(IV) centre acts as the oxidizing species in compound II and can undergo a one-electron gain; regenerating the resting state of HRP. These reactions can be illustrated as shown in scheme 3.



Scheme 3: Catalytic pathway of HRP.

HRP has been applied widely in both mono-enzyme and bi-enzyme biosensors for detection of peroxides [62-64], alcohol, choline and lactase among others [61-63]. It has also been used for detection of its inhibitors [68-69].

2.3 Immobilization methods

Immobilization of enzymes involves retaining the enzymes in functionally active form on the electrode surface or a matrix modified electrode. The immobilization matrix may be a membrane, gels, carbon, graphite, silica and polymeric films among others [1]. The immobilization of these of these protein molecules should be performed under conditions that provide membrane like environment in which all the normal interactions of the proteins are preserved. The method chosen for immobilization of enzymes should therefore prevent loss of enzyme activity by avoiding the change of the chemical nature or reactive groups in the binding site of the enzyme. This calls for a considerable knowledge of the active site of the enzyme to be immobilized. It also implies that there is a need to design electrodes that are compatible with the biological component and that can lead to rapid electron transfer at the electrode surface. Protection of biomolecule's active site may involve incorporation of a protective group; that protects the damage of the active site of the enzyme during attachment to the electrode so long as the protective group can be removed later on without loss of enzyme activity.

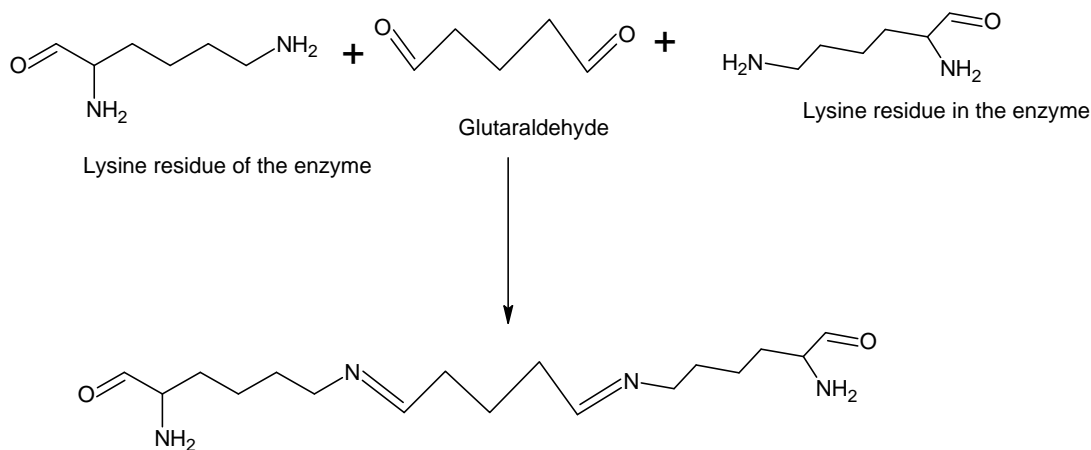
The surface on which the enzyme is immobilized is responsible for retaining the structure of the enzyme through hydrogen bonding or the formation of electron transition complexes. These links will prevent vibration of the enzyme and thus increase thermal stability. The microenvironment of the surface and the enzyme has a charged nature that can cause a shift in the optimum pH of the enzyme up to two units. This may be accompanied by a general

broadening of the pH region in which the enzymes can work effectively allowing enzymes that normally do not have similar regions to work together. Several methods have been proposed, applied and found suitable for retention of the bio molecule on the surface of the electrode. These methods include cross linking, carrier binding, and enzyme entrapping.

2.3.1 Cross linking

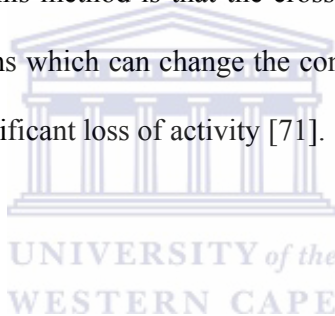
This method involves intermolecular cross-linking of the protein, either to other protein molecules or to functional groups on an insoluble support matrix. Cross-linking an enzyme to itself has been reported to be both expensive and insufficient. This is because; some of the protein material will inevitably be acting mainly as a support. This results in relatively low enzymatic activity. For this reason cross-linking is best used in conjunction with one of the other methods and is used mostly as a means of stabilizing adsorbed enzymes and also for preventing leakage from polyacrylamide gels.

One major advantage of cross linking as a method of immobilizing enzymes is that, very little desorption is likely to occur. This is because the enzyme is covalently linked to the support matrix. Marshall (1973), for example, reported that carbamyl phosphokinase cross-linked to alkyl amine glass with glutaraldehyde lost only 16% of its activity after continuous use in a column at room temperature for fourteen days. Glutaraldehyde is the most common reagent used for cross-linking. Chenghong and Deng, for instance reported successful immobilization of horseradish peroxidase enzyme on glassy carbon electrode using Bovine Serum Albumin (BSA)-Glutaraldehyde matrix crosslinker [70]. During cross linking, glutaraldehyde reacts with lysine residues on the exterior of the proteins (enzyme) as shown in the scheme below.



Scheme 4: Cross linking reactions of glutaraldehyde.

The drawback associated with this method is that the cross linking reactions are carried out under relatively severe conditions which can change the conformation of active centre of the enzyme; and so may lead to significant loss of activity [71].



2.3.2. Carrier-Bonding

This is the oldest immobilization technique for enzymes. In carrier-bonding method, the amount of enzyme bonded to the carrier and the activity after immobilization depend on the nature of the carrier. The selection of the carrier depends on the nature of the enzyme itself, particle size, surface area, molar ratio of hydrophilic to hydrophobic groups and chemical composition. The activity of the immobilized enzymes can generally be boosted by increasing the ratio of hydrophilic groups and in the concentration of bound enzymes. Some of the most commonly used carriers for enzyme immobilization are polysaccharide derivatives such as cellulose, dextran and agarose.

Further subdivisions of carrier bonding occur depending on the bonding mode of the enzyme.

These subdivisions include:

- i. Physical adsorption
- ii. Covalent bonding and
- iii. Ionic bonding

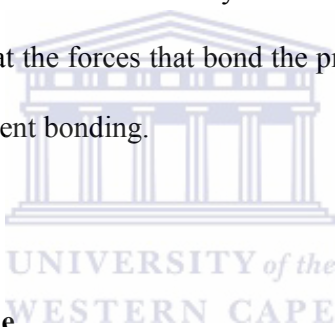
2.3.2.1 Physical adsorption mode

This method for the immobilization of an enzyme is based on the physical adsorption of enzyme protein on the surface of water-insoluble carriers. The main advantages of adsorption as an enzyme immobilization method are: (1) there is little or no conformational change of the enzyme or destruction of its active center, (2) this method can be both simple and cheap, especially if a suitable carrier is found, (3) this method usually requires no reagents and only a minimum of activation steps are required, (4) adsorption tends to be less disruptive to the enzymatic protein than chemical means of attachment. This is because the bonding is mainly by hydrogen bonds, multiple salt linkages, and Van der Waal's forces. In this respect, the method bears the greatest similarity to the situation found in natural biological membranes and has been used to model such systems.

The main disadvantages associated with this method are: (1) the adsorbed enzyme may leak from the carrier during use due to a weak binding force between the enzyme and the carrier, (2) desorption may also result from changes in temperature and pH, (3) non-specific adsorption of other protein substances may occur as the immobilized enzyme is being used. If any of these substances happens to be a substrate to the enzyme, then the enzyme activity towards the target analyte is affected. The rate of enzyme activity will be decreased depending on the surface mobility of the enzyme and the target substrate (analyte).

2.3.2.2 Ionic bonding mode

The ionic bonding method relies on the ionic bonding of the enzyme protein to water-insoluble carriers containing ion-exchange residues. Usual carriers in this method are Polysaccharides and synthetic polymers having ion-exchange centres. The advantages associated with this method are that, there is little change in the conformation and active site of the enzyme. The reason for this is that, the bonding of an enzyme to the carrier is easily carried out, and the conditions are much milder than those needed for the covalent bonding method. For this reason, immobilized enzymes with high activity are obtained with this method. It is however worthy to note that, in substrate solutions of high ionic strength, enzymes may leak from the carrier. The same may be observed if there occurs variation of pH. The reason behind this is that the forces that bond the protein enzymes to the carriers are much weaker than those in covalent bonding.



2.3.2.3 Covalent Bonding Mode

This is the most intensely studied method of the immobilization techniques and it involves the formation of covalent bonds between the enzyme and the support matrix (water-insoluble carriers). Two key factors limit the selection of the type of reaction by which a given protein should be immobilized. One of them involve a bonding reaction such that the conditions under which it is carried do not cause loss of enzymatic activity, and two, the reagents used should preserve the activity of the active site of the enzyme. Several functional groups take part in the bonding of the enzyme to the water-insoluble carriers. These include; amino, carboxyl, hydroxyl, imidazole, phenolic, thiol, threonine and indole groups.

According to the mode of linkage, this method can be further classified into diazo, peptide and alkylation methods. One major challenge of covalent bonding method of enzyme immobilization is that, the conditions for immobilization are much more complicated and less mild than in the cases of physical adsorption and ionic bonding. For this reason, covalent bonding may alter the conformational structure and active centre of the enzyme; therefore resulting in major loss of activity and/or changes of the substrate. However, the bonding forces between enzyme and carrier are strong and guarantees retention of the enzyme to the electrode surface during use as there is no leakage of the enzyme, even in the presence of substrate or solution of high ionic strength.

A thorough understanding of the mode of covalent attachment to a support matrix is necessary. This arises from the fact that, covalent attachment should involve only functional groups of the enzyme that are not essential for catalytic action. It therefore ensures that inactivation reactions with amino acid residues of the active sites are prevented; something that results in higher enzyme activities. Several methods have been devised for prevention of this active site inactivation. They include,

- i. A chemically modified soluble enzyme whose covalent linkage to the matrix is achieved by newly incorporated residues.
- ii. A reversible, covalently linked enzyme-inhibitor complex.
- iii. Covalent attachment of the enzyme in the presence of a competitive inhibitor or substrate. Hence, covalent bonding can be brought about by the forms of bonding shown in table 2.

Table2: Different forms of covalent bonding.

<i>Method</i>	<i>Nature of bonding</i>
Diazotization	SUPPORT--N=N--ENZYME
Amide bond formation	SUPPORT--CO-NH--ENZYME
Alkylation and Arylation	SUPPORT--CH ₂ -NH-ENZYME SUPPORT--CH ₂ -S--ENZYME
Schiff's base formation	SUPPORT--CH=N--ENZYME
Amidation reaction	SUPPORT--CNH-NH--ENZYME
Thiol-Disulfide interchange	SUPPORT--S-S--ENZYME

The nature of bonding in the above given examples ensure a non-hindered active site of the enzyme before, during and after bonding. It also creates a necessary ample space between the enzyme and the backbone.

In order to increase the yield of the immobilized enzyme, the number of reactive residues of an enzyme can be increased. This increased enzyme reactive residues provide alternative reaction sites to those essential for enzymatic activity. The availability of a wide variety of bonding reactions and insoluble carriers; with functional groups either capable of covalent coupling or being activated to give such groups makes this method generally applicable even when little is known about the protein structure of the enzyme to be immobilized. As with cross-linking, covalent bonding should provide stable immobilized enzyme derivatives that do not leach enzyme into the surrounding solution.

2.3.3. Entrapping of enzymes

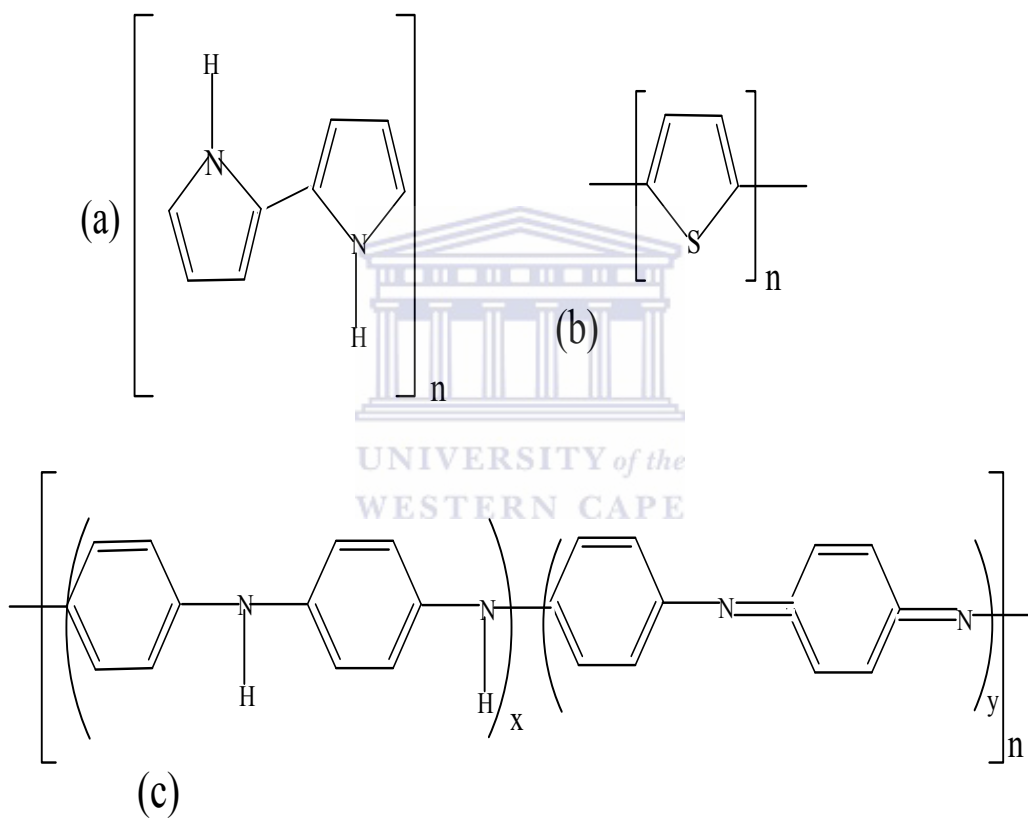
In this method of immobilization, the enzyme is localized within the lattice of a polymer matrix or a membrane. The enzyme immobilization is done in such a way that the protein is retained within the polymer matrix or the membrane while at the same time allowing penetration of the target analyte (substrate). It differs from covalent bonding and cross linking in that, the enzyme itself does not bond to the gel matrix or membrane. Its applicability is therefore wide. However, loss of enzyme activity is likely to occur if this method is employed for its immobilization. This is because, polymerization reactions used in polymer synthesis; both chemical and electrochemical are often carried out under severe conditions. For instance, polyaniline is synthesized for electrochemical purposes under acidic conditions. If not thoroughly washed before immobilization to remove any traces of remaining acid, the immobilized enzyme is likely to lose its activity since acidic conditions are not favorable to working of most enzymes. This calls for careful selection of the most suitable conditions for immobilization of various enzymes.

Entrapment is best achieved when the enzyme is incorporated into conducting polymer films during electrochemical deposition on appropriate electrodes. In this method, a solution of the electropolymerizable monomer and an aqueous buffer containing the enzyme is used for the deposition process [1]. Potentiostatic or galvanostatic mode is then used to electrochemically deposit the polymer film, entrapping the enzyme within it. The main advantage of this method of immobilization is that, the entrapment of enzymes in conducting polymers provides a facile means for ensuring proximity between the active site of the enzyme and the conducting surface of the electrode with considerable potential for biosensor construction. It is however difficult in this method to retain the activity of the enzyme if the polymer film is electrodeposited on the electrode in highly acidic media. This is because, at such a high

acidic media, the enzyme would be denatured and render the enzyme inactive. An example again is polyaniline whose synthesis; either chemically or electrochemically has to be done in acidic media for it to retain its electroactivity as explained above.

2.4 Conducting polymers containing metals (composites).

It has already been pointed out in section 1.1 that enzyme based biosensors rely on mediators to facilitate transfer of electrons. Most previously used enzyme based electrochemical sensors have therefore employed a number of different redox mediators such as monomeric ferrocenes, quinoid-compounds (e.g. benzoquinones), nickel cyclamates, and ruthenium amines among others. For the most part, these redox mediators have had one or more of the following limitations; the solubility of the compound is low, their chemical, light, thermal, or pH stability is poor or they do not exchange electrons rapidly enough with the enzymes or the electrode or both. Additionally, the redox potential of many of these reported redox mediators are so oxidizing that at the potential where the reduced mediator is electro oxidized on the electrode, solution components other than the analyte are also electro oxidized; In other cases, they are so reducing that the solution components such as for example dissolved oxygen are also rapidly electro-reduced. As a result, the sensor utilizing the mediator is not sufficiently specific. Over the years, there has been increasing attempt to synthesize redox mediators that are aimed at addressing the above limitations. Of these mediators, intrinsically conducting polymers have attracted a lot of research attention due to their multiple technological applications. These conducting polymers include polypyrrole, polythiophene and polyaniline (PANI). The structural formulae of each of these conducting polymers are shown in scheme 5 below.



Scheme 5: Structural formulae for the conducting polymers (a) polypyrrole, (b) polythiophene and (c) polyaniline.

Although these polymers can be synthesized chemically, electrochemical synthesis is increasingly becoming a preferred method for preparing electrically conductive polymers [1]. This is because: (1) the electrochemical reactions can be carried out at room temperatures, (2) by varying the potential or the current with time, the thickness of the film can be controlled, (3) electrochemical synthesis can be used to prepare free standing and homogeneous and self doped films, (4) by this method, it is possible to obtain copolymers and graft polymers. During electropolymerization, some monomers such as aniline or pyrrole undergo electrochemical oxidation at a sufficiently high positive (anodic) electrode potential. This leads to formation of cation radicals or other reactive species. Once formed, these species trigger a spontaneous polymerization process which in turn leads to formation of oligomers and/or polymers from the corresponding monomers. Depending on the purpose for which a polymer is formed, a wide range of different structural features of these conducting polymers can be obtained by varying experimental parameters such as monomer concentration, electrolyte used, electrode potential and polymerization time or the number of cycles for cyclic voltammetry. To suit electrical applications, researchers have had to modify the synthesis process of these polymers such that products of high conductivity are obtained. Such attempts have seen the inclusion of metal complexes into the synthesis process such that the polymers formed possess some of the redox properties of the metal complex as well as those of the conducting polymer itself.

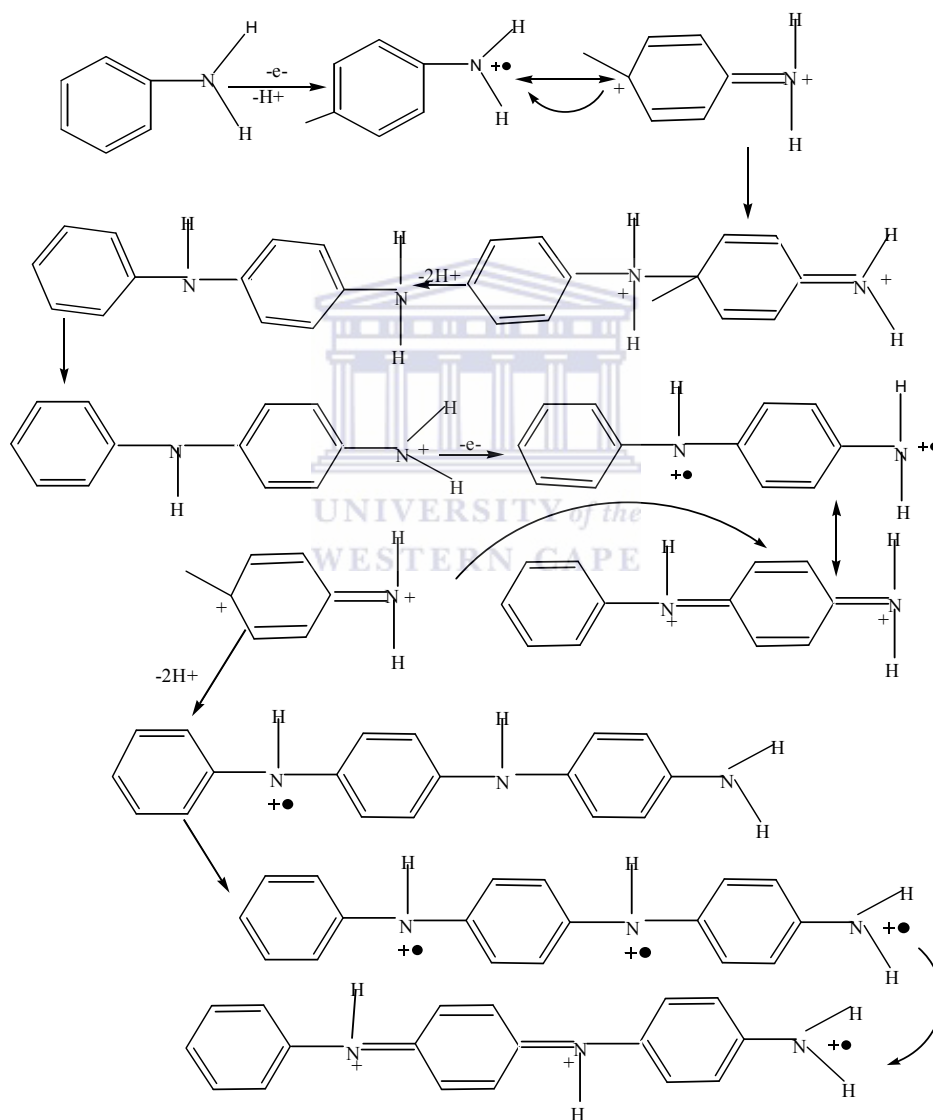
A large number of such polymers have been synthesized and found to be of interest because the electronic, optical, and catalytic properties of the complexes produced are combined in processable form. For instance, conducting electro active polymers containing ferrocenes have been used as (i) ion sensors [72] (ii) biosensors [29], (iii) redox conductors [73], (iv) electroactive Langmuir-Blodgett films [74], (v) free standing redox films [75], (vi) systems for studying monomer adsorption on platinum [76], and (vii) as electro catalysts [77-78].

Generally, metal-containing conducting polymers can be divided into three; the tethered, coupled and incorporated metallopolymers [79]. The tethered metallopolymers have the metal group tethered to the conjugated backbone by a linker moiety such as an alkyl group. The polymer in this type acts as a conductive electrolyte and the metal ions acts in a similar way to the untethered group present in the polymer matrix. In the coupled metallopolymers, the metal is directly coupled to the polymer backbone or to the backbone by a conjugated linker group which makes it easier for the polymer and the metal to affect each other's properties directly. Owing to the redox activity of the conducting polymer backbone and many metal ions, coupled metallopolymers can be electrochemically tuned. In the incorporated metallopolymer, the metal group is directly incorporated into the conjugated backbone. The metal group in this type has the greatest influence on the properties of the conducting polymer.

Several possible methods of synthesizing these co-polymers have been proposed. These include condensation [80], ring open metathesis [81], and electro polymerisation [79]. Tethered and coupled metallopolymers are commonly synthesized by electro polymerisation and often result in insoluble thin films of polymers. Due to their insolubility, electro polymerisation products of tethered and coupled metallopolymers are difficult to characterize because solution methods cannot be used (e.g. accurate molecular weight determination is impossible). This method is however advantageous in that thin films can easily be made alongside control of thickness and morphology via control of the electrochemical parameters such as potential, current density and deposition time. Additionally, the electrochemical properties can be studied in situ, allowing the polymer to be switched from conducting to an insulating state.

2.4.1 Polyaniline

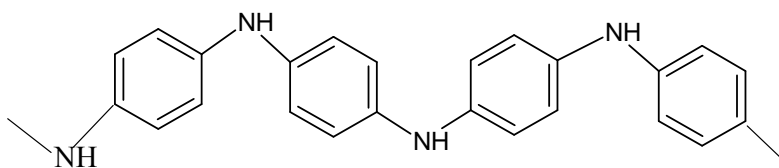
Polyaniline (PANI) is an electroactive polymer obtained by the chemical or electrochemical oxidation of aniline in acidic aqueous and non-aqueous media [82]. The mechanism for electrochemical polymerization of PANI is shown in scheme below.



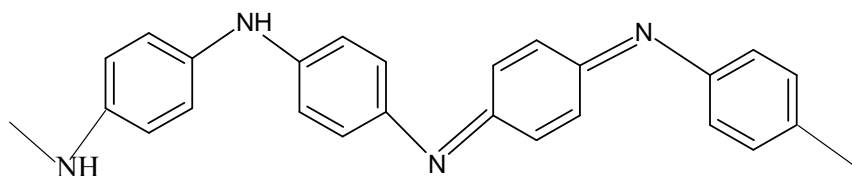
Scheme 6: Aniline to polyaniline electrochemical polymerization mechanism.

The term ‘polyaniline’ refers to a class of polymers consisting of up to 1000 or more *p*-phenyleneimine repeated units [83]. Upon oxidation of leucoemeraldine, iminoquinones in the polymer structure are formed. In acidic solutions, a partially oxidized (emeraldine) form of PANI is obtained. This form of PANI is said to be the most stable and also the most conductive when doped (emeraldine salt) [84]. The fully oxidized form of PANI, poly-*p*-phenylene-iminoquinone is commonly referred to as pernigraniline.

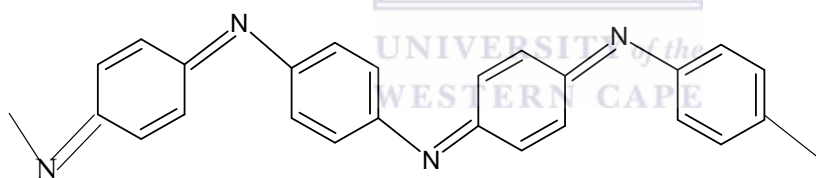




Leucoemeraldine base (fully reduced)



Emeraldine base (partially oxidized)



Pernigraniline base (fully oxidized)

Scheme 7: Different forms of polyaniline

Although polypyrrole polythiophene, polyfuran, polyindole, polycarbazole, polyecetylene and polyphenylene [1] are other previously synthesized conducting polymers, polyaniline has received a lot of research attention in the recent past [84]. This is due to its unique dopability, good redox reversibility, environmental stability, and high electrical conductivity [85-86]. PANI has also been suggested as a potential candidate for numerous electronic applications such as electrochromic displays [87], rechargeable batteries [88] and microelectronic devices [89] among others. Polyaniline based mediated biosensors have also been recently reported [21]. However, the electroactivity of common PANI is restricted to acidic media. To suit its wide applications and more so in biosensors where most biomolecules work best in non-acidic or rather neutral media, the retention of electro activity of polyaniline in these non acidic media is an aspect of concern. Recently, some progress has been reported to address some common drawbacks associated with the synthesis of polyaniline; both chemically and electrochemically. Several composites have been proposed to improve the performance of polyaniline. These recent developments include among others; polyaniline/lignin blends [90], fly ash-polyaniline composites [85], sulfonated polyanilines [91], and polyaniline/poly (*o*-aminophenol) composites [84].

2.4.2 Ferrocenium hexafluorophosphate

Ferrocenium hexafluorophosphate (FcPF₆) is a derivative of ferrocenes, a class of compounds having a central iron cation (Fe²⁺) sandwiched between two cyclopentadienyl (Cp) rings. The central metal iron (II) in ferrocenes is known to undergo a one electron transfer, forming ferricinium ions. This ferrocenium/ferricinium transition involves a fast electron transfer [92]. The heterogeneous electron transfer kinetics and the redox potential of ferrocenes have been extensively studied and established in most organic solvents [93].

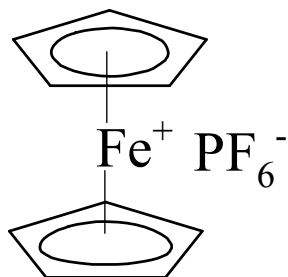


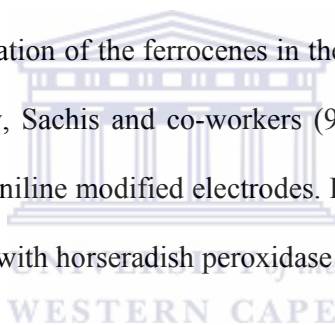
Figure 1: Structure of ferrocenium hexafluorophosphate.

However, the electrochemistry of ferrocenes has not been extensively studied in aqueous solvents. This is due to its very low solubility and lack of good reversibility in aqueous solvents [92].

Ferrocenes have been used as electron transfer mediators in organic phase amperometric biosensors. Their use in biosensors was introduced for the first time for the detection of glucose [45] after it had been claimed as an effective regenerator of the enzyme glucose oxidase [94]. Although the redox behaviour of ferrocenes in organic solvents is good, its application as a redox mediator in biosensors is always met with challenges. This is due to the fact that organic solvents and more so the polar organic solvents are known to strip the biomolecules especially enzymes of their active site water molecule which is highly essential for the enzyme activity [95-96]. To overcome this, researchers have had to mix the organic solvent with water at an appropriate ration. This ensures the solubility and hence redox activity of the ferrocene is guaranteed and that the enzyme activity is maintained.

Ferrocenes have also been used as copolymers in conductive polymers to stabilize and improve the redox properties of such polymers. For instance, the incorporation of ferrocenes

into polypyrrole and polythiophene polymers has been found to have interesting and advantageous features. Firstly, the oxidation of ferrocenes to ferricinium ions has been found to hinder further polymerization of poly (3-substituted pyrrole) [76]. This implies that ferrocenes and its derivatives reduce the rate of polymerization, and therefore their inclusion in the polymerization solution can be used to control the growth of polymer layer thus forming a thin layer on the electrode surface. Secondly, even though no redox conduction is known to occur between the polymer backbone and the ferrocenes, oxidation of ferrocenes groups in the solution can occur by electrons hopping from the ferrocenes groups in the solutions to the ferrocenes groups in the polymer and then directly to the anode [76]. This can be used to form nanostructured materials. Also the expression of ferrocenes in the polymer formed depends on the concentration of the ferrocenes in the polymerization solution and the thickness of the films. Recently, Sachis and co-workers (92) reported strong adsorption of ferrocenium on sulfonated polyaniline modified electrodes. However, the use of ferrocenium-polyaniline modified electrodes with horseradish peroxidase has not been reported.



2.4.3 Characterization methods.

2.4.3.1 Cyclic voltammetry.

Cyclic voltammetry (CV) is an electrolytic method that uses microelectrodes and an unstirred solution so that measured current is limited by analyte diffusion at the electrode surface. It has become an important and widely used electrochemical technique in many areas of chemistry. Although cyclic voltammetry is sometimes for quantitative analysis of samples, it is majorly used for the study of redox processes, for understanding reaction intermediates as well as for obtaining the stability of reaction products. The technique works by varying some applied potential at a working electrode at some scan rate in both forward and reverse directions while monitoring the current. The initial scan can, for instance be negative to the switching potential, in which case if the scan is reversed; it runs in the positive direction. A full cycle, partial cycle or a series of cycles can be performed depending on the analysis targeted. Important parameters are usually obtained from cyclic voltammograms for analysis of redox properties and properties of an electroactive sample. These parameters include anodic and cathodic peak potentials ($E_{p,a}$ and $E_{p,c}$ respectively) as well as anodic and cathodic peak currents ($i_{p,a}$ and $i_{p,c}$ respectively). A typical cyclic voltammogram illustrating these parameters is shown in figure 2 below.

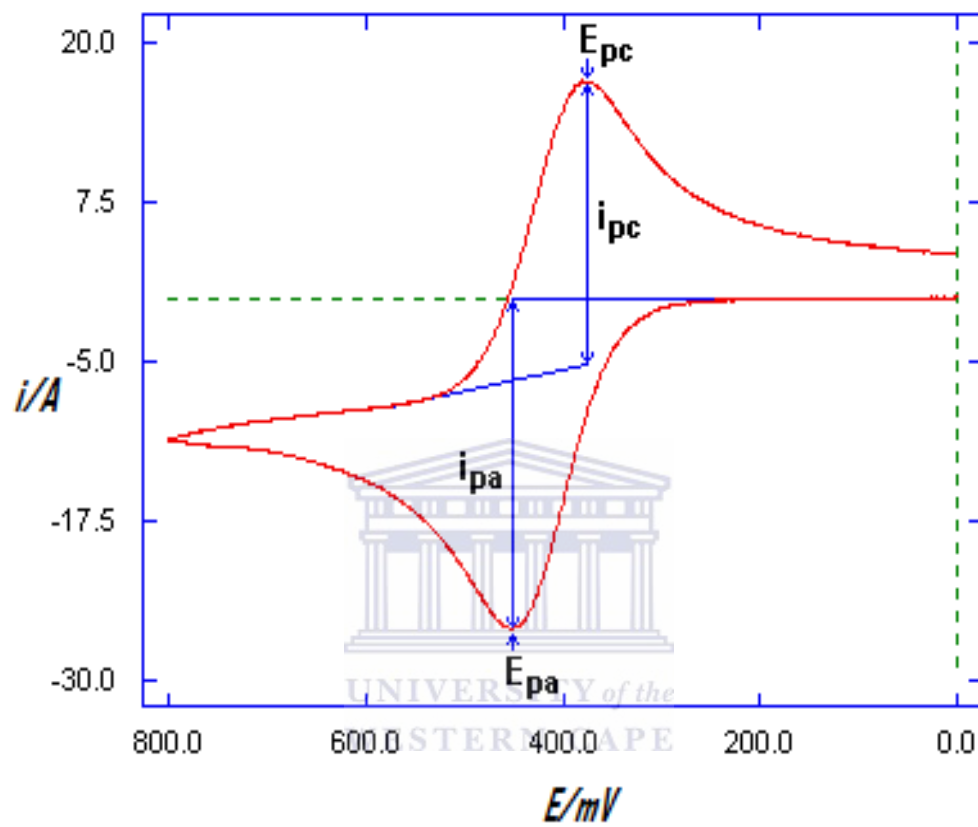
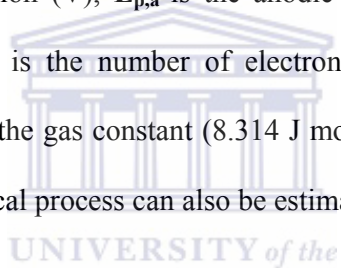


Figure 2: A typical cyclic voltammogram showing the basic peak parameters, $E_{p,a}$, $E_{p,c}$, $i_{p,a}$ and $i_{p,c}$

Important information about the sample under investigation can be obtained from the peak parameters. This includes whether the electrochemical process displayed by the sample is reversible, irreversible or quasi-reversible. It also gives an insight into how fast the electron transfer process is, relative to other processes such as diffusion. For instance, if the electron transfer is fast relative to the diffusion of electroactive species from the bulk solution of the surface of the electrode, the reaction is said to be electrochemically reversible and the peak separation (ΔE_p) is given by equation 5 below.

$$\Delta E_p = |E_{p,a} - E_{p,c}| = 2.230 \frac{RT}{nF} \quad (5)$$

Where ΔE_p is the peak separation (V), $E_{p,a}$ is the anodic peak potential (V), $E_{p,c}$ is the cathodic peak potential (V), n is the number of electrons transferred, F is the Faraday constant (96,584 C mol⁻¹), R is the gas constant (8.314 J mol⁻¹K⁻¹). The number of electrons (n) involved in the electrochemical process can also be estimated from the equation above.



Several voltammograms performed at different scan rates can lead to preparation of several linear plots whose slopes could give further information about the redox properties of the sample in question. For instance, when the peak current is plotted against the square root of the scan rate, the slope of the linear plot can be used to estimate the diffusion coefficient according to the Randles-Sevcik equation 6 shown below

$$i_p = 2.86 \times 10^5 n^{3/2} A C_0 D^{1/2} \nu^{1/2} \quad (6)$$

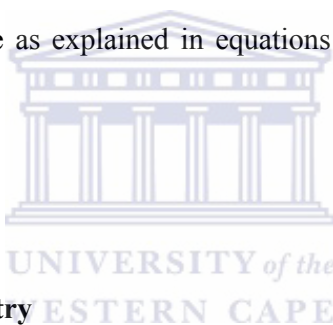
Where i_p is the peak current (A), ν is the rate at which the potential is swept (V / sec), F is Faraday's constant (96485 C / mol), A is the electrode area (cm²), R is the universal gas constant (8.314 J / mol K), T is the absolute temperature (K), and D is the analyte's diffusion coefficient (cm²/sec) and C is the concentration of the analyte. When plotted, the log of peak

current versus the log of scan rate gives a linear plot whose slope distinguishes between diffusion controlled peaks, adsorption controlled peaks or even a mixture of the two.

In some cases, the sample to be characterized may be deposited on the surface of a working electrode (chemically modified electrodes). It is usually important to estimate the surface concentration of the adsorbed material. In such cases, a plot of peak current versus scan rate would be of great importance in estimating the surface area of the adsorbed species, in accordance with Brown-Anson model using the equation 7.

$$\frac{i_p}{\nu} = \frac{n^2 F^2 A \Gamma_{adsorbed\ species}}{4RT} \quad (7)$$

Where i_p , n , F , A , R and T are as explained in equations 5 and 6 and $\Gamma_{adsorbed\ species}$ is the electrode modifier.



2.4.3.2 Square wave voltammetry

Square wave voltammetry (SWV) has proved to be a suitable method to investigate redox reactions with overlapping waves. The excitation signal in SWV consists of a symmetrical square wave pulse of amplitude superimposed on staircase wave form of step height ΔE . The forward pulse coincides with the staircase step. A typical square wave voltammogram is shown in figure 3 below.

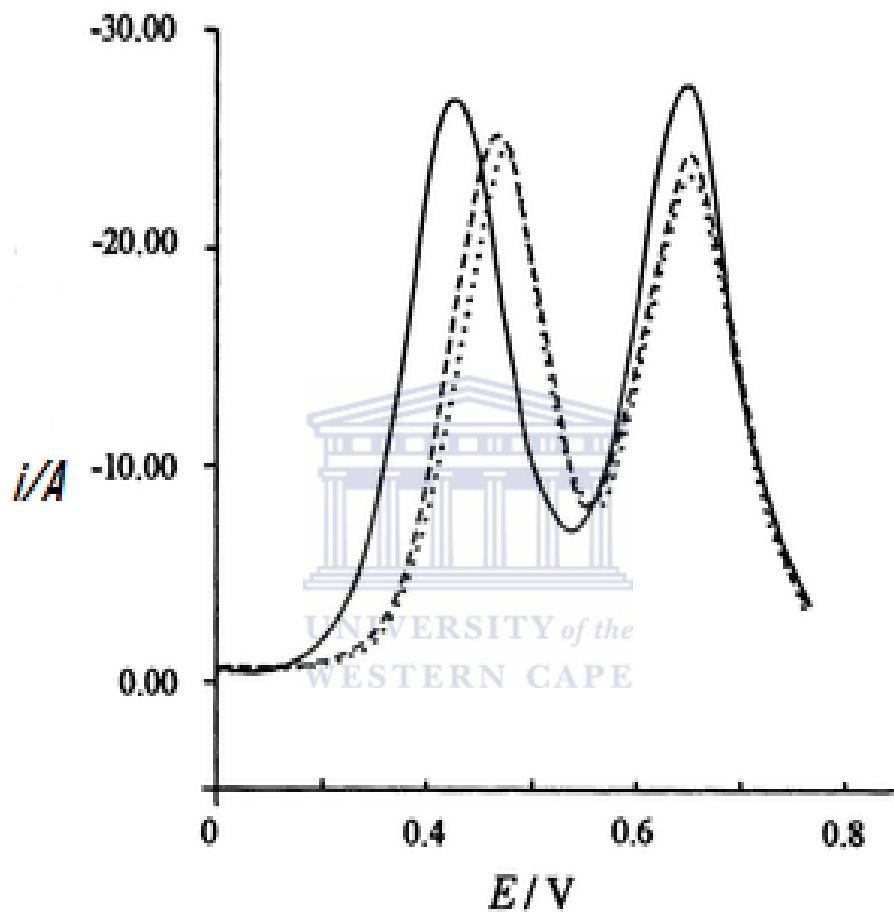
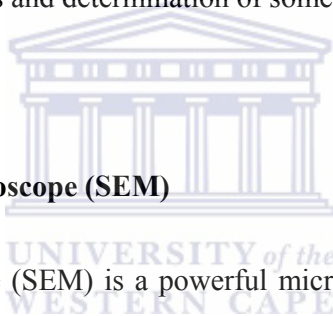


Figure 3: A typical square wave voltammogram.

The net current (i_{net}) is obtained by taking the difference between the forward and the reverse currents ($i_{\text{fwd}}-i_{\text{rev}}$) and is centred on the redox potential. In SWV, the peak height is directly proportional to the concentration of the electroactive species and direct detection limit as low as 10^{-8} M is possible.

SWV is associated with some advantages over cyclic voltammetry. These advantages include excellent sensitivity and rejection of back ground currents. The scanning speed in SWV is also high. This high speed coupled with computer control and signal averaging allows for experiments to be performed repetitively and increases the signal to noise ratio. SWV is also applied in study of electrode kinetics with regard to preceding, following or catalytic homogeneous chemical reactions and determination of some species at trace levels.



2.4.3.3 Scanning electron microscope (SEM)

A scanning electron microscope (SEM) is a powerful microscope that uses electrons rather than light to form an image of objects such as fractured metal components, foreign particles and residues, polymers, electronic components and biological samples among others. It uses a focused beam of high energy electrons to generate a variety of signals at the surface of solid specimens. The signals derive from electron-sample interaction and reveal information about the sample including external morphology (texture), chemical composition, crystalline structure and orientation of materials making up the sample. The advantages associated with SEM include among others its ability to perform analyses of selected point locations on the sample. Areas ranging from approximately 1 cm to 5 microns can also be imaged in a scanning mode using conventional SEM techniques (magnification ranging from 20X to approximately 30,000X and a spatial resolution of 50 to 100 nm). Coupled with energy dispersive spectroscopy (EDS), information about the atomic composition of the compound

under investigation is obtained. Furthermore, the data collected from selected area of the surface of the sample generates a 2-dimensional image which displays spatial variation of the sample properties.



Chapter 3

3.0 Experimental

3.1 Instrumentation

All electrochemical experiments were carried using a BAS100W integrated and automated electrochemical work station from Bio Analytical Systems (BAS), Lafayette, USA+. Hydrodynamic amperograms and voltammograms; both cyclic and square wave, were recorded with a computer interfaced to the BAS 100W electrochemical workstation. A 3 mL electrochemical cell with a conventional three electrode set up was used. The electrodes were: (1) GC working electrode ($A = 0.071 \text{ cm}^2$) from BAS modified with Pani-FcPF₆, (2) platinum wire, from Sigma Aldrich, South Africa acted as a counter electrode and (3) Ag/AgCl (3 M KCl) from BAS was the reference electrode. Screen printed carbon electrodes (SPEs) with a surface area of 0.09 cm^2 ; previously donated by National Centre for Sensor Research, Dublin City University, Ireland were used as working electrodes to prepare the composite materials for SEM analysis. The SEM images of gold sputtered samples were taken using the JEOL JSM-7500F Scanning Electron Microscope from USA. Alumina micropolish and polishing pads were obtained from Buehler, IL, USA and were used for polishing the GCE.

3.2 Reagents

The reagents used in this study included: aniline (99%), hydrogen peroxide (32%), ferrocenium hexafluorophosphate, Hydrochloric acid (30%), sodium dihydrogen phosphate, disodium hydrogen phosphate, glutaraldehyde (50 wt % sol in water), which in this work will be abbreviated as “Glu”, bovine serum albumin (BSA) sulphuric acid and polyvinyl sulfonic

acid. They were all purchased from Sigma-Aldrich and were of analytical grade. The enzyme horseradish peroxidase (EC 1.11.1.7 type II from horse radish containing 150-250 units mg^{-1}) was used for biosensor preparation. Phosphate buffer solution (PBS), 0.1 M and pH 7.0 was prepared from anhydrous disodium hydrogen phosphate and sodium dihydrogen phosphate monohydrate. This was used as the solvent for preparation of HRP enzyme and BSA solutions. Deionized water; previously prepared by passing distilled water through milli-QTM water purification system (Millipore) was used for preparation of the PBS. Aniline was vacuum-distilled before use and analytical grade argon (Afrox, South Africa) was used to degas the system.

3.3 Preparation of Pani-FcPF₆ nano-composites

Before each experiment, the GCE was thoroughly polished in 1.0, 0.3, and 0.05 μm slurries of alumina respectively and rinsing with de-ionized water after each polishing step. This was followed by ultrasonication for 5 min. The polymerization solution contained 0.02 M FcPF₆, 0.2 M aniline per 1 M HCl and 1 mL of poly(vinyl sulfonic acid sodium salt)- PVSNa. The total volume of this solution was 5 mL. Before applying potential, the solution was degassed by bubbling argon gas through for 8 min and then maintained oxygen free by keeping a blanket of argon above the solution. The potential was then cycled from -100 mV to +1000 mV at 100 mV s^{-1} scan rate for 10 cycles. It is during this process that Pani-FcPF₆ nano-composites were electrodeposited on the surface of the electrode. The electrode was then removed from the solution, washed thoroughly in de-ionized water to remove traces of monomers and HCl and kept in readiness for either characterization or enzyme immobilization.

3.4 Characterization of the Pani-FcPF₆ nano-composites

3.4.1 Electrochemical characterization.

A three electrode system, same as that used for electrodeposition of the nano-composites was used in this characterization. The characterization solution contained 3 mL of 1 M HCl. The Pani-FcPF₆ modified GCE was anodically scanned from -100 mV to +1000 mV at scan rates 10, 20, 30, 40, 50, 60, 70, 80, 90, and 100 mV s⁻¹. In these scan rates; the cyclic voltammetry was performed for only one cycle.

3.4.2 Scanning Electron microscopy (SEM).

The procedure for preparation of the Pani-FcPF₆ nano-composite materials for SEM analysis was similar to that described in sec. 3.3. However, screen printed carbon electrode were used as the working electrode instead of the GCE. Pre-treatment of the screen printed electrodes involved repeated potential scanning in 0.2 M H₂SO₄ in the potential range of -1200 mV to +1500 mV at a scan rate of 100 mV s⁻¹ until reproducible voltammograms were obtained. After electrodeposition, the Pani-FcPF₆ modified electrodes were thoroughly washed in deionised water and kept in sealed Petri dish containers in readiness for SEM analysis. The SEM analysis was performed on a JEOL JSM-7500F Scanning Electron Microscope. Micrographs were obtained for samples of the composites on SPEs; mounted on aluminium stubs using conductive glue and coated with a thin layer of gold.

3.5 Fabrication of the biosensor

The enzyme solution was prepared as follows. 3 mg of horseradish peroxidase enzyme was dissolved in 120 μL of PBS pH 7.0 containing 4 mg of BSA per 100 μL of the buffer. 10 μL of this enzyme solution was added to 4 μL of 2.5% glutaraldehyde and thoroughly mixed. 5 μL of the resulting solution was placed on the GCE/Pani-FcPF₆ surface and allowed to dry. The GCE/Pani-FcPF₆/HRP electrode hereby referred to as the enzyme electrode or biosensor was kept in the working buffer at 4° C when not in use.

3.5.1 Illustrating the necessity of (HRP) in the biosensor.

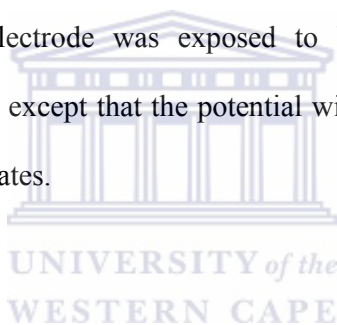
The aim of this part was to determine whether or not, the HRP was necessary for detection of hydrogen peroxide. It was also aimed at evaluating possible response effects emanating from BSA or Glu or both. Freshly prepared electrodes which included Pani-FcPF₆/Glu/BSA/HRP, Pani-FcPF₆, Pani-FcPF₆/Glu and Pani-FcPF₆/Glu/BSA were used in this part. 5 mmol L⁻¹ of the standard hydrogen peroxide was prepared in the working buffer and used as the analyte. The cell for electrocatalytic reduction of hydrogen peroxide consisted of the enzyme electrode, platinum counter electrode and Ag/AgCl (3 M KCl) reference electrode. A 3 mL test solution consisting of PBS pH 7.0 was degassed with argon before the experiment and after each successive addition of small amounts (5 μL) of 5 mmol L⁻¹ hydrogen peroxide. A blanket of argon was also kept during the experiment to maintain an oxygen free solution. Each of the freshly prepared electrodes subjected to voltammetric measurements without, and with successive additions of 5 μL of 5 mmol L⁻¹ H₂O₂ in 3 mL of PBS, pH 7.0. A multiscan of voltammograms obtained from a bare enzyme electrode the 20th μL of H₂O₂ of each of the other four electrodes was used to evaluate the necessity of HRP in this study.

3.5.2 Choice of potential window.

A freshly prepared enzyme electrode was used in this part. The cell set up was as described in section 3.5.1 above. Cyclic voltammetric measurements were performed on the enzyme electrode in 3 ml of PBS, pH 7.0 with successive additions of 5 μL of 5 mmol L^{-1} H_2O_2 at different potential windows.

3.5.3 Choice of scan rate.

A freshly prepared enzyme electrode was exposed to Voltammetric measurements as described in section 3.5.2 above except that the potential window was held constant at +200 to -700 mV while varying scan rates.

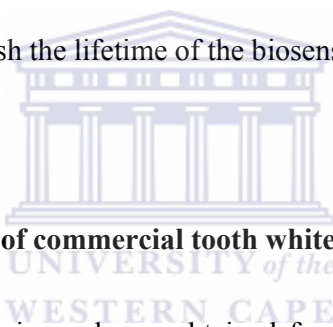


3.6 Biosensor measurements.

3.6.1 Preparation and analysis of standard hydrogen peroxide

5 mmol L^{-1} of the standard hydrogen peroxide was prepared in the working buffer and kept for biosensor measurements. The cell for electrocatalytic reduction of hydrogen peroxide was as described in section 3.5.1. Degassing with argon prior to measurements and continuous flow of the same gas above the solution during the experiment was also observed. Both cyclic voltammetry and square wave voltammetry were used for the characterization of enzyme electrode. This was done in order to determine the response of the biosensor to H_2O_2 and the potential at which any generated signal would be detected for further steady state amperometric measurements. After being established that H_2O_2 was catalytically reduced at -

400 mV, amperometric measurement was made at this constant potential. This was achieved as follows. The degassed 3 mL of the working buffer was excited at a constant potential of -400 mV. The current was initially allowed to attain a steady state. The first 5 μL of 5 mmol L^{-1} hydrogen peroxide was then injected into the cell. The increase in the catalytic current was then monitored, allowed to attain steady state, then followed by another addition of 5 μL of 5 mmol L^{-1} hydrogen peroxide. This was repeated until no further increase in catalytic current was observed after addition of hydrogen peroxide. Besides keeping the solution oxygen free by use of argon, the solution was also constantly stirred at 300 rotations per minute (300 rpm) using a magnetic stirrer. After each biosensor experiment, the electrode was washed in de-ionized water and kept in the working buffer at 4°C for successive measurements in order to establish the lifetime of the biosensor.



3.6.2 Preparation and analysis of commercial tooth whiteners.

The DAYWHITE® tooth whitening gel was obtained from a cosmetic dentist at Intercare medical and dental centre in Cape Town, South Africa. During its pretreatment, DAYWHITE® tooth whitening gel was diluted in 0.1 M PBS, pH 7.0 under stirring until complete dilution. It was further diluted with the same buffer to 5 mL and left for three (3) hours to equilibrate and attain homogeneity. No further treatment was necessary. Both SWV and steady state amperometric techniques were used to monitor the increase in catalytic after injection of small amounts of this solution as described in sec. 3.6.1 above.

The Colgate Plax Whitening Blancheua, abbreviated in this study as CPWB was obtained as an over-the-counter product in Cape Town, South Africa. This product was used as received, that is, no pre-treatment was carried out. This was because; the product was received in liquid form, a form that allowed for pipetting and eventual injection into the cell solution. Both

SWV and steady state amperometric techniques were used to monitor the current response upon addition of small amounts (5 μL) of the analyte.

3.7 Interference studies.

Several substances suspected to interfere with the detection of hydrogen peroxide by the developed biosensor were investigated. They included glucose, acetic acid and ethanol. Special attention was paid to ethanol because it was present in CPWB; one of the commercial tooth whitening products investigated in this study. Solutions containing 3 mmol L^{-1} of each of these substances were prepared. Each solution was mixed with a similar concentration of hydrogen peroxide at a ratio of 1:1. SWV was carried out on each of the resulting mixtures. The catalytic current emanating from each of these solutions was compared to that of a similar concentration of standard hydrogen peroxide alone at the 20th μL addition. Expressed as a ratio of $I(\text{H}_2\text{O}_2)/I(\text{H}_2\text{O}_2+\text{suspected interference})$, the value obtained was used to assess the level of possible interference by each investigated substance.

RESULTS AND DISCUSSION



UNIVERSITY *of the*
WESTERN CAPE

Chapter 4.

4.0 Results and discussion 1

4.1 The Pani-FcPF₆ nano-composites

Pani-FcPF₆ nano-composites were electrochemically deposited on the GCE in acidic media by sweeping the potential from -100 mV to +1000 mV at 100 mV s⁻¹. The electropolymerization voltammograms in figures 4 and 5 show increasing current amplitude as the cycles increase. This is an indication of deposition of a conducting polymer on the surface of the electrode. A close analysis of the peaks in the first and subsequent cycles in the anodic scan shows that the peaks in the first cycle occur at potentials more positive than in the subsequent cycles. For instance, the innermost peak in d of the first scan occurs at 900 mV whereas the subsequent peaks are observed at 780 mV. This results from the initial nucleation of aniline during the first anodic scan. In the subsequent scans, the catalytic effect of polyaniline causes oxidation at much lower potentials and results in deposition of polymer on the electrode surface. Electropolymerization of PANI has been observed to show three redox peaks. These peaks are clearly seen in figure 5 for polyaniline in acidic media. In Pani-FcPF₆, four redox peaks were observed. Of particular interest was the redox peak b/b' (b' at 220 mV and b at 350 mV) because it showed relatively strong intensity in figure 4 but was not observed in figure 5. Moreover, when different concentrations of FcPF₆ were incorporated into the polymerization solution, it was observed that the intensity of the peak b/b' increased with increasing concentration of FcPF₆. For instance with a 0.01 M FcPF₆ in the polymerization solution (Ref. Appendix A), the peak b' almost becomes invisible whereas peak b disappears completely. The intensities of the other redox peaks, a/a', c/c', and d/d' were not affected by changes in the concentration of the FcPF₆ in the polymerization solution. It was further observed that, when the polymerization voltammograms of

polyaniline and poly(aniline-ferrocenium hexafluorophosphate) were compared, the inclusion of FcPF_6 in the polymerization solution did not shift the redox peaks for polyaniline to either lower or higher potentials. However, the current amplitude in the electro polymerization Pani-FcPF_6 was observed to be higher than that of PANI. This was an indication that the Pani-FcPF_6 composites formed were more conducting than the polyaniline. The redox peak b/b' was therefore associated with $[\text{FcPF}_6]^+ / [\text{FcPF}_6]$ reactions. To further confirm this, cyclic voltammetry was performed on 0.02 M FcPF_6 in 1 M HCl and voltammograms for this experiment are shown in figure 6. It is evident from this figure that the redox couple b/b' occurs at the same potentials as those observed in figure 2 (b' at 220 mV and b at 350 mV).



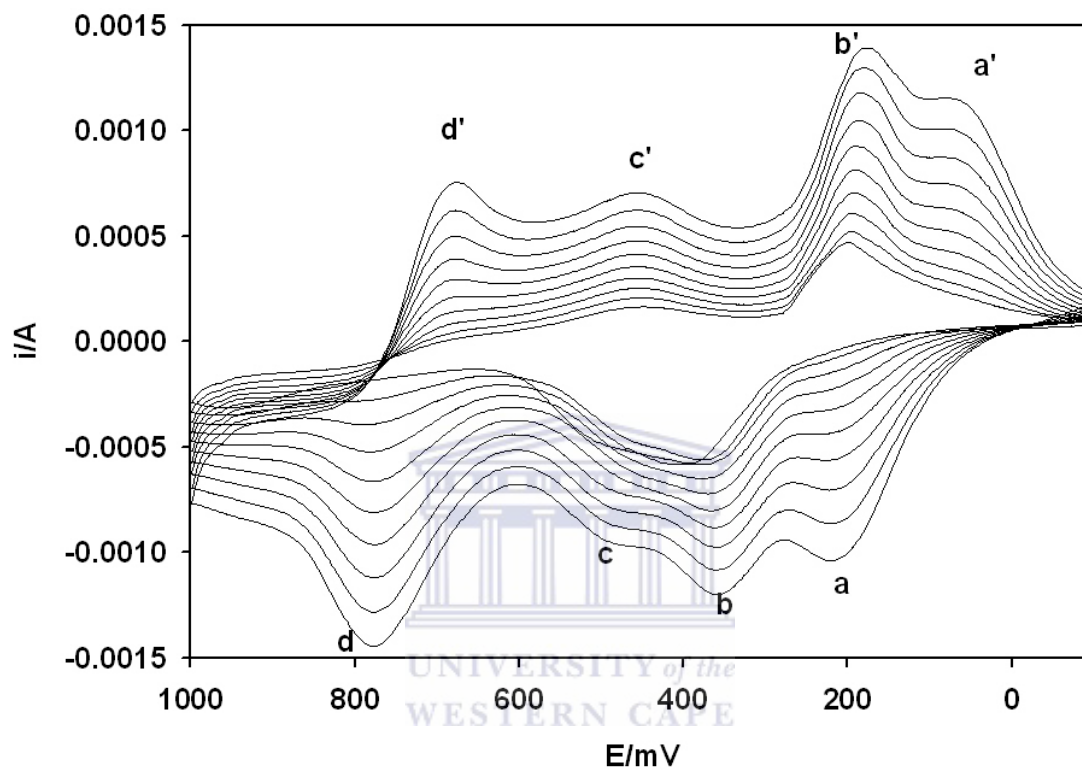


Figure 4: Voltammograms for the electropolymerization of poly(aniline-ferrocenium hexafluorophosphate) nano-composites in 1 M HCl at a scan rate of 100 mV s^{-1} .

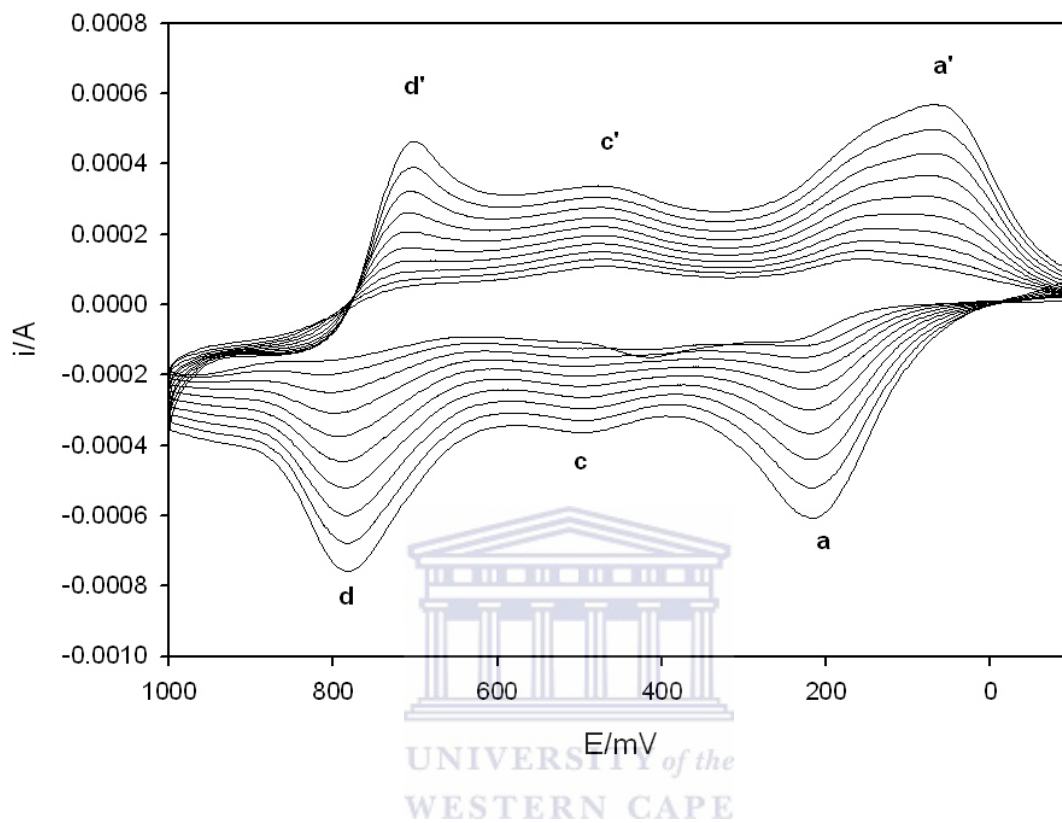


Figure 5: Voltammograms for electropolymerization of polyaniline in 1 M HCl, initial potential: -100 mV; scan rate 100 mV s^{-1} .

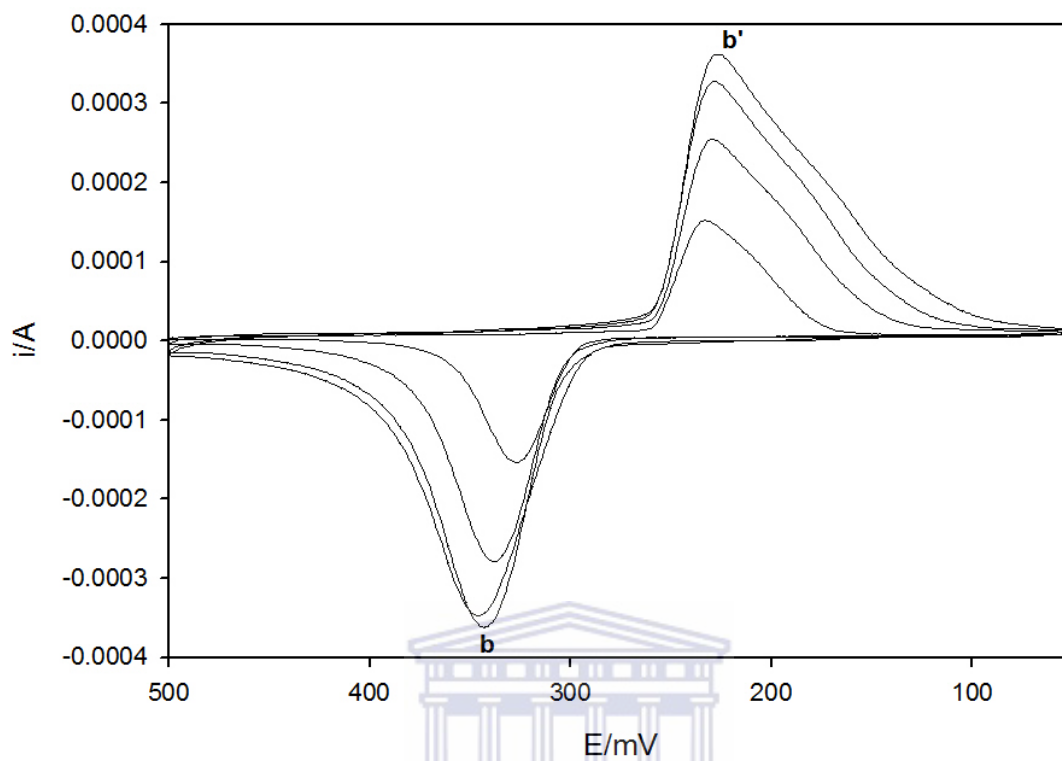
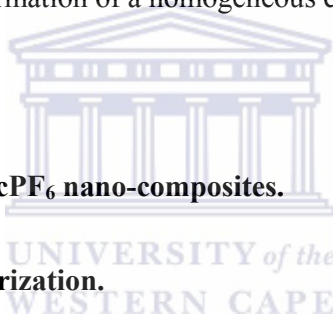


Figure 6: Voltammograms of 0.02 M FcPF₆ in 1 M HCl, initial potential: -100 mV, scan rates: 20, 50, 80 and 100 mV s⁻¹

The other redox couples a/a' , c/c' and d/d' in figure 4 corresponds to those observed in figure 5 and are characteristic peaks of polyaniline. They have previously been assigned redox processes as follows; (i) a/a' – Leucoemeraldine radical cation/leucoemeraldine transition; (ii) c/c' - Emeraldine/emeraldine radical cation; and (iii) d/d' – Pernigraniline/pernigraniline radical cation [84].

As discussed in section 1.0, no redox conduction occurs between the polymer backbone and the ferrocenes, In this study however, oxidation of ferrocenes groups in the solution occurred by electrons hopping from the ferrocenes groups in the solutions to the ferrocenes groups in the polymer and then directly to the anode. In the process, $FcPF_6$ groups were trapped within the polymer matrix leading to formation of a homogeneous composite.



4.2 Characterization of Pani- $FcPF_6$ nano-composites.

4.2.1 Electrochemical characterization.

From figure 7, it is evident that both leucoemeraldine radical cation/leucoemeraldine (a/a') and Pernigraniline/pernigraniline radical cation (d/d' , d'') transitions are highly expressed. The redox peak due to emeraldine/ emeraldine radical cation transition observed during polymerization was almost invisible. However a broad anodic peak was observed between 300 mV and 500 mV. The peaks d' and d'' were observed at scan rates greater than 10 mV s^{-1} . At scan rates lower than 10 mV s^{-1} (voltammograms not shown), only a single peak instead of two was observed. It was therefore concluded that, at around 600 mV, the Pernigraniline/pernigraniline radical cation transition involved a multi-electron transfer process in which case gaining of the second electron in the cathodic scan was a slow process compared to the gaining of the first one.

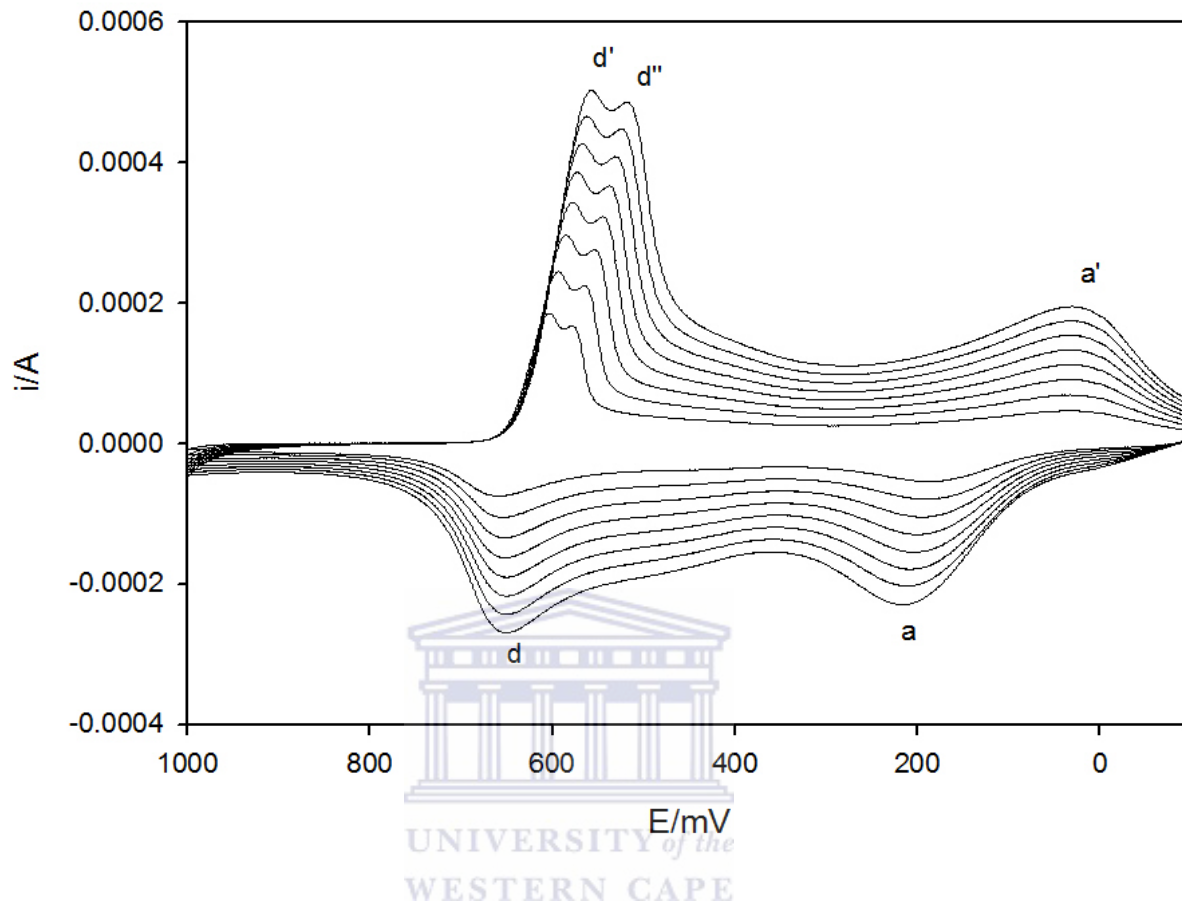


Figure 7: Multiscan voltammograms of Pani-FcPF₆ characterization in 1 M HCl at different scan rates (20 to 90 $mV s^{-1}$ in steps of 10 $mV s^{-1}$). Initial potential: -100 mV.

Although the peak due to FcPF_6 was not expressed in the above characterization, cyclic voltammograms of the composite taken with in a wider potential window (-1300 mV to +1300 mV) in PBS, pH 7.0, showed a redox peak; characteristic of $\text{FcPF}_6^+/\text{FcPF}_6$ [Ref. Appendix E].

In order to understand the nature of reactions influencing each peak in figure 7, several plots were prepared. The plots; root of scan rate versus peak current scan rate versus peak current and log scan rate versus log peak current are; one shown in figure 8 and the rest in appendix B. However, the major characteristic features of all the plots are shown in table 3.



Table 3: The slopes and correlation coefficients for various plots of peaks a, a', d, and d'

		Root scan rate <i>versus</i> peak current	Scan rate <i>versus</i> peak current	Log of scan rate <i>versus</i> log of peak current
Peak a	Slope	-6.1822×10^{-4}	-1.183×10^{-3}	0.738
	r^2	0.9892	0.9943	0.9938
Peak a'	Slope	4.3636×10^{-4}	8.325×10^{-4}	0.6477
	r^2	0.9998	0.9990	0.9999
Peak d	Slope	-4.255×10^{-5}	-8.000×10^{-5}	0.7300
	r^2	0.8488	0.8237	0.8656
Peak d'	Slope	2.0718×10^{-3}	3.952×10^{-3}	0.8590
	r^2	0.9999	0.9988	0.9997

All plots had a non-zero intercept. The slopes of plots of $\log v$ versus $\log i$ have been used to identify diffusion controlled or adsorption controlled peaks or even a mixture of the two. In such plots, a slope of 1 indicates an adsorption controlled peak, 0.5 indicates a diffusion controlled peak while intermediate values indicate mixed diffusion/adsorption controlled peaks [97]. In this study, all plots of $\log v$ versus $\log i$ gave intermediate slopes between 0.5 and 1. This is an indication that Pani-FcPF₆ film exhibits both diffusion and adsorbed electrochemistry. First, adsorption behaviour is observed because, the film being deposited on the GCE undergoes electrochemical reactions on the electrode or polymer film surface. Secondly, diffusion behaviour exists due to hopping of electrons from one unit to another along the polymer chain and eventually to the electrode surface. It was also observed that plots emanating from the peak a' were the most linear. The redox peak a'/a which involves polyleucoemeraldine/polyleucuemeraldine radical cation transition has been shown to be a one electron reaction [84]. A plot of scan rate versus peak current for this peak is shown in figure 8. The plot gave a slope of 8.325×10^{-4} with a non-zero intercept. This agrees with the behaviour of a thin film adsorbed electro active species undergoing a Nernstian reaction [84].

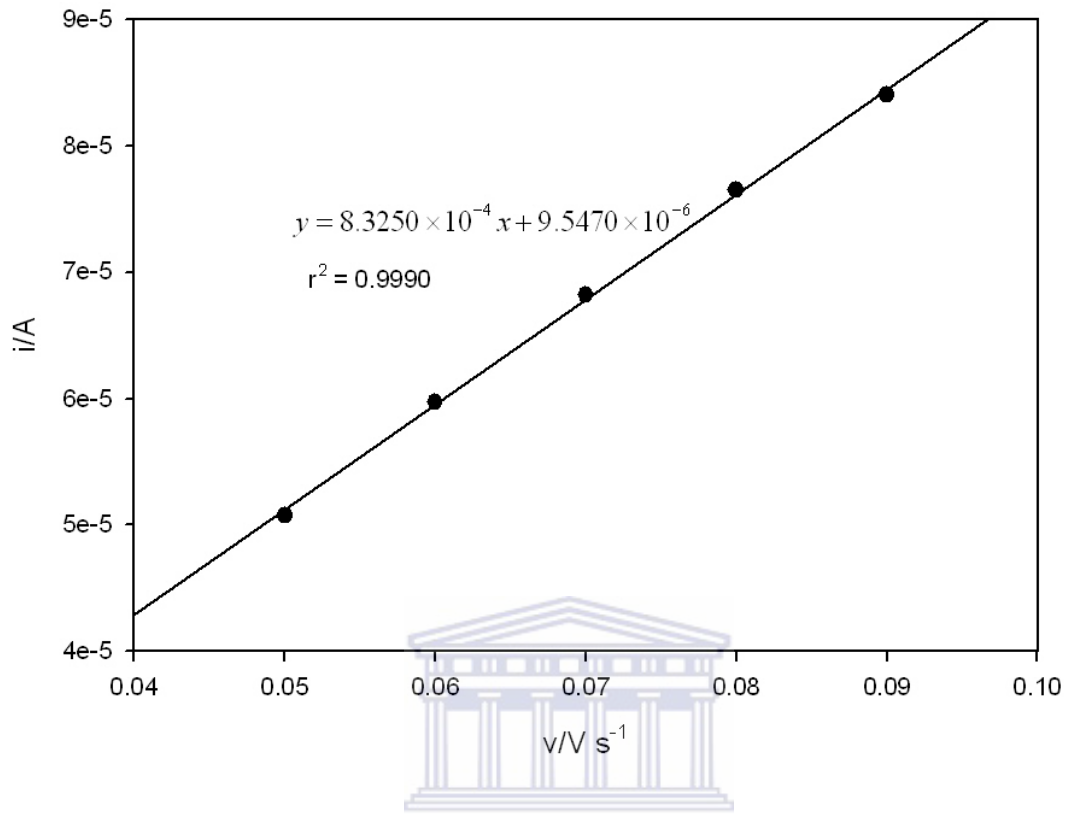
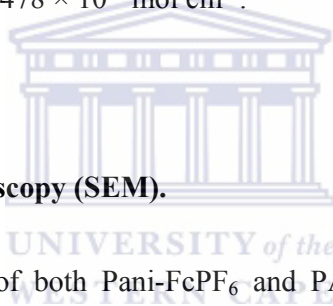


Figure 8: A plot of scan rate versus peak current for peak a'

In the adsorption phenomenon, the surface concentration of the adsorbed electroactive species may be calculated from equation (8)

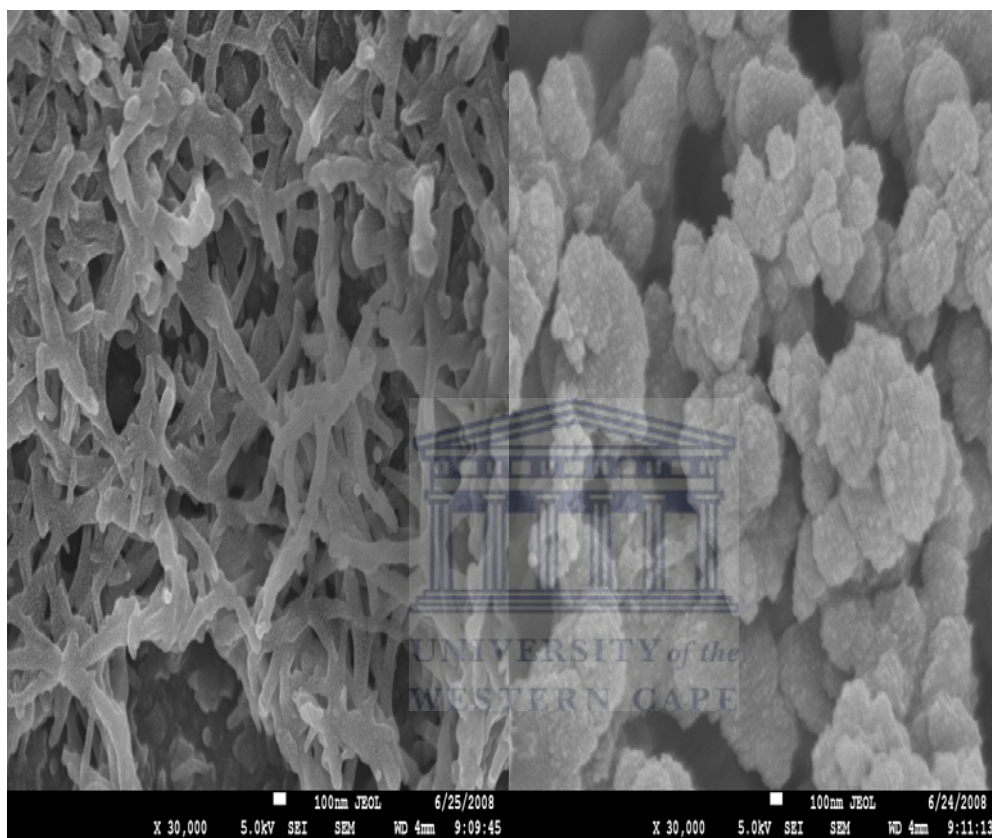
$$\frac{i_p}{\nu} = \frac{n^2 F^2 A \Gamma_{Pani-FcPF_6}}{4RT} \quad (8)$$

where n is the number of electrons transferred, F is the Faraday constant ($96,584 \text{ C mol}^{-1}$), $\Gamma_{Pani-FcPF_6}$ is the surface concentration of the composite film (mol cm^{-2}), A is the surface area of the electrode (0.071 cm^2), ν is the scan rate (V s^{-1}), R is the gas constant ($8.314 \text{ J mol}^{-1}\text{K}^{-1}$) and T is the operating absolute temperature (T in Kelvin). Thus for a one electron transfer at 25°C (298 K) the surface concentration ($\Gamma_{Pani-FcPF_6}$) of the adsorbed electroactive species evaluated from the slope was $1.2478 \times 10^{-8} \text{ mol cm}^{-2}$.



4.2.2 Scanning Electron Microscopy (SEM).

Scanning electron micrograph of both Pani-FcPF₆ and PANI are shown in the figure 9. Although both micrographs show nano-sized particles, it is evident that whereas PANI gives a cauliflower-like structure, the Pani-FcPF₆ shows some well-defined nano fibrous clusters with an average cross sectional diameter of 100 nm. A follow up elemental analysis using Electron dispersion spectroscopy (EDS) showed presence of Fluorine (F), phosphorus (P) and iron (Fe) in the composite (Ref. Appendix D). This confirmed retention of ferrocenium hexafluorophosphate in the composite. It was therefore suggested that, the presence of ferrocenium hexafluorophosphate activated self organization of polyaniline into fibrous morphology.



(a) (b)
Figure 9: Scanning electron micrograph of (a) Pani-FcPF₆ and (b) PANI

In this study, the Pani-FcPF₆ serves two major purposes. Firstly, it forms a platform for the immobilization of HRP and secondly to shuttle electrons between the GCE and the HRP. During immobilization of the HRP, the inter-nano fibre spaces as can be seen from the micrographs were of great importance. This is because, such spaces provided for entrapment of the enzyme, therefore minimizing chances of the enzyme leaching out during use. Furthermore, the spaces increased the surface area for enzyme immobilization thus allowing attachment of a large amount of the enzyme for improved interaction with the target analyte. Being entrapped within the composite spaces, the enzyme was also kept in close contact with the film and led to direct electron communication between the HRP and the conducting composite and through it to the GCE. This enhanced efficient reduction of hydrogen peroxide at -400 mV (Versus Ag/AgCl) thus improving the performance of the biosensor.



Chapter 5.

5.0 Results and discussion 2

5.1 The necessity of horseradish peroxidase (HRP) enzyme in the biosensor.

In order to illustrate that HRP was necessary for the catalytic reduction of hydrogen peroxide; catalytic signals upon addition of H_2O_2 were recorded in presence and absence of HRP. Figure 10 shows multiscan of voltammograms recorded with Pani-FcPF₆ alone, Pani-FcPF₆/BSA/Glu/HRP (enzyme electrode), Pani-FcPF₆/Glu, Pani-FcPF₆/BSA/Glu; each with 20 μL of 5 mmol L^{-1} of H_2O_2 as well as the enzyme electrode without H_2O_2 .



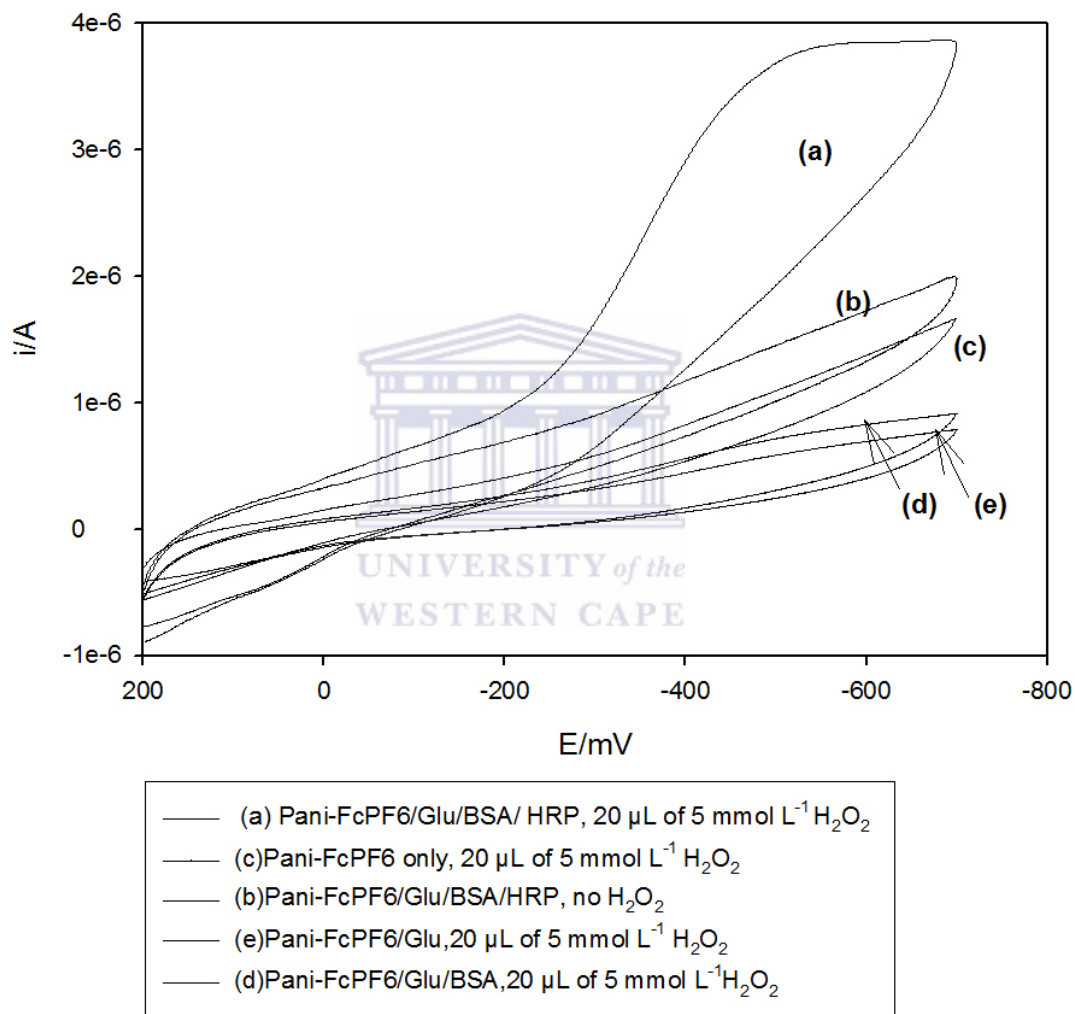


Figure 10: Multiscan voltammograms of Pani-FcPF₆/Glu/BSA/HRP, Pani-FcPF₆, Pani-FcPF₆/Glu and Pani-FcPF₆/Glu/BSA; all with 20 μL of 5 mmol L⁻¹ of H₂O₂ as well as Pani-FcPF₆Glu/BSA/HRP without H₂O₂; each performed in PBS, pH 7.0 at a scan rate of 10 mV s⁻¹

Both Pani-FcPF₆/BSA/Glu (d) and Pani-FcPF₆/Glu (e) give low lying voltammograms with no observable increase in current when H₂O₂ is added. The probable reason for this is that both Glu and BSA form a protective cover on the surface of the Pani-FcPF₆, thus hindering any electron communication between either the hydrogen peroxide or the buffer itself and the electroactive Pani-FcPF₆. When 20 μL of 5 mmol L⁻¹ H₂O₂ is injected into the buffer solution in presence of Pani-FcPF₆ modified GCE (c), a higher current than the former case is recorded. This may result from electrochemistry of the Pani-FcPF₆ and the buffer or the hydrogen peroxide itself. However, a cyclic voltammogram recorded by the enzyme electrode without hydrogen peroxide gives even higher current. This shows that Pani-FcPF₆ alone has no effect on hydrogen peroxide. When 20 μL of 5 mmol L⁻¹ H₂O₂ is injected into the buffer solution in presence the enzyme electrode (a), a high increase in catalytic current is observed at around -400 mV which levels off at -500 mV. This current which occurs only when HRP is incorporated into the modified electrode confirms that the enzyme is necessary for the catalytic reduction of hydrogen peroxide. The pH and enzyme concentration for this study were adopted from references [98] and [9] and worked well in this study.

5.2 Choice of potential window

The reduction of hydrogen peroxide; catalyzed by hydrogen peroxide leads to formation of Fe⁴⁺ (compounds I and II), as described in section 2.2.1. It is this bio-catalytically Fe⁴⁺ species which is reduced to Fe³⁺ on the surface of the electrode. The best potential window for the reduction of Fe⁴⁺ was investigated in detail. The figure 11 shows voltammograms obtained when the first addition of 5 μL of 5 mmol L⁻¹ of H₂O₂ was added to the PBS, pH 7.0 at a scan rate of 10 mV s⁻¹; at different potential windows.

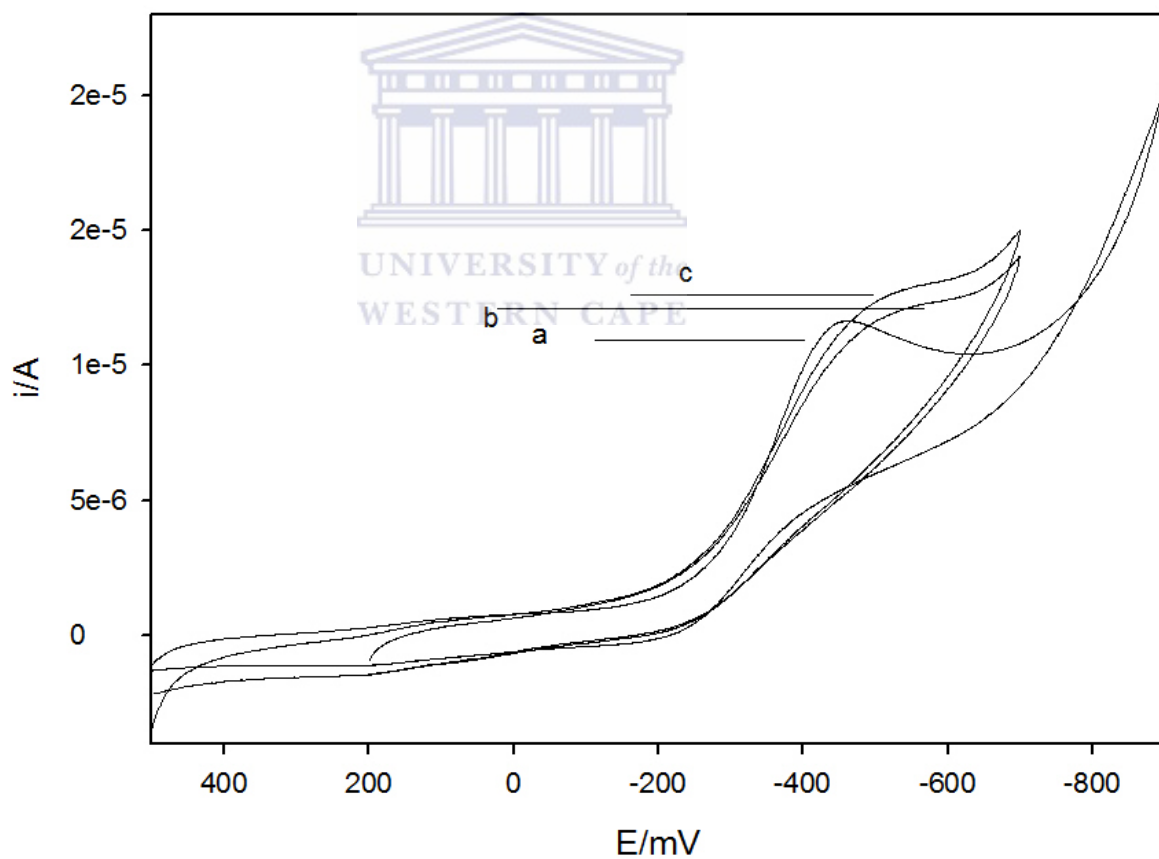
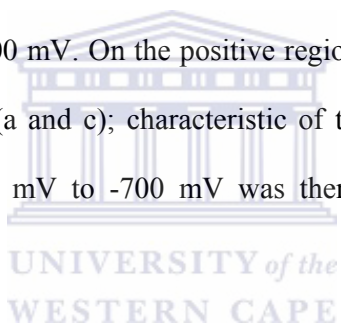


Figure 11: Multiscan voltammograms of the enzyme electrode in presence of $5 \mu\text{L}$ of $5 \text{ mmol L}^{-1} \text{H}_2\text{O}_2$ in PBS, pH 7.0 at a scan rate of 10 mV s^{-1} within different potential windows.

Within a potential window of +500 mV to -900 mV (voltammogram **a**), an increase in current was observed when H₂O₂ was added, showing a peak at -400 mV. A further increase in current was observed beyond -600 mV which crossed on the reverse scan at -750 mV. The appearance of the peak at -400 mV suggests diffusion controlled current at this potential (-400 mV) whereas the crossing of the voltammograms at -750 mV may be attributed to a number of factors which include: (1) Oxidation of an adsorbed species formed during the forward scan and whose reaction generates more current than that generated during the forward scan [99] or (2) Potential oscillations by current scan that appear beyond the first peak [100]. This behaviour was not observed when the potential was reduced to -600 mV (b and c). Both b and c gave a plateau limiting current in the region between -400 and -500 mV. On the positive region, a redox peak was observed at potentials beyond 200 mV (a and c); characteristic of the ferrocene redox reactions. A potential window of + 200 mV to -700 mV was therefore chosen for further cyclic voltammetry measurements.



5.3 Choice of scan rate.

The figure 12 shows a multiscan of cyclic voltammograms obtained after 4th addition of 5 μ L of 5 mmol L⁻¹ of hydrogen peroxide (20 μ L H₂O₂) at scan rates 5, 10 and 20 mV s⁻¹. At 5 mV s⁻¹, a reductive current is observed at -380 mV; a potential slightly less negative than -400 mV. However, this reduction signal is not clearly seen. The voltammogram also appears to cross at -560 mV. At 20 mV s⁻¹, an unclear signal appears at around -490 mV. A clearly defined catalytic signal was observed at -400 mV s⁻¹ when the scan rate was adjusted to 10 mV s⁻¹.

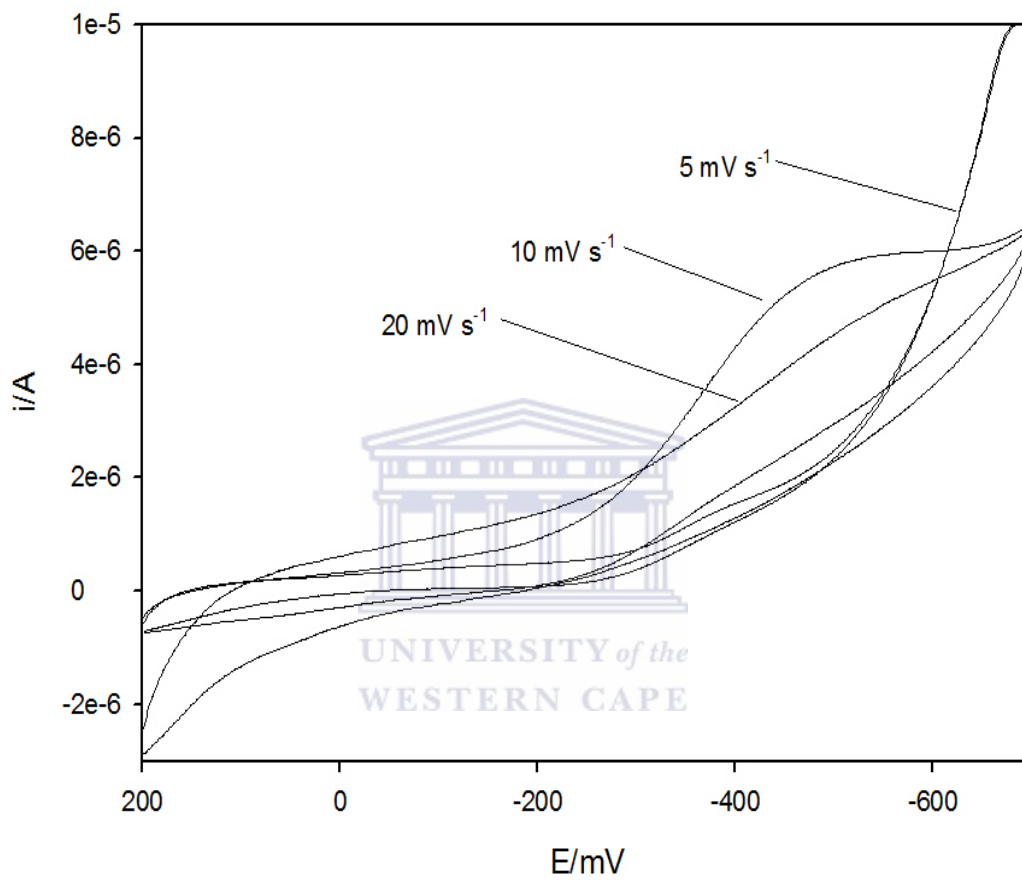


Figure 12: Multiscan voltammograms of enzyme electrode in presence of $20 \mu\text{L}$ of $5 \text{ mmol L}^{-1} \text{H}_2\text{O}_2$ in PBS, pH 7.0 at different scan rates.

It is important to mention that the biosensor described here works via catalytic process involving both chemical and electrode reactions. This involves three (3) sequential steps. The first step is the diffusion of the substrate (hydrogen peroxide) from the bulk solution to the surface of the enzyme (active centre) and its subsequent conversion into product. This is then followed by electron transfer from the reaction centre of the enzyme to the mediator. The third step involves the transport of the electron from the mediator to the electrode. This implies that the whole catalytic reaction is characterized by slow electron transfer. A fast scan rate would therefore lead to existence of non-Nernstian concentrations at the electrode surface [97]. The result of this is that as the scan rate increases, reduction potential shifts to more negative values as was observed in this work when the scan rate was progressively increased from 5 mV s^{-1} to 20 mV s^{-1} (reduction potential shifts progressively as -380 , -400 and -490 mV respectively). Although the scan rate of 10 mV s^{-1} showed a signal at a potential more negative than that observed for 5 mV s^{-1} , a scan rate of 10 mV s^{-1} was chosen for further cyclic measurements. This is because, its signal was clearest of the three.

5.4 Response characteristics of the hydrogen peroxide biosensor.

In order to determine the potential for steady state amperometric measurements, cyclic voltammetry was carried out on the enzyme electrode in PBS pH 7.0 without and with successive additions of small amounts of hydrogen peroxide. Figure 13 shows cyclic voltammetry biosensor response to H_2O_2 in PBS pH 7.0. When the first $5 \mu\text{L}$ of 5 mmol L^{-1} H_2O_2 was added to the PBS of pH 7.0 under diffusion controlled reactions, catalytic current resulting from the reduction of H_2O_2 was observed at -400 mV . Upon successive additions of H_2O_2 , the reduction peak at -400 was observed to proportionally increase with increase in H_2O_2 concentration

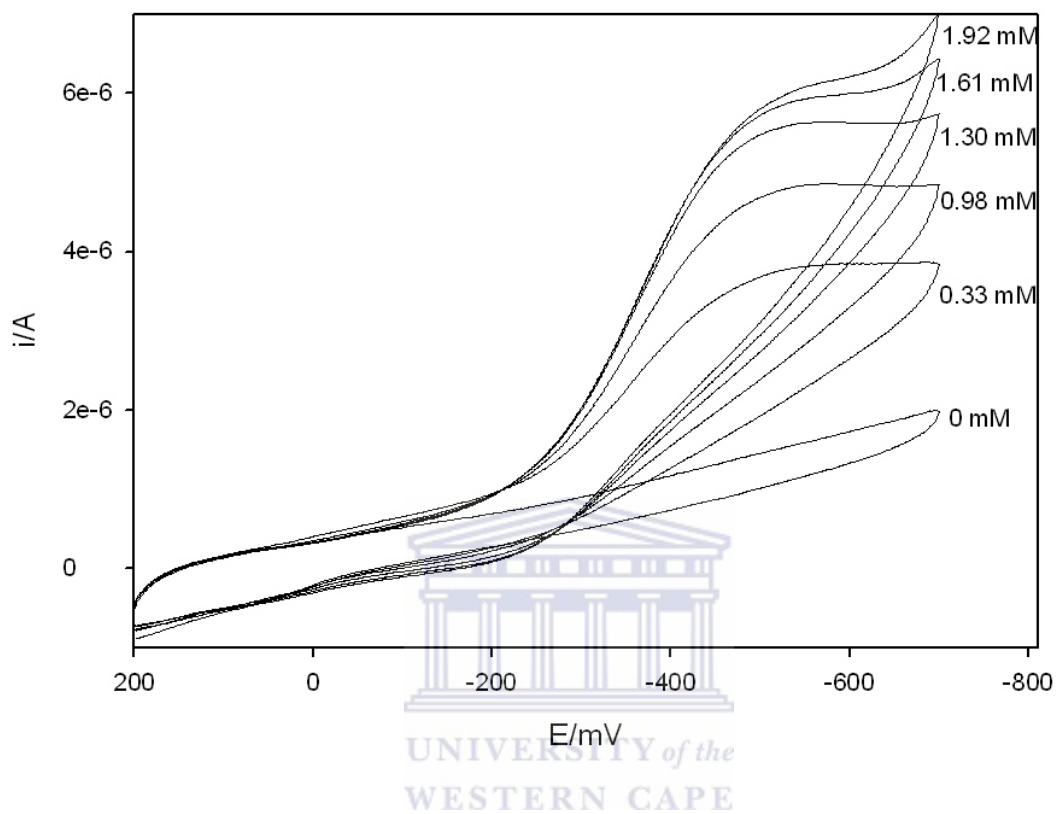


Figure 13: Cyclic Voltammetric biosensor response to successive additions of standard H₂O₂ in PBS, pH 7.0 at a scan rate of 10 mV s⁻¹

A similar behaviour was observed when square wave voltammetry was used as shown in figure 14.

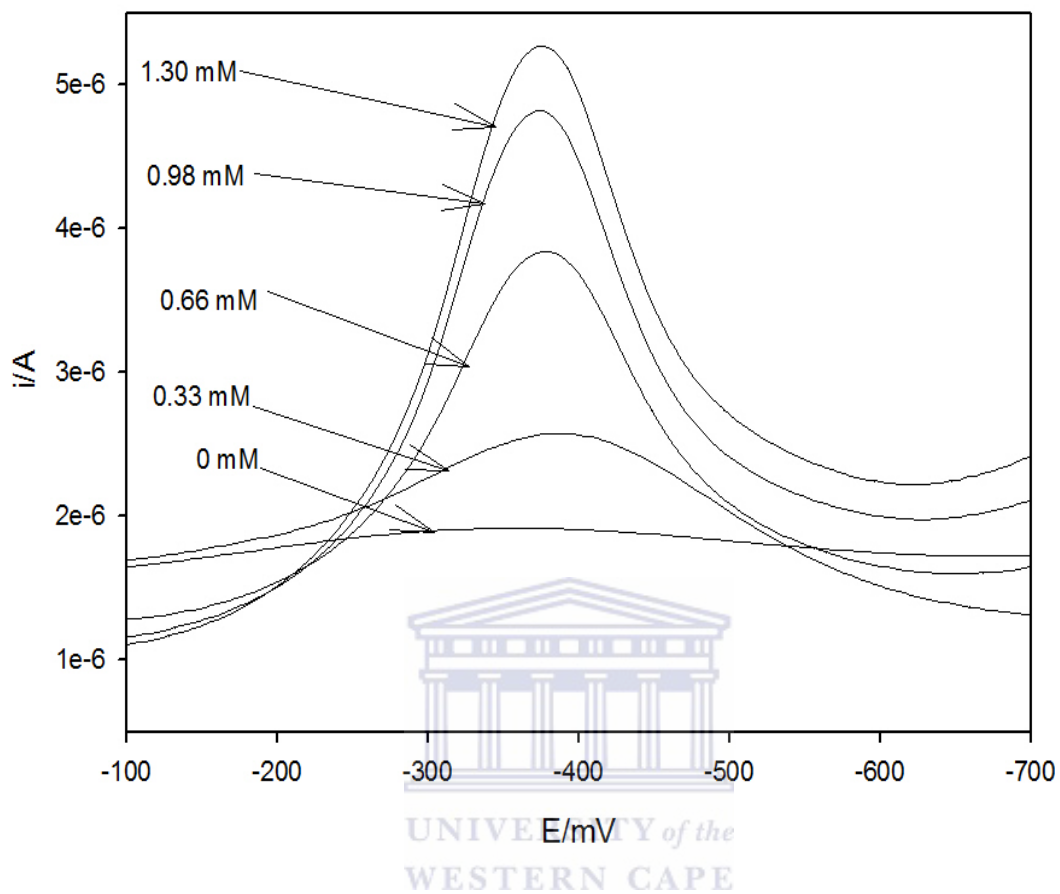
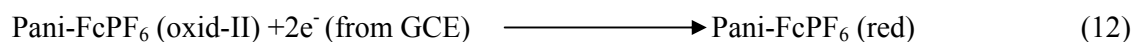
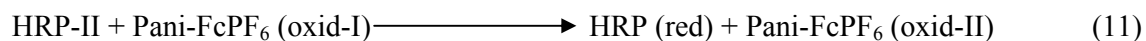
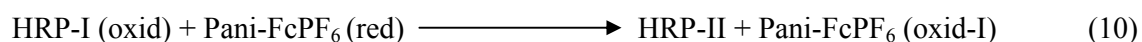
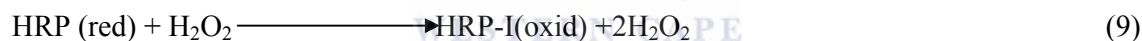


Figure 14: Square wave voltammetric response to successive additions of standard H_2O_2 in PBS, pH 7.0

The mechanism for catalytic reduction of H_2O_2 in a mediated biosensor has been proposed [98] and discussed in section 1.2.1.

In this study, the first step in the catalytic cycle involves a reaction between H_2O_2 and Fe^{3+} (the resting state of HRP) [90]. This reaction forms HRP-I, which is a high oxidation state intermediate comprising a Fe^{4+} oxoferryl centre and a porphyrin based cation radical. The HRP-I undergoes a one electron reaction with the reduced form of Pani-FcPF₆ in which case HRP-II is formed while Pani-FcPF₆ assumes one oxidation state higher than its reduced form - Pani-FcPF₆ (oxid-1). The HRP-II comprises a Fe^{4+} oxoferryl species that is one oxidation state above the resting state of HRP. The second one-electron returns HRP-II to the resting state while Pani-FcPF₆ attains an even higher oxidized state [Pani-FcPF₆ (oxid-II)]. This oxidized form of Pani-FcPF₆ (oxid-II) undergoes a two-electron reduction with GCE giving its reduced form [Pani-FcPF₆ (red.)]. This sequential set of reactions can be summarized by equations 9 to 12 below.



As seen from the cyclic voltammograms and also confirmed by square wave voltammetry, a potential of -400 mV was chosen for steady state amperometric measurements of the biosensor response to H_2O_2 .

The figure 15 shows the typical amperometric response for a freshly prepared enzyme electrode for successive additions of 5 μ L of 5 mmol L^{-1} H_2O_2 . The bioelectrode exhibits a rapid response to H_2O_2 . For instance, the average time required to reach 95% of the steady

state current after each addition was observed to be less than 6 s. This possibly indicates a low diffusional resistance and high electrical conductance of the Pani-FcPF₆ nano fibres. This response time was comparable to that reported by Zhu and co-workers (6 s) [101] and Kozan and co-workers (7 s) [22].

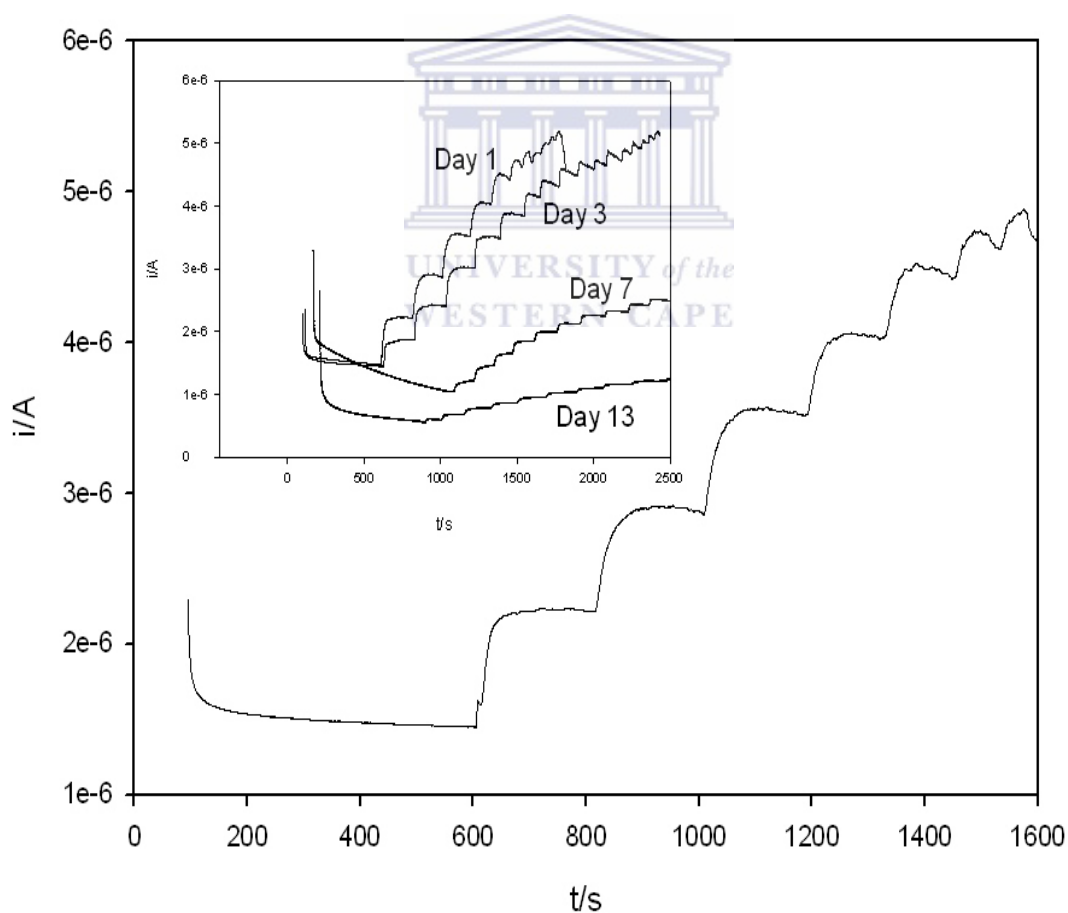


Figure 15: Current-time plot for biosensor response to standard H₂O₂ at a constant potential of -400 mV in PBS, pH 7.0 (inset are similar plots for days 1, 3, 7 and 13)

To assess the stability of the biosensor, a single enzyme electrode was used for analytical determination of hydrogen peroxide standard solution for two weeks, storing it in the working buffer in between experiments. The steady state amperograms for days 1, 3, 7 and 13 are shown in figure 15 inset. Although a significant decrease in the current generated after each successive addition of H_2O_2 in days 3, 7 and 13 was observed, steady state currents were still observed on the 13th day. This decrease in current response may be attributed to loss of biosensor activity, which in turn may have resulted from (1) partial inactivity of HRP induced by treatment of the enzyme electrode after each experiment and storage conditions as explained in sec. 2.5, (2) Possible H_2O_2 oxidation might have caused deterioration of the electrical conductivity of the Pani-FcPF_6 , (3) intrinsic instability of the nano-composite resulting from possible irreversible chemical reaction between polyaniline and its dopant (polyvinyl sulfonic acid) which breaks the conjugation, (4) loss of the dopant via thermal related mechanisms especially when the charged sites become unstable due to conformational changes in the polymer backbone and (5) leaching of enzyme from the composite film. However, significant enzyme leaching is not expected because of the stable configuration and morphology of the composite as explained earlier. Other possible causes of this decrease in current may be composite stability related. Four similar enzyme electrodes were also used for amperometric determination of hydrogen peroxide under similar conditions. The results obtained were comparable [standard deviation (σ) = 0.1408, n = 4], thus assuring some reproducibility of the biosensor.

Figure 16 below shows the calibration curve for the biosensor response to H_2O_2 obtained from steady state amperometric response data. From this curve, we can say that the biosensor obeyed the normal Michaelis-Menten kinetics

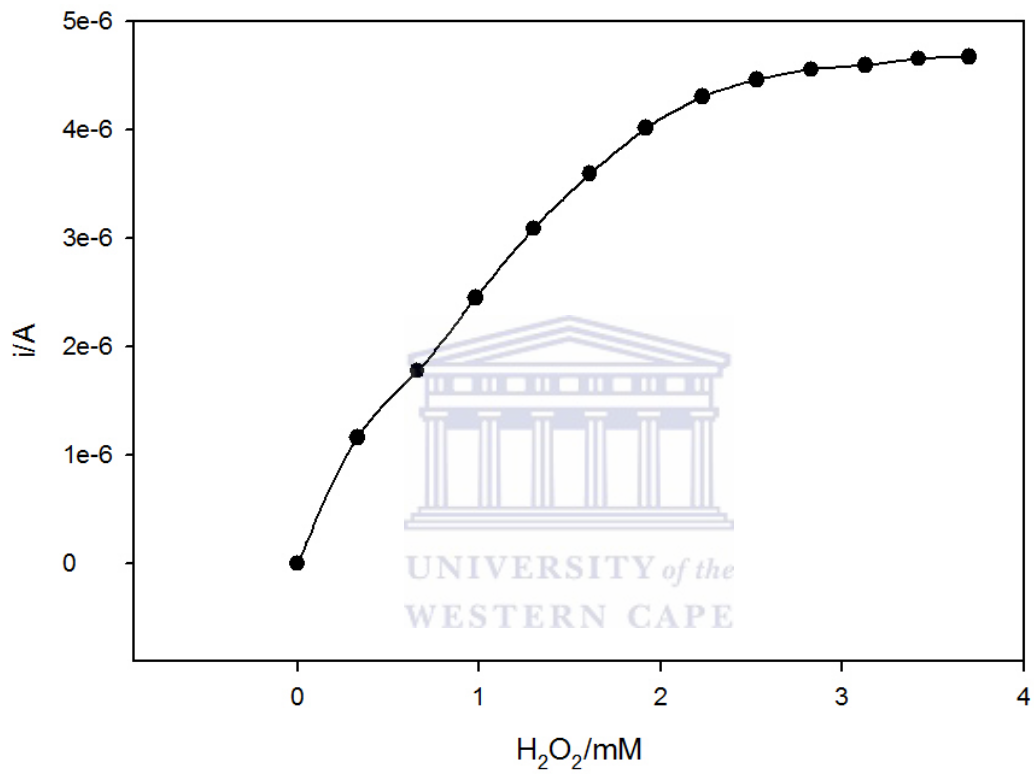


Figure 16: Calibration curve for the biosensor response to standard H₂O₂ in PBS, pH 7.0. with a freshly prepared enzyme electrode.

A statistic analysis of the calibration curve and equation (13) were used to evaluate the apparent Michaelis-Menten constant (K_m^{app}).

$$I = \frac{I_{\max}[H_2O_2]}{[H_2O_2] + K_m^{app}} \quad (13)$$

Where I is the steady state current after substrate addition, $[H_2O_2]$ is the bulk concentration of the substrate; I_{\max} is the maximum current measured under saturated substrate concentration and K_m^{app} is the apparent Michaelis-Menten constant. The value of K_m^{app} evaluated from standard hyperbolic curve fitting in sigma plot 8.0 was $1.6890 \text{ mmol L}^{-1}$. This value is lower than 3.69 mmol L^{-1} , reported by Liu and co-workers [102], 8.9 mmol L^{-1} reported by Kozan and co-workers [22] and 5.5 mmol L^{-1} reported by Ferri and co-workers [103]. The K_m^{app} obtained in this work indicates that the enzymatic activity of the immobilized HRP is high. We can also conclude from this value that the enzyme electrode exhibited a relatively high affinity for H_2O_2 . The minimum concentration of H_2O_2 that could be detected using this biosensor was $6.6 \times 10^{-5} \text{ M}$ which was one order of magnitude lower than $2.5 \times 10^{-4} \text{ M}$; reported by Mathebe and co-workers [21], for a polyaniline/peroxidase based biosensor. The detection of such low concentrations in this study could be attributed to several factors such as (1) The inclusion of ferrocenium hexafluorophosphate in the nano-composite mediator may have improved the sensitivity of the biosensor, (2) The large surface area of the composite allowed for attachment of large amount of HRP thus improving the interaction between the H_2O_2 and the enzyme. The current response of the enzyme electrode increased linearly with increase of H_2O_2 concentration from $6.6 \times 10^{-5} \text{ M}$ to $2.23 \times 10^{-3} \text{ mmol L}^{-1}$ (linear range), with a correlation coefficient of 0.9983. A linear plot for this is shown in figure 17. This range suggests that lower levels of hydrogen peroxide can be detected by this method than when calorimetric method is used in a similar media as discussed in section 1.3.

It further suggests that, higher levels of hydrogen peroxide than 1.46×10^{-4} M (reported for titrimetric method, section 1.3) can be detected by this method in a similar media. A sensitivity of $1.9305 \text{ A } \mu\text{M}^{-1}$ and a detection limit of $2.930 \times 10^{-5} \text{ mmol L}^{-1}$ were obtained for this biosensor. The detection limit was calculated from $3\sigma/\text{slope}$ of the linear plot in figure 17, where σ is the standard deviation of the current in the buffer solution.

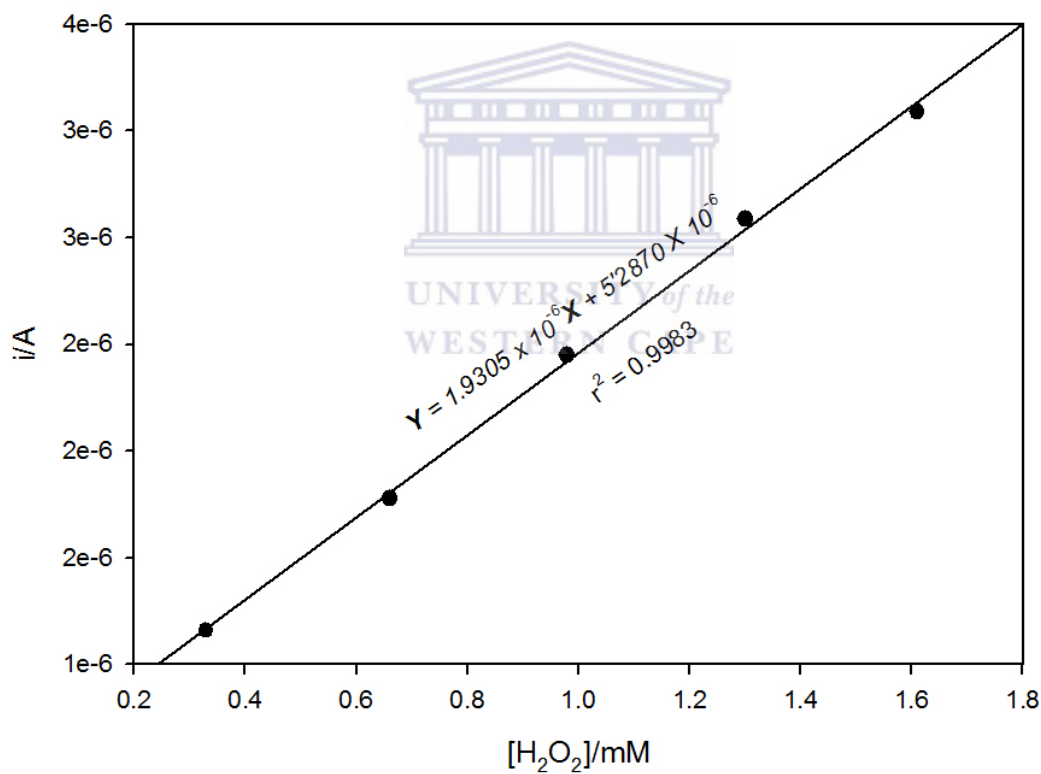


Figure 17: A current-H₂O₂ concentration plot for the biosensor response to standard H₂O₂ in PBS, pH 7.0

5.5 Interference to hydrogen peroxide detection by the enzyme electrode.

In the catalytic reduction of peroxides by HRP, several interfering substances have been reported. These substances include glucose, sucrose, acetic acid, oxalic acid, citric acid, ethanol, ascorbic acid, nitrates (NO_3^-), fluorides (F^-) and sulphides (S^-) [104]. The action of peroxides by HRP is also inhibited by sodium azide, cyanide, L-cystine, dichromate, ethylenethiourea, hydroxylamine, vanadate, P-aminobenzoic acid, Cd^{2+} , Pb^{4+} , Co^{2+} , Cu^{2+} , Fe^{3+} , Mn^{2+} , Ni^{2+} , and Pb^{2+} . In the two tooth whitening products covered in this study (DAYWHITE® and CPWB), the possible interfering substance was ethanol, present in the latter. None of these products contained any inhibiting chemical substance reported above. A comparative study was therefore made between the current generated for ethanol at a concentration of 3 mmol L^{-1} in presence of the same concentration of hydrogen peroxide and that obtained for standard hydrogen peroxide alone. The ratio of the current generated; i.e $I(\text{H}_2\text{O}_2)/I(\text{H}_2\text{O}_2+\text{C}_2\text{H}_5\text{OH})$ was obtained to give an insight in to the magnitude of interference if any. Square wave voltammetric response for this study is shown in the figure 18. At this studied concentration (3 mmol L^{-1}), H_2O_2 alone generated $2.569 \times 10^{-6} \text{ A}$ whereas $\text{H}_2\text{O}_2 + \text{C}_2\text{H}_5\text{OH}$ generated $2.461 \times 10^{-6} \text{ A}$, resulting to a ratio of 1.0440 (4% interference). Ethanol therefore was expected to cause no meaningful interference in the detection of H_2O_2 in the studied tooth whitening products.

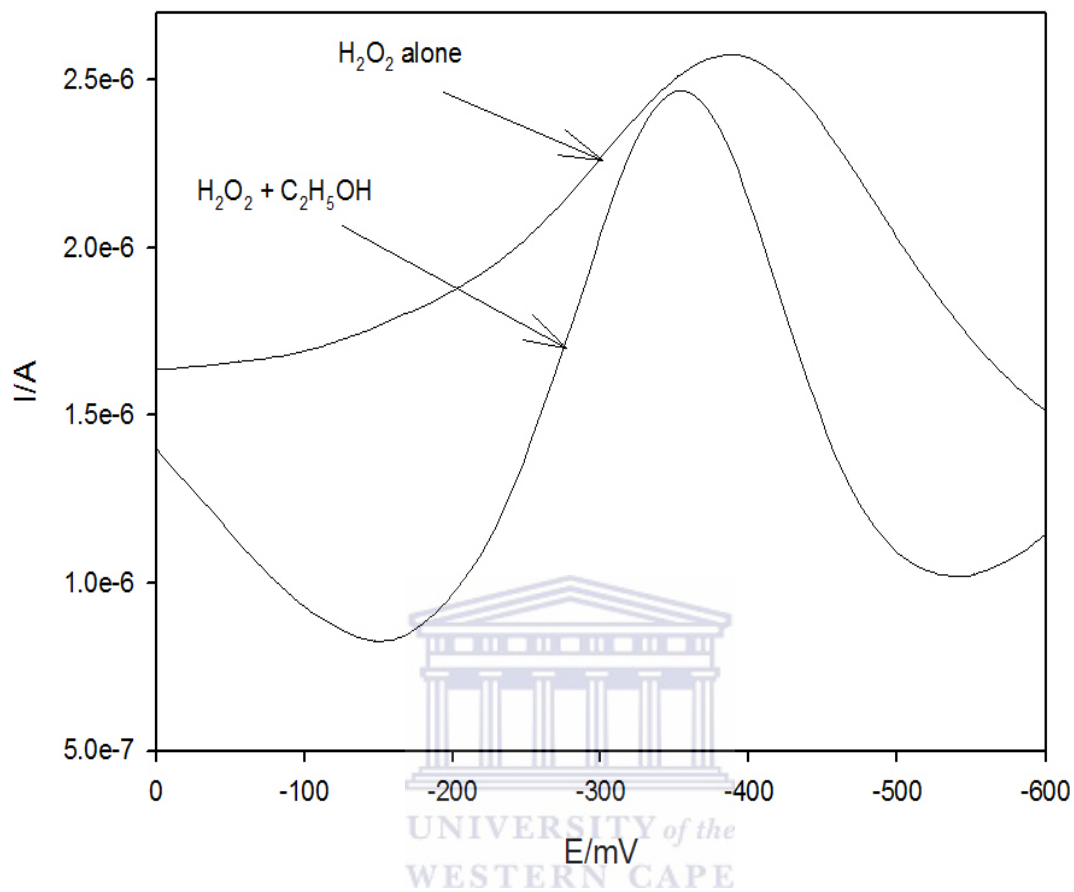


Figure 18: Square wave voltammetric biosensor response to 3 mmol L⁻¹ H₂O₂ alone and H₂O₂ + C₂H₅OH in PBS, pH 7.0.

Other interference substances investigated in this study were glucose and acetic acid. Glucose gave a ratio of 1.02 while acetic acid gave 1.22.

5.6 Biosensor response to hydrogen peroxide in selected tooth whiteners.

5.6.1 DAYWHITE®

The proposed hydrogen peroxide biosensor was used for the detection of hydrogen peroxide in DAYWHITE® tooth whitening gel. The catalytic response of the biosensor to hydrogen peroxide in DAYWHITE® is shown in figures 19 (steady state response) and 20 (square wave response). A comparison of figure 14 (square wave voltammetric response of the biosensor to standard H₂O₂) and figure 20 (square wave voltammetric response of the biosensor to DAYWHITE®) shows similar trend when small amounts (5 µL) of analyte were added to the PBS of pH 7.0. This is an indication that the developed biosensor was able to detect, isolate and reduce hydrogen peroxide in DAYWHITE® tooth whitening gel.

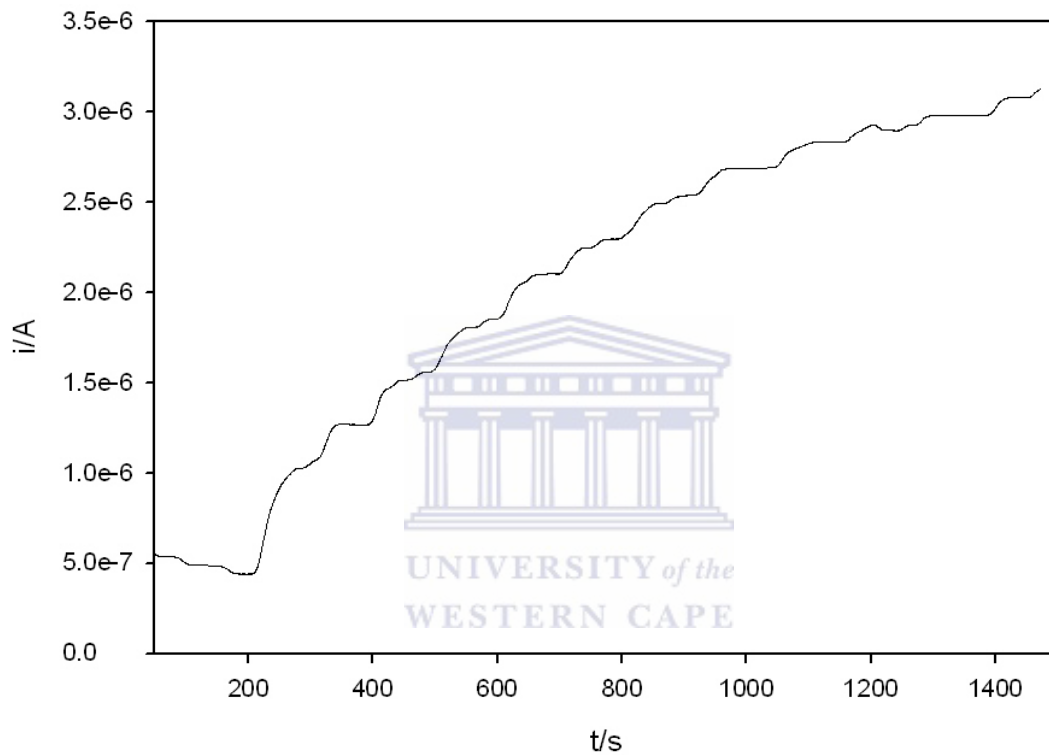


Figure 19: Current-time plot for the biosensor response to successive additions of DAYWHITE® at a constant potential of -400 mV in PBS, pH 7.0.

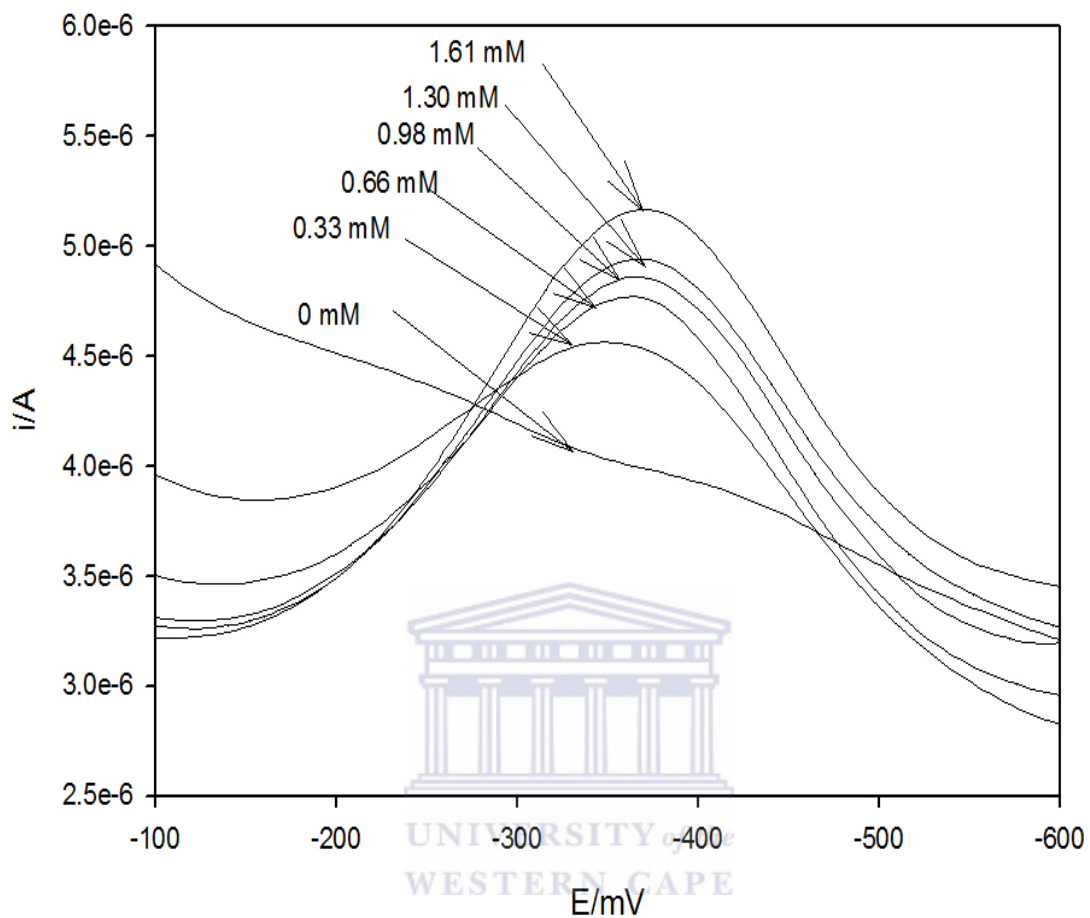


Figure 20: Square wave voltammetric response to successive additions of DAYWHITE® in PBS, pH 7.0.

5.6.2. Colgate Plax whitening Blancheua (CPWB).

Colgate Plax Whitening Blancheua was the second tooth whitening product whose hydrogen peroxide concentration was investigated using the developed biosensor. Upon addition of small amounts (5 μ L) of the analyte into the cell solution, an increase in catalytic current; proportional to the amount of analyte added was observed. This was in agreement with the results obtained for standard hydrogen peroxide and DAYWHITE® tooth whitening gel. Biosensor responses to this product using the two techniques are shown in figures 21 and 22.

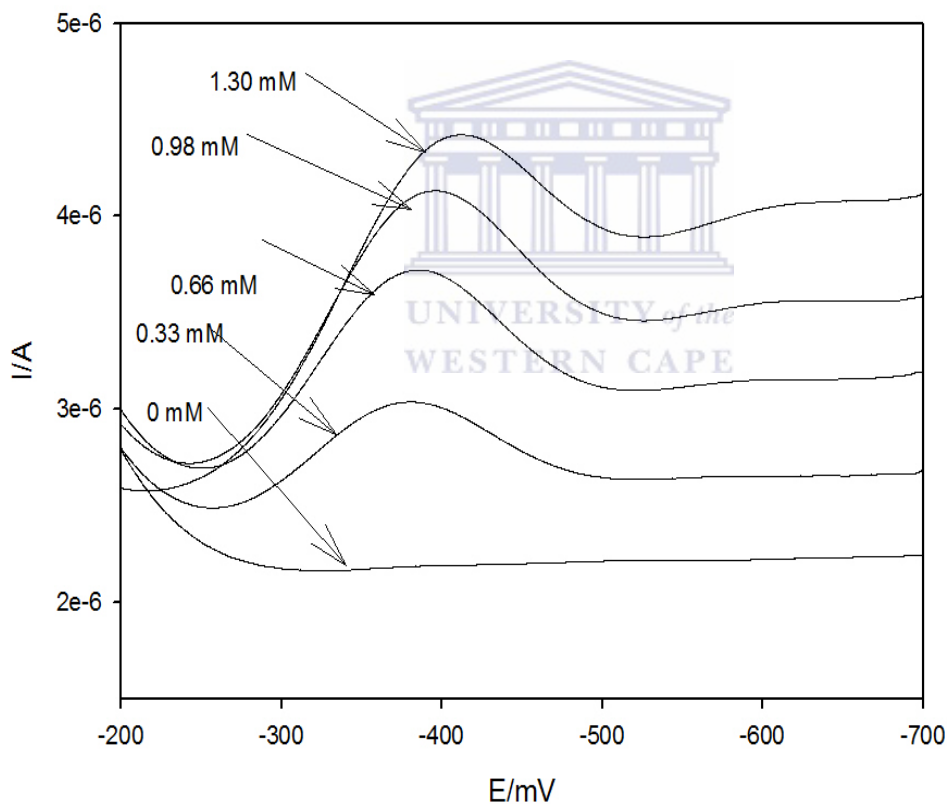


Figure 21: Square wave voltammetric response to successive additions of CPWB in PBS, pH 7.0.

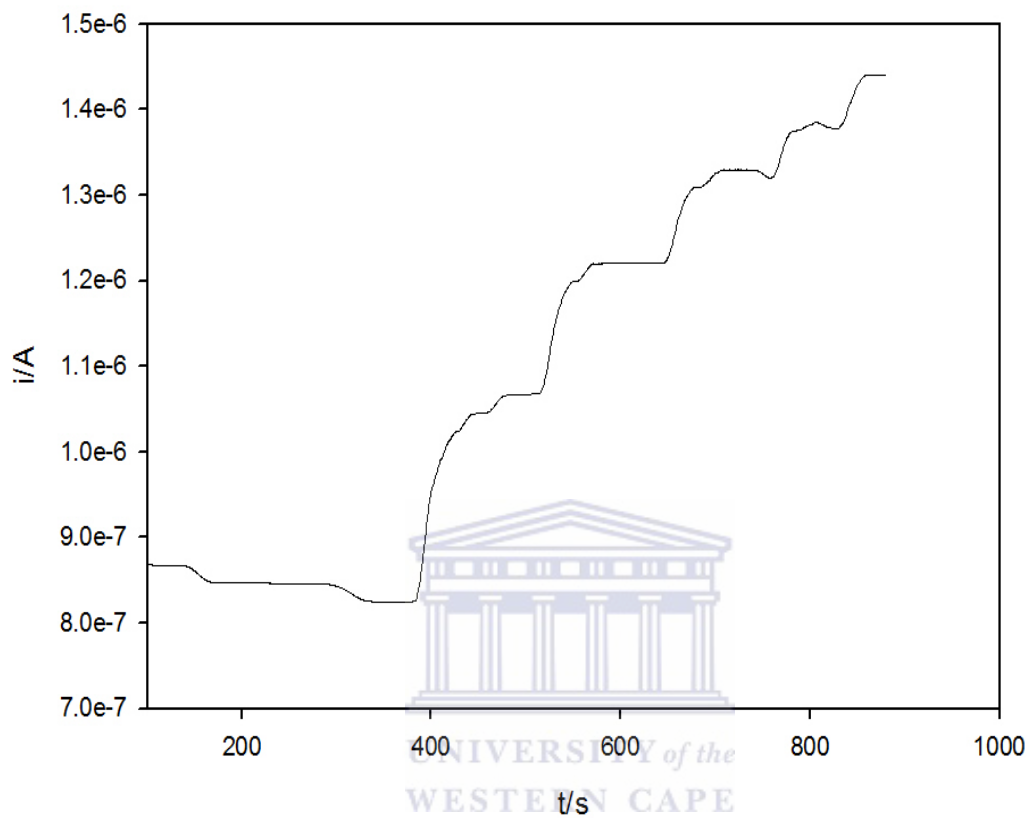


Figure 22: Current-time plot for the biosensor response to successive additions of CPWB at a constant potential of -400 mV in PBS, pH 7.0.

5.6.3 Quantitative evaluation of H₂O₂ in DAYWHITE® and CPWB.

Quantitative evaluation of H₂O₂ in both DAYWHITE® and CPWB was based on the steady state current generated upon injection of the first matrix sample of the tooth whitening gel. This was then checked against the calibration curve (Figure 16) to obtain the corresponding concentration (mM). It is important to mention here that, the calibration curve was obtained from analysis of 5 mM of standard H₂O₂; prepared from a solution containing 32% of H₂O₂ by composition. This means that a concentration of 5 mM read from the calibration curve translates to 32% composition of H₂O₂ in the sample analyzed. In view of this, the percentage composition of H₂O₂ in any sample can be evaluated from the calibration curve using the equation.

$$\%H_2O_2 = \frac{x \times 32}{5} \quad (14)$$

Where x is the concentration (mM) read from calibration curve.

Table 4 summarises the quantitative information about the tooth whiteners studied in this work.

Table 4: Quantitative composition of H₂O₂ in tooth whiteners.

Tooth whitener	Steady state current (A)	H ₂ O ₂ concentration (mM)	H ₂ O ₂ concentration (%)
DAYWHITE®	2.8690 × 10 ⁻⁶ A	1.190	7.168
CPWB	5.1500 × 10 ⁻⁷ A	0.470	3.008

Attempts to get either percentage or molar concentration of hydrogen peroxide in CPWB from the manufacture's description of ingredients or any other previously used method were unsuccessful. For this reason, this study does not compare the results obtained for CPWB with any previously obtained data. The percentage composition of hydrogen peroxide in DAYWHITE® is labelled by the manufacture as 7.5. Holding this value true, we can conclude that for reasons stated earlier in sec.5.4, this method recorded an under-detection of 0.3320%.



Chapter 6

6.0 Conclusions and recommendations

6.1 Conclusions

Poly(aniline-ferrocenium hexafluorophosphate) nano-composites were successfully prepared on a glassy carbon electrode by a relatively simple and inexpensive electrochemical method. A close analysis of the polymerization voltammograms of both Pani-FcPF₆ and PANI showed a higher current density in Pani-FcPF₆ than in PANI. This was an indication that the nano-composites obtained in this study were more conducting than PANI itself. Physical adsorption of horseradish peroxidase/glutaraldehyde matrix mixture on the surface of the Poly(aniline-ferrocenium hexafluorophosphate) nano-composite modified GCE showed that the nano-composites provided a suitable platform for attachment of HRP. Biosensor measurements of standard hydrogen peroxide with the fabricated enzyme electrode, in a PBS of pH 7.0 showed that increase in concentration of hydrogen peroxide led to a proportional increase in catalytic current. This was an indication that HRP retained its catalytic activity after immobilization. It further confirmed that the prepared nano-composite materials suitable shuttled electrons between the redox centre of the HRP and the GCE. In this study, successful detection of hydrogen peroxide concentrations as low as 6.60×10^{-5} M. This was an order of magnitude lower than 2.5×10^{-4} M reported in literature for a polyaniline/peroxidase based biosensor; implying an improved performance of the biosensor in this study. The biosensor also successfully detected, isolated and reduced hydrogen peroxide in DAYWHITE® and CPWB. The results obtained in this study at a pH of 7.0 provided reliable information that led to quantitative determination of hydrogen peroxide concentration in the studied tooth whiteners.

6.2 Recommendations

Recommended further studies on this work include optimization of factors such as pH and concentration of the immobilized horseradish peroxide enzyme. This would possibly improve the performance of the biosensor and make it more reliable than reported here. Other enzymes such as glucose oxidase, acetylcholine esterase and cytochrome P450 among others can also be tried with the Pani-FcPF₆. If successful, this would open opportunities for fabrication of biosensors for the respective enzyme substrates (analytes), thus widening the applications of the Pani-FcPF₆.



References

1. Gerard, M., Chaubey, A., Malhotra, B.D. 2002. Application of conducting polymers to biosensors. *Biosensors and Bioelectronics* 17, 345-359.
2. Castillo, J., Gaspar, S., Leth, S., Niculescu, N., Mortari, A., Bontidean, I., Soukharev, V., Dorneanu, S.A., Rybov, A.D., Csoregi, E. 2004. Biosensors for life quality Design, development and applications. *Sensors and Actuators B* 102, 179-194.
3. Salimi, A., Hallaj, R., Soltanian, S., Mamkhezri, H. 2007. Nanomolar detection of hydrogen peroxide on glassy carbon electrode modified with electrodeposited cobalt oxide nanoparticles. *Analytica Chimica Acta* 594, 24-31.
4. Joiner, A., Thakker, G. 2004. In vitro evaluation of a novel 6% hydrogen peroxide tooth whitening product. *Journal of dentistry* 32, 19-25.
5. Berry, J. 1991. What about whiteners? Safety concerns explored. *Journal of American Dental Association* 121, 223-225.
6. Christensen, G. J. 1989a. Tooth bleaching, home use products. *Clinical Research Associates Newsletter* 13, 1-3.
7. Haywood, V. B. 1991. Overview and status of mouth guard bleaching. *Journal of Esthetic Dentistry* 3, 157-161.
8. Sinensky, M.C., Leiser, A.L., Babich, H. 1995. Oxidative stress aspects of the cytotoxicity of carbamide peroxide: in vitro studies. *Toxicology letters* 75, 101-109.
9. Li, Y 1996. Biological properties of peroxide-containing tooth whiteners. *Food and Chemical Toxicology* 34, 887-904.

10. Chan, P.C., Peller, O.G., Kesner, L. 1982. Copper (II)-catalyzed lipid peroxidation in liposomes and erythrocyte membranes. *Lipids* 17, 331-337.
11. Floyd, R.A. 1990. Role of oxygen free radicals in carcinogenesis and brain ischemia. *FASEB Journal* 4, 2587-2597.
12. Floyd, R.A and Schneider, J.E. 1990. Hydroxyl free radical damage to DNA. *In Lipid Membrane Oxidation* 34, 768-773.
13. Harman, D. 1981. The aging process. *Proceedings of the National Academy of Sciences of the U.S.A* 78, 7124-7132.
14. Chen, D., Bernstein, C., 1987. Recombinational repair of hydrogen peroxide-induced damages in DNA of phage T4. *Mutation Research* 184, 87-98.
15. Hochstein, P. and Atallah, A.S. 1988. The nature of antioxidant systems in the inhibition of mutation cancer. *Mutation Research* 202, 363-375.
16. Bates, E. J, Johnson, C.C, Lowther, D.A. 1985. Inhibition of proteoglycan synthesis by hydrogen peroxide in cultured bovine cartilage. *Biochemica et Biophysica Acta* 838, 221-226.
17. Hanks, C.T., Fat, J.C., Wataha, J.C., Corcaran, J.F. 1993. Cytotoxicity and dentine permeability of carbamide peroxide and hydrogen peroxide vital bleaching materials, in vitro. *Journal of Dental research* 72, 931-938.
18. Li, Y., Martin, M.J., Noblitt, T., Stookey, G. 1992. Cytotoxicity of hydrogen peroxide and peroxide-containing bleaching gels. *Proceedings of Second Annual Research day, Indiana University School of Dentistry and Indiana Section, American Association of Dental Research, Indianapolis, Indiana U.S.A.*
19. Ramp, W.K., Arnold, R.R., Russel, J.E, Yancey, J.M. 1987. Hydrogen peroxide inhibits glucose metabolism and collagen synthesis in bone. *Journal of Periodontology* 58, 340-344.

20. Rubin, R., Farber, J.L. 1984. Mechanisms of killing of cultured hepatocytes by hydrogen peroxide. *Archives of Biochemistry and Biophysics* 228, 450-459.
21. Mathebe, N.G.R., Morrin, A., Iwuoha, E.I. 2004. Electrochemistry and scanning electron microscopy of polyaniline/peroxidase-based biosensor. *Talanta* 64, 115-120.
22. Kozan, J.V.B., Silva, R.P., Serrano, S.H.P., Lima, A.W.O., Agnes, L. 2007. Biosensing hydrogen peroxide utilizing carbon paste electrodes containing peroxidase naturally immobilized on coconut (*Cocos nucifera L.*) fibres. *Analytica Chimica Acta* 591, 200-207.
23. <http://www.solvaychemicals.us/static/wma/pdf/6/6/2/5/XX-122.pdf>
24. Hsien C., Wei, Su, Hua., Huang, Yeun-Chung, Lee 2008. Development of a Novel BIA Enzyme Calorimetric biosensor and Detection System for Hydrogen Peroxide determination at hazardous level. Published by the American Society of Agricultural and Biological Engineers, St. Joseph, Michigan www.asabe.org
25. <http://www.hdrinc.com/Assets/documents/Publications/Waterscapes/spring2006/HydrogenPeroxide.pdf>
26. <http://www.assaydesigns.com/commerce/ccp1171-1171-hydrogen-peroxide-chemiluminescent-detection-kit.htm?gclid=CJGvlnlrZYCFQO11AodWkRyzg#>
27. Corton, E., Battaglini, F. 2001. Effect of milk proteins on the behaviour of a biosensor based on poly(allylamine) containing an osmium complex wired to redox enzymes: Part B. Bienzymatic configuration. *Electroanalytical Chemistry* 511, 5-12.
28. Eloi, J.C., Chabanne, L., Whittell, G.R., Manners, I. 2008. Metallopolymers with emerging applications, *Materials Today* 11, 28-36.

29. Chen, J., Too, C.O., Wallace, G.G., Swiegers, G.F. Skelton, B.W., white, A.H. 2002. Redox- active conducting polymers incorporating ferrocenes, Preparation, characterization and bio-sensing properties of ferrocenylpropyl and butyl polypyrroles. *Electrochimica Acta* 47, 4227-4238.
30. Clark, L. C Jr. Lyons, C, 1962. Electrode systems for continuous monitoring in cardiovascular surgery. *Annals of the New York Academy of Sciences* 102, 29-45.
31. You, L., Chan, S.K., Bruce, J.M., Engle, S.A., Casanova, M., Corton, J.A., Heck, H.D. 1999. Modulation of testosterone-Metabolizing Hepatic Cytochrome P-450 Enzymes in Developing Sprague-Dawley Rats Following in Utero Exposure to P,P'-DDE. *Toxicology and Applied Pharmacology* 158, 197-205.
32. Bentley, A., Atkinson, A., Jezek, J., Rawson, D.M. 2001. Whole cell biosensors- electrochemical and optical approaches to ecotoxicity testing. *Toxicology in vitro* 15, 469-475.
33. Rotodo, F., Vidal, S., Bell, D., Horvath, E., Kovacs, K., Scheithauer, B.W., Lioyd, R.V. 2003. Immunohistochemical localization of amylin in human pancreas, thyroid, pituitary and their tumors. *Acta Histochemica* 105, 303-307.
34. Moench, J.S., Scott, C.B., Erman, E., Satterlee, J.D. 1989. Physical and spectroscopic studied of yeast Cytochrome c peroxidase and yeast iso-1-Cytochrome c. *Journal of Inorganic Biochemistry* 36, 219.
35. Armstrong, F.A., Butt, J.N., Sucheta, A. 1993. Voltammetric studies of redox-active centres in metalloproteins adsorbed on electrodes. *Methods in Enzymology* 227, 479-500.
36. Ho, W.O., Athey, D., McNeil, C.J., Hager, H.J., Evans, G.P., Mullen, W.H. 1993. Mediatorless horseradish peroxidase enzyme electrodes based on activated

- carbon: Potential application to specific binding assay. *Journal of Electroanalytical Chemistry* 351, 185-197.
37. Tatsuma, T., Watanabe, T., 1991. Oxidase/oxidase bilayer modified electrodes as sensors for lactase, pyruvate, cholesterol and uric acid. *Analytica Chimica Acta* 242, 85-89.
38. Razumas, V., Kazlauskaitė, J., Ruzgas, T., Kulys, J. 1992. Bioelectrochemistry of microperoxidases. *Journal of Electroanalytical Chemistry* 343, 159-176.
39. Danilowicz, C., Corton, E., Battaglini, F., Calvo, E.J. 1998. An Os(byp)₂CIPyCH₂NHPpoly(allylamine) hydrogel mediator for enzyme wiring at electrodes. *Electrochimica Acta* 43, 3525-3531.
40. Wollenberger, U., Drungiliene, A., Stocklein, W., Kulys, J.J., Scheller, W.F. 1995. Direct electrocatalytic determination of dissolved peroxidases. *Analytica Chimica Acta* 329, 231-237.
41. Suzuki, Y., Nakao, T., Ito, T., Watanabe, N., Toda, Y., Guiyun, X., Suzuki, T., Kobayashi, T., Kimura, Y., Yamada, A., Sugawara, K., Nishimura, H., Kitame, F., Nakamura, K., Deya, E., Kiso, M., Hasegawa, A. 1992. Structural determination of gangliosides that bind to influenza A, B, and C viruses by an improved binding assay: Strain-specific receptor epitopes in sialo-sugar chains. *Virology* 189, 121-131.
42. Kiefer, R., Kreutzberg, G.W. 1990. Gamma interferon-like immunoreactivity in the rat nervous system. *Neuroscience* 37, 725-734.
43. Omotayo, A.A., Ignaszak, A., Malgas, R., Ahmed, A.A., Baker, P.G.L., Mapolie, S.F., Iwuoha, E.I. 2007. An electrochemical DNA biosensor developed on novel multinuclear nickel(II) salicylaldimine metallodendrimer platform. *Electrochimica Acta* 53, 1689-1696.

44. Copel, J.A., Grannum, P.A., Hobbins, J.C. 1991. Interventional procedures in obstetrics. *Seminars in Roentgenology* 26, 87-94.
45. Cass, A.E.G., David, G., Francis, G.D., Hill, H.A.O., Aston, W.J., Higgins, I.J., Plotkin, E.V., Scott, L.D.L., Turner, A.P.F., 1984. Ferrocene mediated enzyme electrode for amperometric determination of glucose. *Analytical Chemistry* 56, 667-671
46. Cooper, J.C., Hall, E.A.H. 1992. Electrochemical response of an enzyme loaded polyaniline film. *Biosensors and Bioelectronics* 7, 473-485.
47. Shinohara, H., Chiba, T. Aizawa, M 1998. Enzyme micro sensor for glucose with electrochemically synthesized enzyme-polyaniline film. *Sensors and Actuators* 13, 79-86.
48. Iwuoha, E.I., Williams-Doltin, A.R., Hall, I.A., Morin, A., Mathebe, G.N., Smyth, M.R., Killard, A. 2004. Electrochemistry and application of a novel nanosubstituted squarate electron transfer mediator in a glucose oxidase-doped poly(phenol)sensor. *Journal of Pure Applied Chemistry* 79,789-799
49. Ivanov A.N., Lukachova, L.V., Evtugyn, G.A., Karyakina, E.E., Kiseleva, G.P., Karyakin, A.A. 2002. Polyaniline modified cholinesterase sensor for pesticide determination. *Bioelectrochemistry* 55, 75-77.
50. Iwuoha, E.I., Joseph, S., Zang, Z., Smyth, M.R., Fuhr, U., Ortiz de Montellano, P.R. 1998. Drug metabolism biosensors: electrochemical reactivities of Cytochrome P450_{cam} immobilized in synthetic vascular systems. *Journal of Pharmacy and Biomedical Analysis* 17, 1101-1110.
51. Iwuoha, E.I., Smyth, M.R. 2003. Reactivities of organic phase biosensors. 6 square wave and differential pulse studies of genetically engineered cytochrome

- P450_{cam} (CYP101) bioelectrodes in selected solvents. *Biosensors and Bioelectronics* 18, 237-244.
52. Iwuoha, E.I., Kane, S. Ania, C.O., Smyth, M.R., Ortiz de Montellano, P.R., Fuhr, U. 2002. Reactivities of organic phase biosensors. 3. Electrochemical study of cytochrome P450_{cam} immobilized on a methyltriethoxysilane sol-gel. *Electroanalysis* 12, 980-986.
53. Iwuoha, E.I. Wilson, A., Howel, M., Mathebe, N.G.R., Montane Jaime, K., Narinesingh, D., Guiseppi-Elie, A. 2004. Cytochrome P450_{2D6} (CYP_{2D6}) bioelectrode for fluoxetine. *Analytical letters* 37, 929-941.
54. Joseph, S., Rusling, J.F., Lvov, Y.M., Friedberg, T., Fuhr, U. 2003. An amperometric biosensor with human CYP3A4 as a novel drug screening tool. *Biochemical Pharmacology* 65, 1817-1826.
55. Schubert, F. 1991. Mediated amperometric enzyme electrode incorporating peroxidase for the determination of hydrogen peroxide in organic solvents. *Analytica Chimica Acta*. 245, 133-138.
56. Mulchandani, A., Wang, C.L., Weetall, H. 1995. Amperometric detection of peroxides with poly(anilinomethyl ferrocene) modified enzyme electrodes. *Analytical Chemistry* 67, 94-100.
57. Yabuki, S., Mizutani, F., Hirata, Y. 2000. Hydrogen peroxide determination based on a glassy carbon electrode covered with polyion complex membrane containing peroxidase and mediator. *Sensors and Actuators B* 65, 49-51.
58. Huang, R., Hu, N. 2001. Direct electrochemistry and electrocatalysis with horseradish peroxidase I Eastman AQ films. *Bioelectrochemistry* 54, 75-81.
59. Razola, S.S., Ruiz, B.L., Diez, N.M., Mark Jr. H.B., Kauffmann, J.M. 2002. Hydrogen peroxide sensitive amperometric biosensor based on horseradish

- peroxidase entrapped in polypyrrole electrode. *Biosensors and Bioelectronics* 17, 921-928.
60. Lan, J., Guo, S.D., Yuan, X.Y. 2007. Influence of Cu(II) on the interaction between sulfite and horseradish peroxidase in vitro. *Spectrochimica Acta Part A: Molecular and Biomolecular Spectroscopy* 67,536-539.
61. Feng, Y.J., Liu, J.Z., Liang, N.J. 2008. Thermostability, solvent tolerance, catalytic activity and conformation of cofactor modified horseradish peroxidase. *Biochimie* 90, 1337-1346.
62. Yang, Y., Mu, S., 1997. Bioelectrochemical responses of polyaniline horseradish peroxidase. *Journal of Electroanalytical Chemistry* 432, 71-78.
63. Csoregi, E., Corton, L., Marko-Varga, G. 1994, Peroxidase modified carbon microelectrodes in flow through detection of hydrogen peroxide and organic peroxides. *Analytical Chemistry* 66, 3604-3610.
64. Adeyolu, O., Iwuoha, E.I., Smyth, M.R. 1994. Amperometric determination of butanone peroxide and hydroxylamine via direct electron transfer at a horseradish peroxidase modified platinum electrode. *Analytical Processes and Analytical Communications* 31, 177-179.
65. Vijayakumar, A.R., Csoregi, E., Heller, A., Corton, L. 1996. Alcohol biosensors based on coupled oxidase peroxidase systems. *Analytica Chimica Acta* 327, 223-234.
66. Tatsuma, T., Watanabe, T., 1991. Oxidase/peroxidase bilayer modified electrodes as sensors for lactase, pyruvate, cholesterol and uric acid. *Analytica Chimica Acta* 242, 85-89.
67. Garguilo, M.G., Huyhn, N., Proctor, A., Michael, A.C. 1991. Amperometric sensors for peroxide, choline and acetylcholine, based on electron transfer

- between horseradish peroxidase and a redox polymer. *Analytical Chemistry* 65, 523-528.
68. Wang, J., Liu, Y., Chen, L. 1993. Organic phase biosensors for monitoring phenol and hydrogen peroxide in pharmaceutical antibacterial products. *Analyst* 118, 277-280.
69. Tatsuma, T., Ariyama, K., Oyama, N. 1996. Peroxidase incorporated hydrophilic polythiophene electrode for the determination of hydrogen peroxide in acetonitrile. *Analytica Chimica Acta* 318, 297-301.
70. Chenghong, L., deng, J., Hydrogen peroxide sensor based on coimmobilized Methylene Green and Horseradish Peroxidase in the Same Montmorillonite-modified Bovine Serum Albumin-Glutaraldehyde Matrix on a Glassy Carbon Electrode Surface. *Journal of Electroanalytical Chemistry* 413, 519-531.
71. Chaubey, A., Pande, K.K., Singh, V.S., Malhotra, B.D. 2000. Co-immobilization of the lactate oxidase and lactate dehydrogenase on conducting polyaniline films. *Analytica Chimica Acta* 407, 97-103.
72. Moutet, J.C., Aman, S.E., Ungurreanu, M., Visan, T. 1996. Electropolymerization of ferrocene bis-amide derivatives: a possible route to an electrochemical sensor device. *Journal of Electroanalytical Chemistry* 410, 79-85.
73. Zotti, G., Gallazi, M.C., Zerbi, G., Meille, S.V. 1995. Conducting polymers from anodic coupling of some regiochemically defined dialkoxy-substituted thiophene oligomers, *Synthetic Metals* 73, 217-225.
74. Inagaki, S., Kutoba, Y., Kito, S., Fukuda, M., Ono, T., Yamano, M., Tohyama, M. 1986. Ultrastructural evidence of enkephalinergetic input to glucoreceptor neurons in ventromedial hypothalamic nucleus. *Brain Research* 378, 420-424.

75. Merz, A., Haimerl, A., Owen, A.J., 1988. Free-standing, conducting films of pyrrole/N-(4-ferrocenylbutyl)-pyrrole benzenesulphonate copolymers. *Synthetic Metals* 25, 89-102.
76. Zotti, G., Sciavon, G., Zecchin, S., Berlin, A., Canavesi, A., Pagani, G. 1997. Self-assembly and electropolymerization of pyrrole-and bithiophene-*n*-hexyl-ferrocene molecules on ITO electrodes. *Synthetic Metals* 84,239-240.
77. Gulce, H., Celebi, S.S., Ozyoruk, H., Yildiz, A. 1995. Amperometric enzyme electrode for sucrose determination prepared from glucose oxidase and invertase co-immobilized in poly(vinylferrocenium). *Journal of electroanalytical Chemistry* 397, 217-223.
78. Dong, S., Che, G. 1991. Electrocatalytic oxidation of ascorbic acid at Prussian blue film modified microdisk electrode. *Journal of Electroanalytical Chemistry* 315, 191-199.
79. Koch, S, Wolf, H., Danapel, C., Feller, K.A. 2001. Optical flow-cell multichannel immunosensor for the detection of warfare agents. *Biosensors and Bioelectronics* 14, 779-784.
80. Allen, K.D., Bruck, M.A., Gray, S.D., Kingsborough, R.P., Smith, D.P., Weller, K.J, Wigley, D.E. 1995. Quinoline binding mode as a function of oxidation state in aryloxide-supported tantalum complexes: Models for hydrodenitrogenation catalysis. *Polyhedron* 14, 3315-3333.
81. Herber, R.H., Temple, K., Manners, I., Buretea, M., Tilley, T.D. 1999. Strained, ring tilted dicarbon-bridged[2]ferrocenophanes and ferrocene revisited: ⁵⁷Fe Mossbauer spectroscopic study of bonding, hyperfine interactions, and lattice dynamics. *Inorganica Chimica Acta* 287, 152-158.

82. Karyakin, A.A. Maltsev, I.A. Lukachova, L. V. 1996. The influence of defects in polyaniline structure on its electroactivity; optimization of 'self-doped' polyaniline synthesis. *Journal of Electroanalytical Chemistry* 402, 217-219.
83. Ray, A., Asturias, G.E., Kershner, D.L., Richter, A.F., MacDiarmid, A.G., Epstein, A.J. 1989. Polyaniline: Doping, structure and derivatives. *Synthetic Metals* 29, 141-150.
84. Shah, A.A. Holze, R. 2008. Spectroelectrochemistry of two-layered composites of polyaniline and poly(o-aminophenol). *Electrochimica Acta* 53, 4642-4653.
85. Iwuoha, E. I. Mavundla, S. E. Somerset, V. S. Pertik, L. F. Klink, M. J. Sekota, M., Bakers, P. 2006. Electrochemical and Spectroscopic Properties of Fly Ash-Polyaniline Matrix Nanorod Composites. *Microchim Acta* 155, 453 – 458.
86. Yong, C., Liping, Guo., Min, A., Liande, Z., Xiujun, C. 2006. Effects of Ethanol on properties of polyaniline-modified Electrode Doped with planar Binuclear Cobalt Phthalocyanine. *Chinese Journal of Analytical Chemistry* 34, 469-473.
87. Ryu, K.S., Kim, M.K., Park, J.Y., Park, G.N., Kang, M.G., Chang, S.O. 2002. Redox supercapacitor using polyaniline doped with Li salts as electrode. *Solid State Ionics* 152-153, 861-866.
88. Zhu, L., Yang, R., Zhai, J., Tian, C. 2007. Bionzymatic glucose biosensor based on co-immobilization of peroxidase and glucose oxidase on carbon nanotubes electrode. *Biosensors and Bioelectronics* 23, 528-535.
89. Schultze, J.W., Heidelberg, A., Rosenkranz, C., Schapers, T., Staikov, G. 2005. Principles of electrochemical nanotechnology and their application for materials and systems.

90. Rodrigues, P.C., Cantao, M.P. Jannisek, P., Scarpa. P.C.N., Mathias, A. L., Ramos, L.P., Gomes, M.A.B. 2002. Polyaniline/lignin blends: FTIR, MEV and electrochemical characterization. *European Polymer Journal* 38, 2213-2217.
91. Zheng, L., Xiong, L., Liu, C., Jin, L. 2006. Electrochemical synthesis of a novel sulfonated polyaniline and its electrochemical properties. *European Polymer Journal* 42, 2328-2333.
92. Sanchis, C., Salavagione, H J. Morallon, E. 2008. Ferrocenium strong adsorption on sulfonated polyaniline modified electrodes. *Journal of Electroanalytical Chemistry* 618, 67-73.
93. Matsumiya, M., Tokuraku, K., Matsuura, H., Hinoue, K. 2006. Consecutive recovery of rare earth and alkaline earth elements by countercurrent electromigration in room temperature molten salts. *Journal of Electroanalytical Chemistry* 586, 12-17.
94. Marr, G., Rockett, B.W. 1982. Ferrocene annual survey covering the year 1980. *Journal of Organometallic Chemistry* 227, 373-440.
95. Iwuoha, E.I, Smyth, M.R. 1996. Organic phase enzyme electrodes: kinetics and analytical applications. *Biosensors and bioelectronics* 12, 53-75.
96. Iwuoha, E.I., Smyth M.R., Lyons, M.E.G., 1995. Solvent effects on the reactivities of an amperometric glucose sensor. *Journal of Electroanalytical Chemistry* 390, 35-45.
97. Gosser, Jr. D.K. 1993. Cyclic Voltammetry, simulations and Analysis of Reaction Mechanisms. *VCH Publishers Inc. Newyork*.97-102
98. Cao, Z., Jiang, X., Xie, Q., Yao, S. 2008. A third generation hydrogen peroxide biosensor based on horseradish peroxidase immobilized in a tetrathiafulvalene-

- tetracyanoquinodimethane/multiwalled carbon nanotubes film. *Biosensors and Bioelectronics* 24, 222-227.
99. Li, L.Z., Huang, J.H., Xiao, X.M., Zeng, Y., Chu, X. 2002. Modulation of Electrochemical Oscillations by specific adsorption of Cl^- during electrooxidation of methanol on Pt electrode. *Chinese Chemical letters* 13, 277-278.
100. Li, L.Z., Huang, Q.H., Ren, B., Xiao, X.M., Zeng, Y., Tian, Z.Q. 2001. A new experimental method to distinguish two different mechanisms for a category of Oscillators involving mass transfer. *Electrochemistry Communications* 3, 654-658.
101. Zhu, L., Yang, R., Zhai, J., Tian, C. 2007. Bionzymatic glucose biosensor based on co-immobilization of peroxidase and glucose oxidase on carbon nanotubes electrodes. *Biosensors and Bioelectronics* 23, 528-535.
102. Liu, S.Q., Ju, H.X. 2002. Renewable reagentless hydrogen peroxide sensor based on direct electron transfer of horseradish peroxidase immobilized on colloidal gold modified electrode. *Analytica Biochemistry* 307, 110-116.
103. Ferri, T., Poscia, A., Santucci, R. 1998. Direct electrochemistry of membrane-entrapped horseradish peroxidase: Part 1. A voltammetric and spectroscopic study. *Bioelectrochemistry and Bioenergetics* 44, 177-181.
104. Liu, Z.M., Yang, Y., Wang, H., Liu, Y.L., Shen, G.L., Yu, R.Q. 2005. A hydrogen peroxide biosensor based on nano-Au/PAMAM dendrimer/cystamine modified gold electrode. *Sensors and Actuators B* 106, 394-400.

APPENDIX A

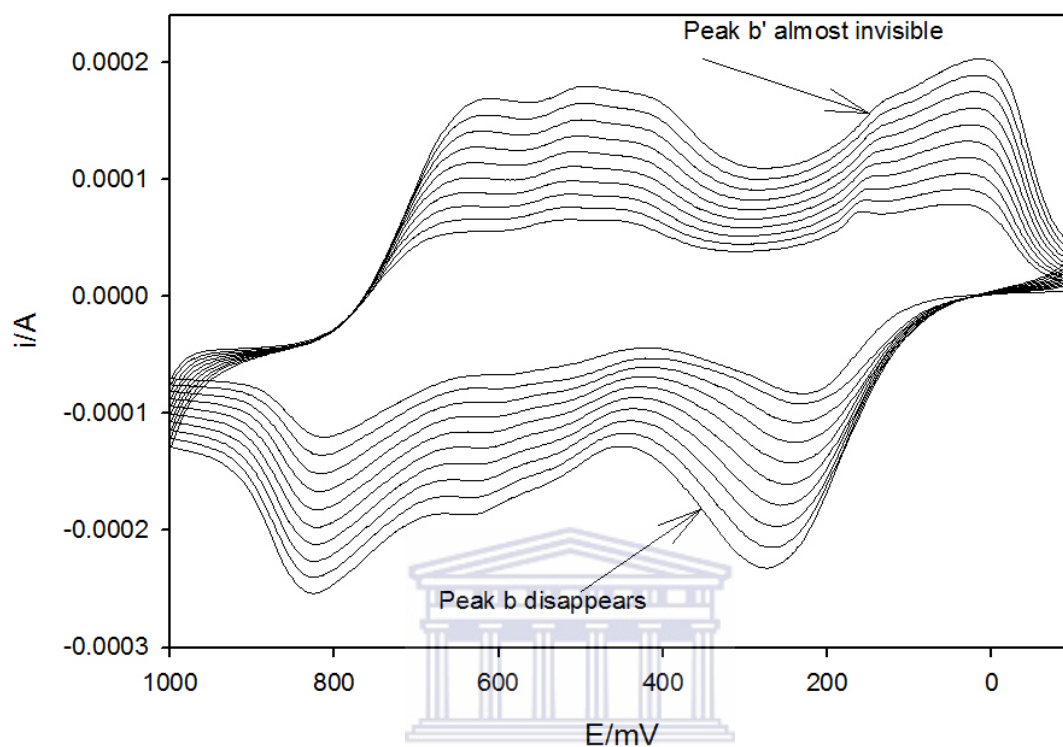


Figure A. Voltammograms for the electropolymerization of poly(aniline-ferrocenium hexafluorophosphate) nano-composites when 0.01 M of ferrocenium hexafluorophosphate is used in the electropolymerization solution (1 M HCl at a scan rate of 100 mV s^{-1} .)

APPENDIX B

Peak a

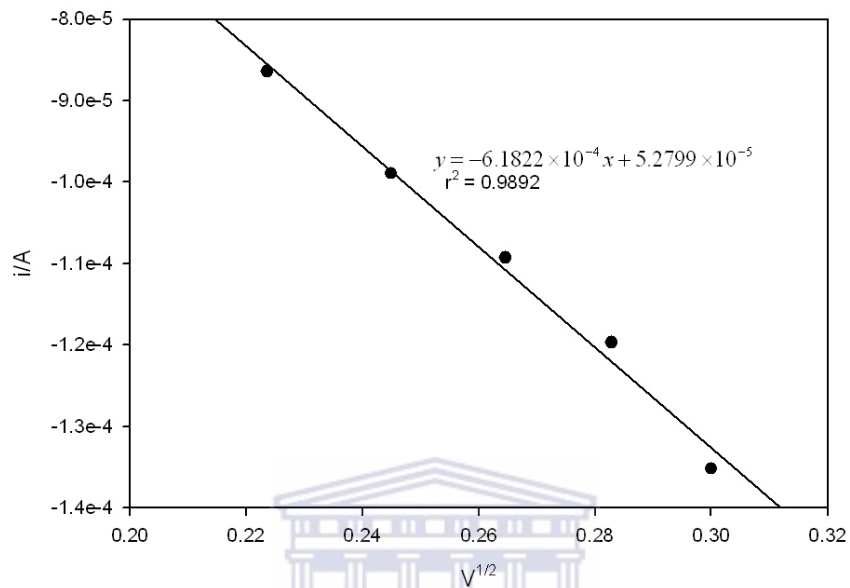


Figure B (i): A plot of root scan rate versus peak current for peak a (Ref Fig. 7).

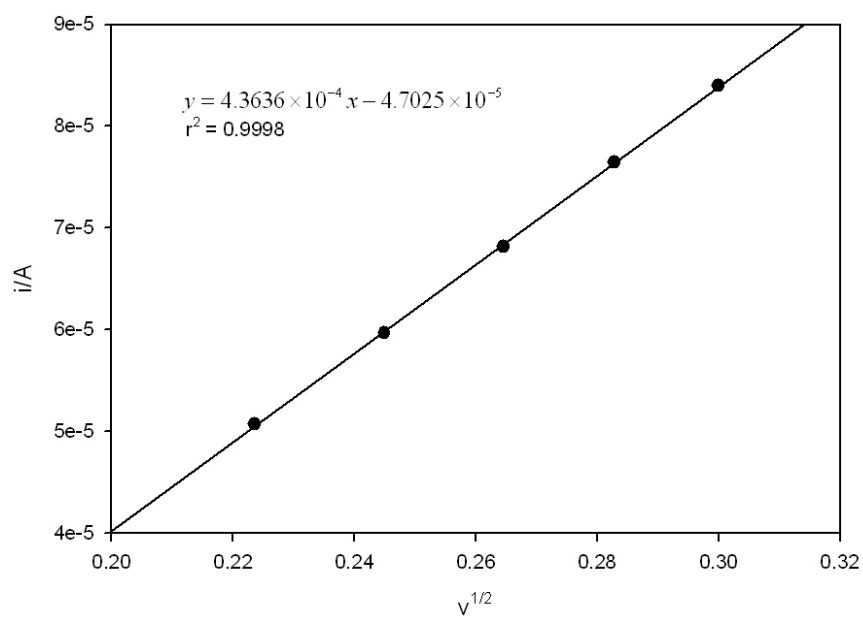


Figure B (ii): A plot of root scan rate versus peak current for peak a' (Ref. Fig.7).

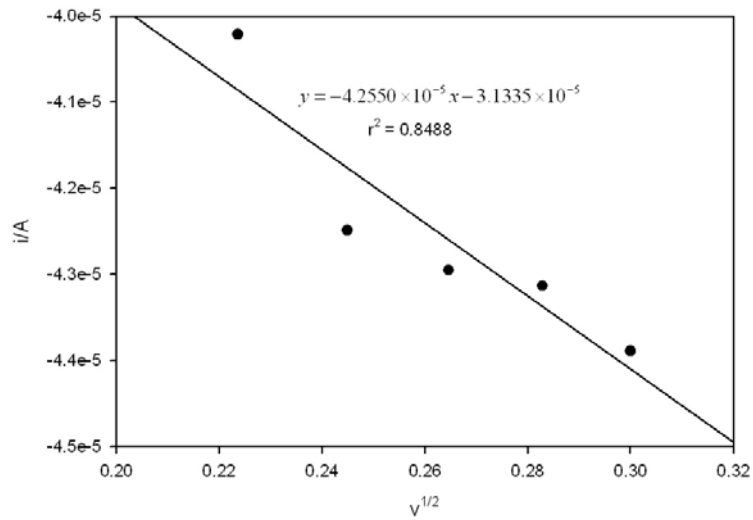


Figure B (iii): A plot of root scan rate versus peak current for peak d (Ref. Fig.7).

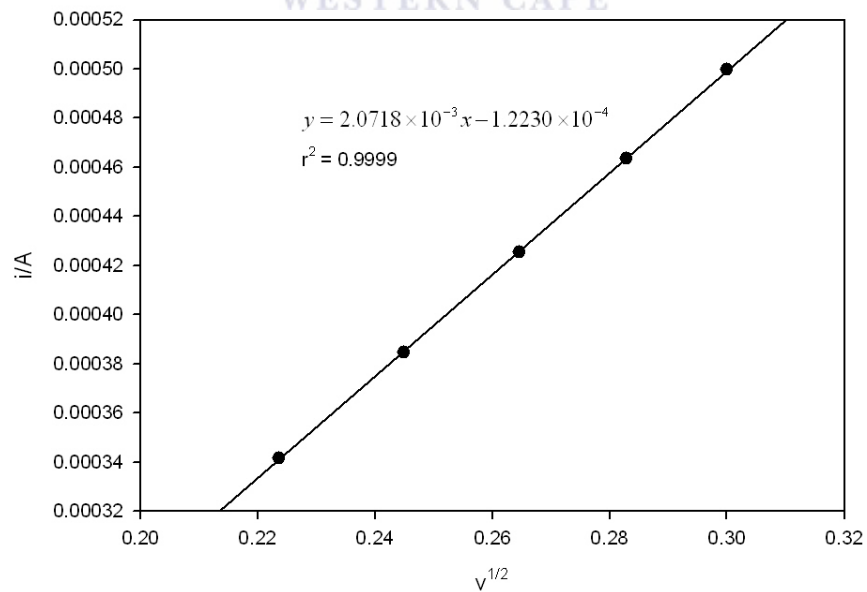


Figure B (iv): A plot of root scan rate versus peak current for peak d' (Ref. Fig.7).

peak a

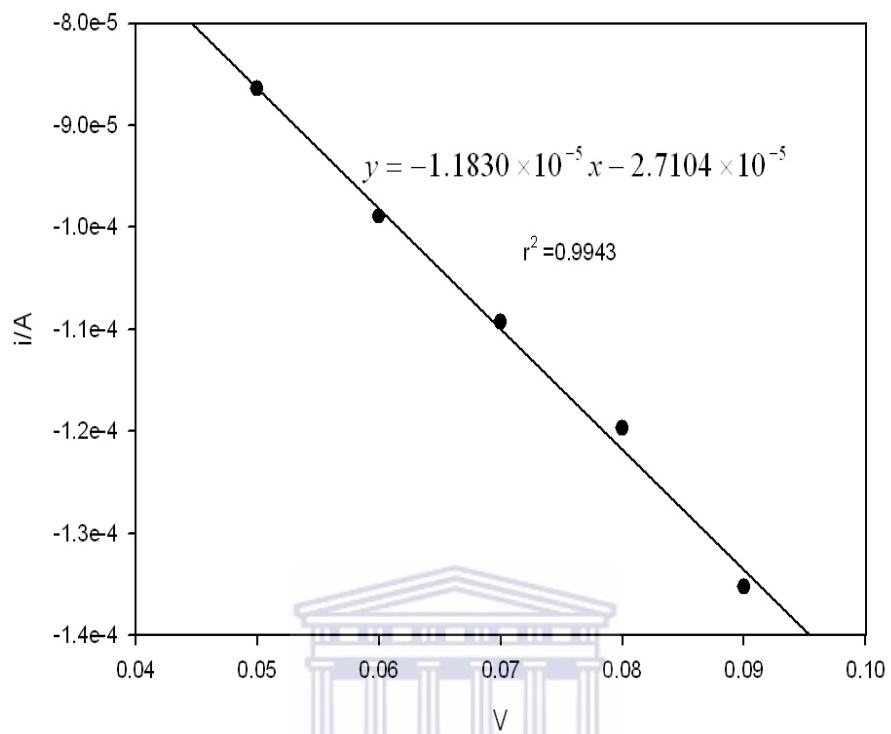
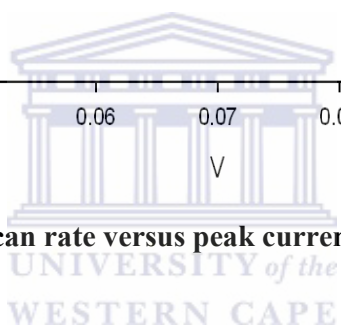


Figure B (v): A plot of scan rate versus peak current for peak a (Ref. Fig 7).



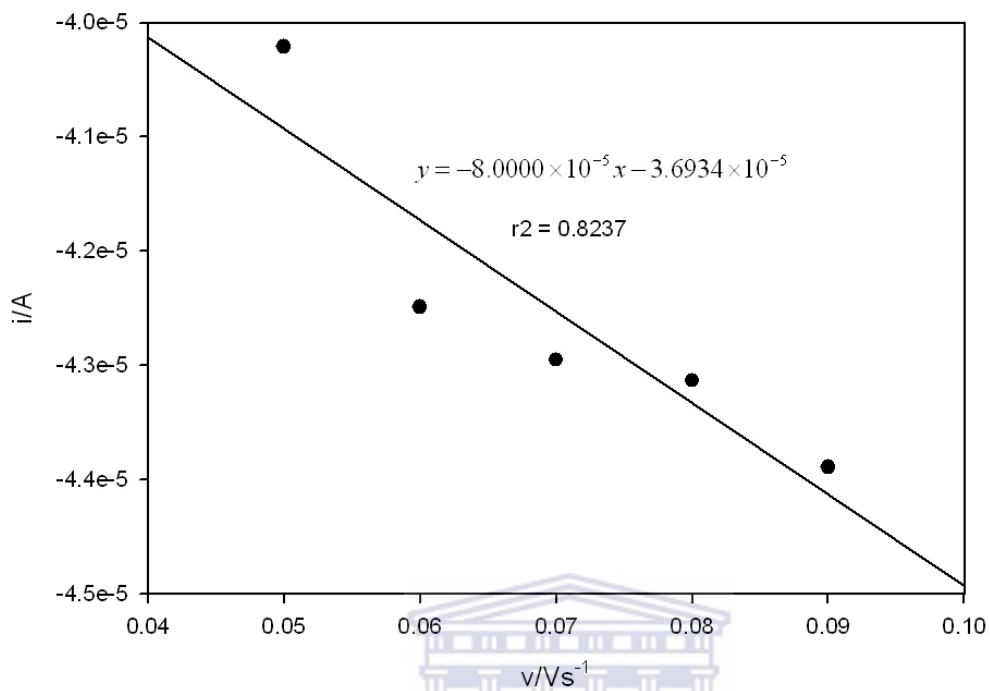


Figure B (vi): A plot of scan rate versus peak current for peak d (Ref. Fig.7).

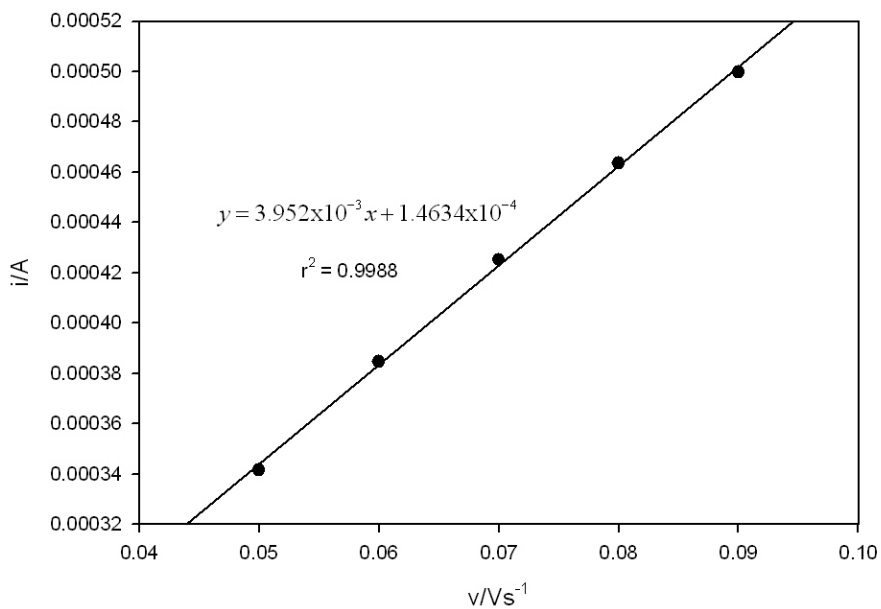


Figure B (vii): A plot of scan rate versus peak current for peak d' (Ref. Fig. 7).

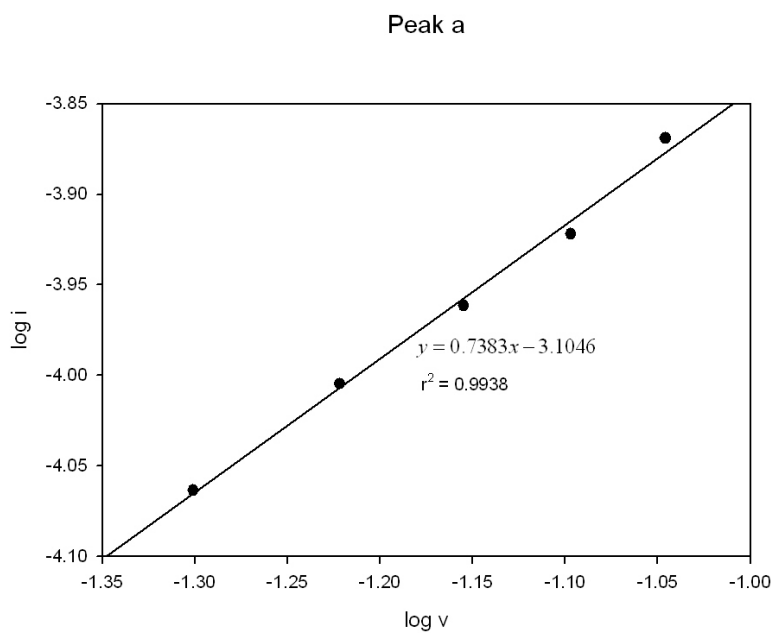


Figure B (viii): A plot of log scan rate versus log peak current for peak a (Ref.Fig.7).

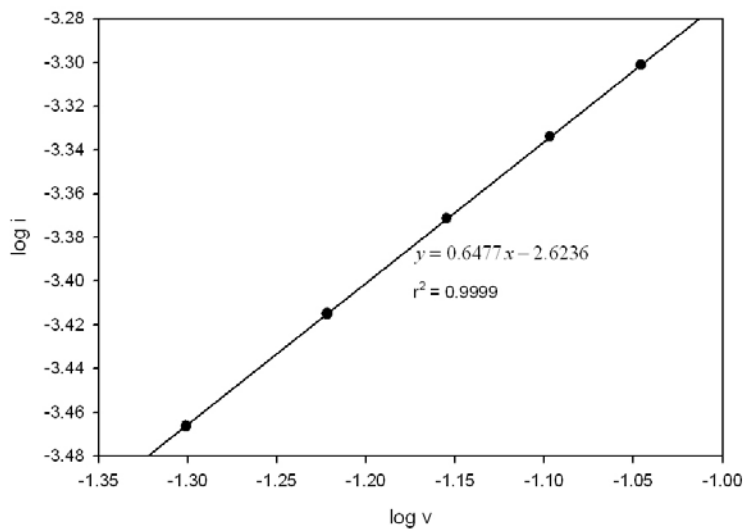
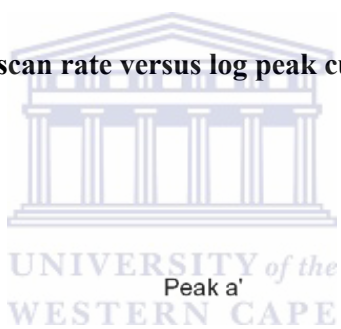


Figure B (ix): A plot of log scan rate versus log peak current for peak a' (Ref. Fig 7).

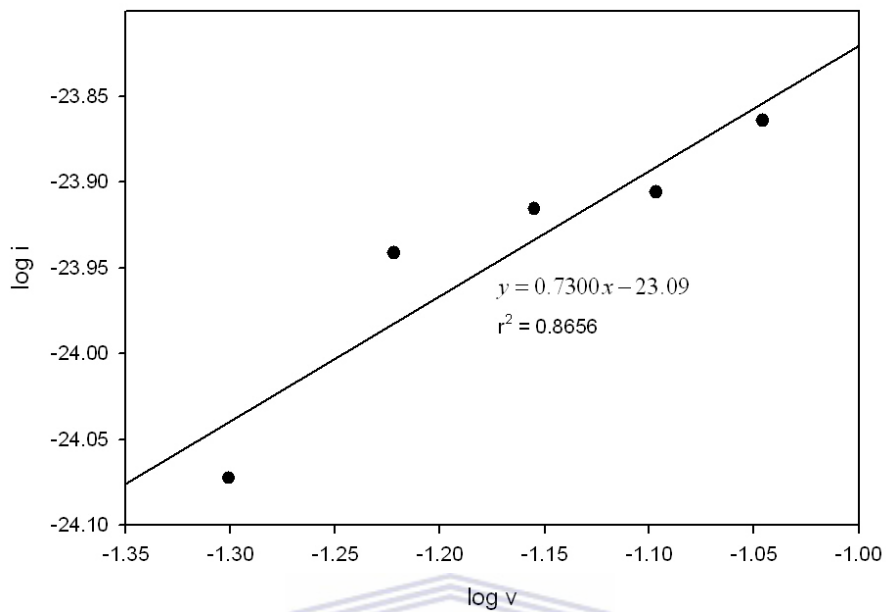


Figure B (x): A plot of log scan rate versus log peak current for peak d (Ref. Fig.7).

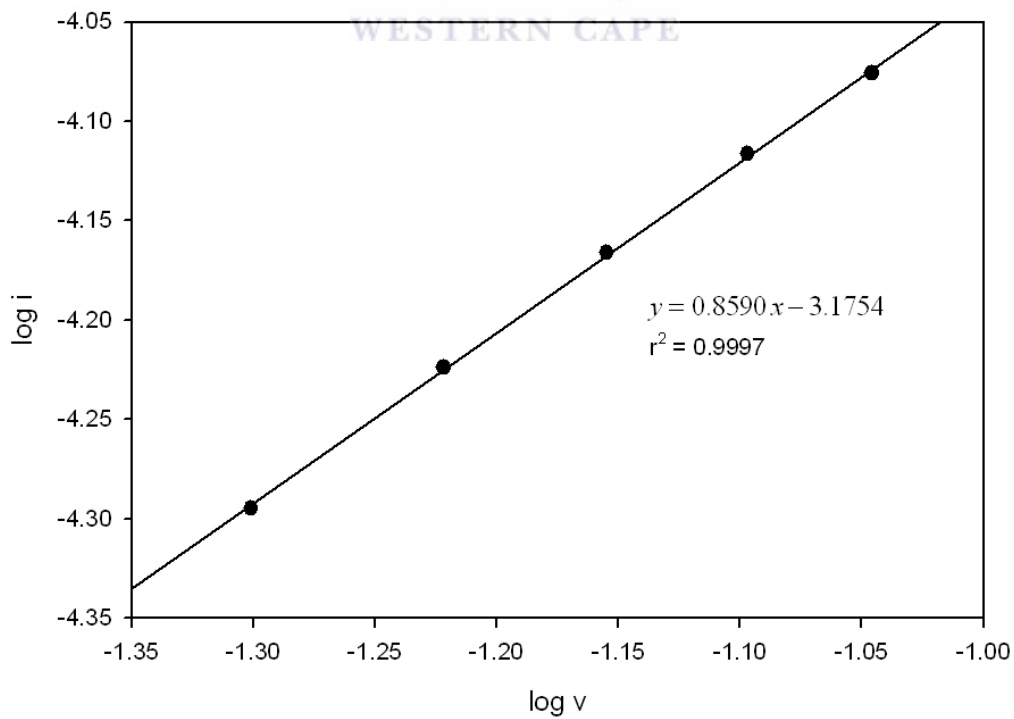
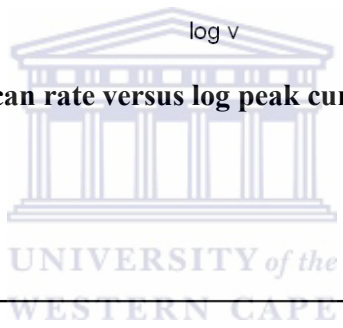


Figure B (xi): A plot of log scan rate versus log peak current for peak d' (Ref. Fig 7)

APPENDIX C

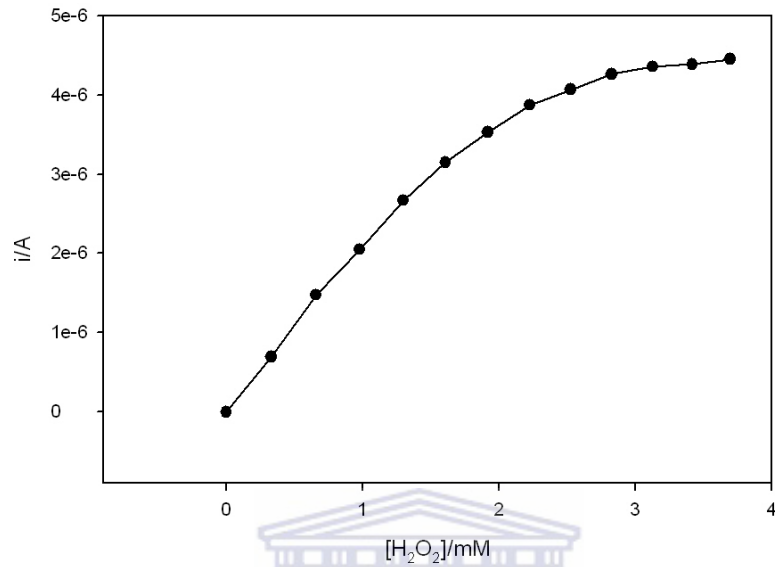


Figure C (i): Calibration curve for biosensor response to standard H_2O_2 in PBS, pH 7.0 on day 3.

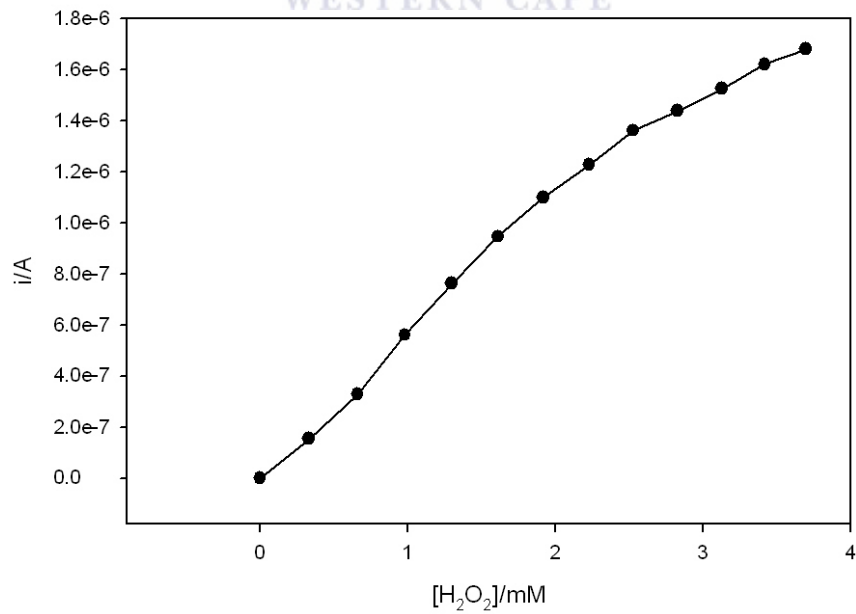


Figure C (ii): Calibration curve for biosensor response to standard H_2O_2 in PBS, pH 7.0 on day 7.

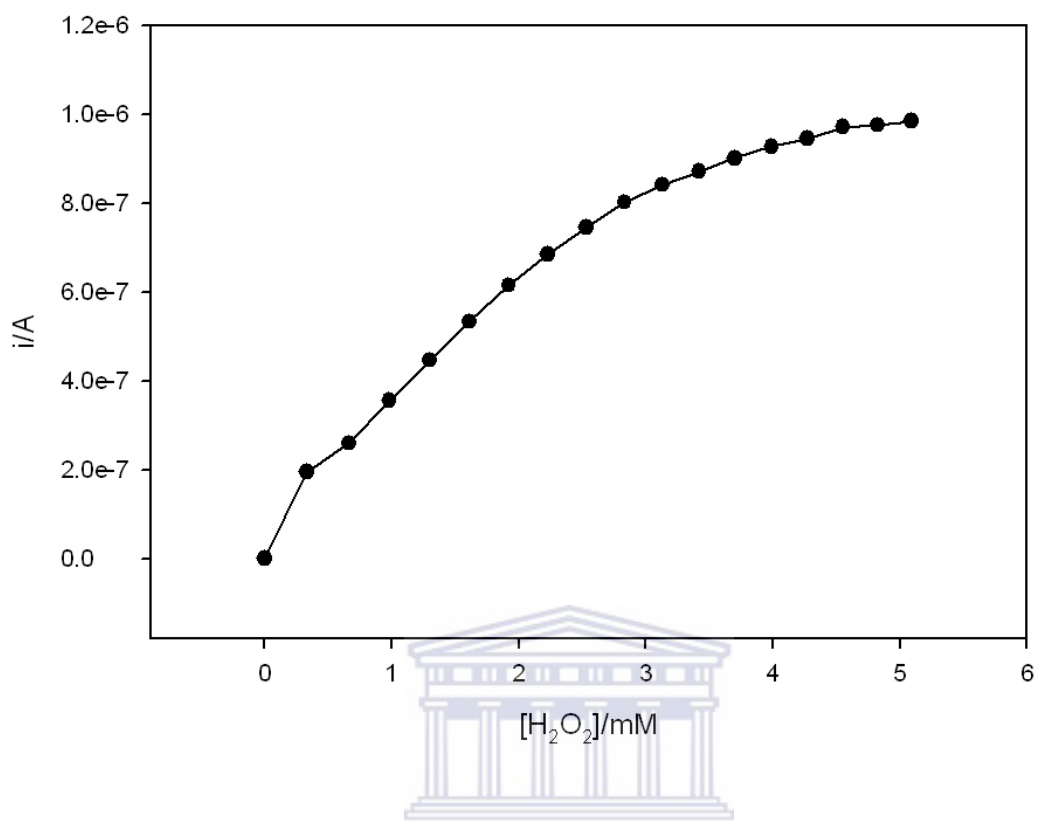


Figure C (iii): Calibration curve for biosensor response to standard H₂O₂ in PBS, pH 7.0 on day 1

APPENDIX D

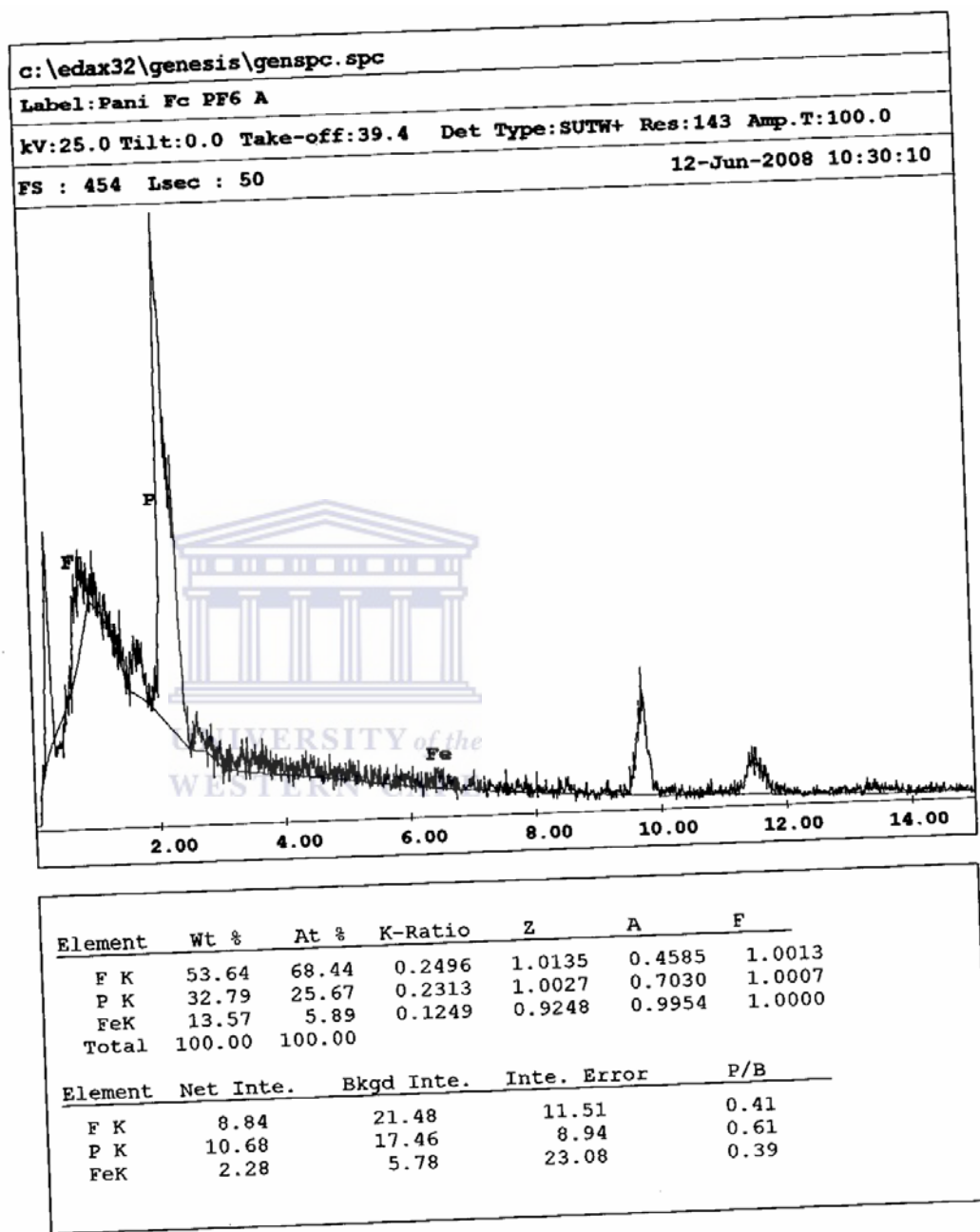


Fig D. Electron Dispersion Spectra (EDS) for Pani-FcPF₆.

APPENDIX E

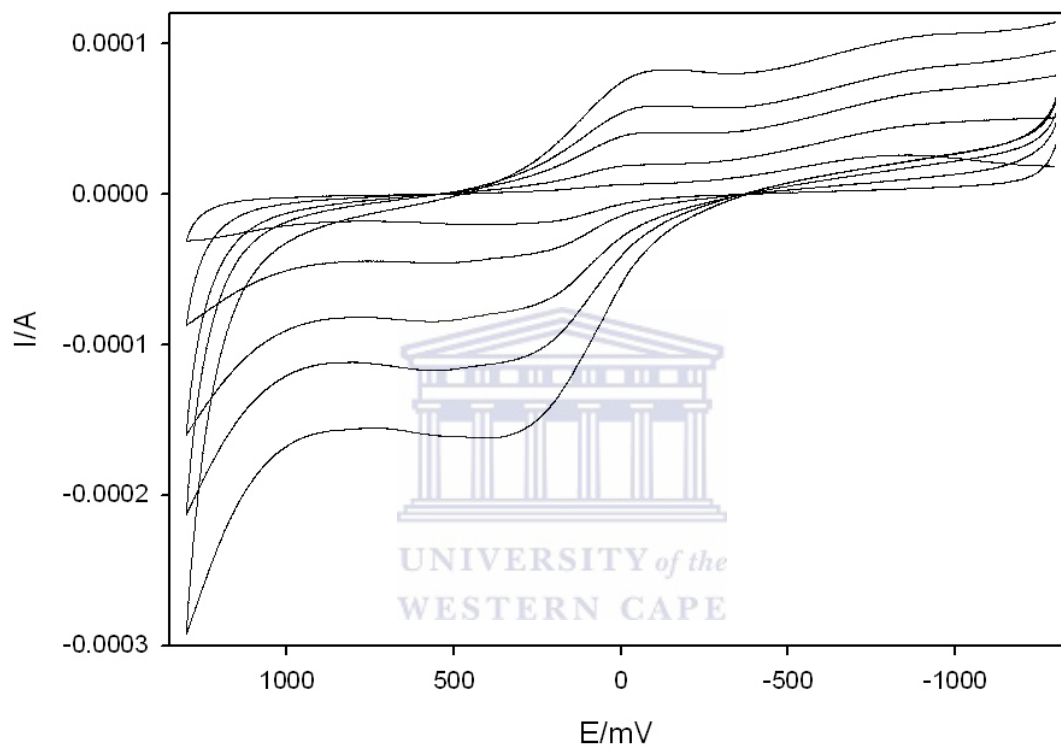


Figure E: Cyclic voltammograms of Pani-FcPF₆ in 0.1 M PBS, pH 7.0 at scan rates 10, 30, 60, 80 and 100 mV s⁻¹.